Developed at the request of:

Research conducted by:

Climate: Observations, projections and impacts: United States of America

Met Office
Simon N. Gosling, University of Nottingham
Robert Dunn, Met Office
Fiona Carrol, Met Office
Nikos Christidis, Met Office
John Fullwood, Met Office
Diogo de Gusmao, Met Office
Nicola Golding, Met Office
Lizzie Good, Met Office
Trish Hall, Met Office
Lizzie Kendon, Met Office
John Kennedy, Met Office
Kirsty Lewis, Met Office
Rachel McCarthy, Met Office
Carol McSweeney, Met Office
Colin Morice, Met Office
David Parker, Met Office
Matthew Perry, Met Office
Peter Stott, Met Office
Kate Willett, Met Office
Myles Allen, University of Oxford
Nigel Arnell, Walker Institute, University of Reading
Dan Bernie, Met Office
Richard Betts, Met Office
Niel Bowerman, Centre for Ecology and Hydrology
Bastiaan Brak, University of Leeds
John Caesar, Met Office
Andy Challinor, University of Leeds
Rutger Dankers, Met Office
Fiona Hewer, Fiona's Red Kite
Chris Huntingford, Centre for Ecology and Hydrology
Alan Jenkins, Centre for Ecology and Hydrology
Nick Klingaman, Walker Institute, University of Reading
Kirsty Lewis, Met Office
Ben Lloyd-Hughes, Walker Institute, University of Reading
Jason Lowe, Met Office
Rachel McCarthy, Met Office
James Miller, Centre for Ecology and Hydrology
Robert Nicholls, University of Southampton
Maria Noguer, Walker Institute, University of Reading
Friedreike Otto, Centre for Ecology and Hydrology
Paul van der Linden, Met Office
Rachel Warren, University of East Anglia

The country reports were written by a range of climate researchers, chosen for their subject expertise, who were drawn from institutes across the UK. Authors from the Met Office and the University of Nottingham collated the contributions in to a coherent narrative which was then reviewed. The authors and contributors of the reports are as above.

Developed at the request of:

DEPARTMENT OF ENERGY & CLIMATE CHANGE

Research conducted by:

Met Office Hadley Centre

The University of Nottingham
UNITED KINGDOM · CHINA · MALAYSIA

Walker INSTITUTE

Centre for Ecology & Hydrology
NATURAL ENVIRONMENT RESEARCH COUNCIL

UNIVERSITY OF LEEDS

Tyndall Centre
for Climate Change Research

Climate: Observations, projections and impacts

United States of America

We have reached a critical year in our response to climate change. The decisions that we made in Cancún put the UNFCCC process back on track, saw us agree to limit temperature rise to 2 °C and set us in the right direction for reaching a climate change deal to achieve this. However, we still have considerable work to do and I believe that key economies and major emitters have a leadership role in ensuring a successful outcome in Durban and beyond.

To help us articulate a meaningful response to climate change, I believe that it is important to have a robust scientific assessment of the likely impacts on individual countries across the globe. This report demonstrates that the risks of a changing climate are wide-ranging and that no country will be left untouched by climate change.

I thank the UK's Met Office Hadley Centre for their hard work in putting together such a comprehensive piece of work. I also thank the scientists and officials from the countries included in this project for their interest and valuable advice in putting it together. I hope this report will inform this key debate on one of the greatest threats to humanity.

The Rt Hon. Chris Huhne MP, Secretary of State for Energy and Climate Change

There is already strong scientific evidence that the climate has changed and will continue to change in future in response to human activities. Across the world, this is already being felt as changes to the local weather that people experience every day.

Our ability to provide useful information to help everyone understand how their environment has changed, and plan for future, is improving all the time. But there is still a long way to go. These reports – led by the Met Office Hadley Centre in collaboration with many institutes and scientists around the world – aim to provide useful, up to date and impartial information, based on the best climate science now available. This new scientific material will also contribute to the next assessment from the Intergovernmental Panel on Climate Change.

However, we must also remember that while we can provide a lot of useful information, a great many uncertainties remain. That's why I have put in place a long-term strategy at the Met Office to work ever more closely with scientists across the world. Together, we'll look for ways to combine more and better observations of the real world with improved computer models of the weather and climate; which, over time, will lead to even more detailed and confident advice being issued.

Julia Slingo, Met Office Chief Scientist

Introduction

Understanding the potential impacts of climate change is essential for informing both adaptation strategies and actions to avoid dangerous levels of climate change. A range of valuable national studies have been carried out and published, and the Intergovernmental Panel on Climate Change (IPCC) has collated and reported impacts at the global and regional scales. But assessing the impacts is scientifically challenging and has, until now, been fragmented. To date, only a limited amount of information about past climate change and its future impacts has been available at national level, while approaches to the science itself have varied between countries.

In April 2011, the Met Office Hadley Centre was asked by the United Kingdom's Secretary of State for Energy and Climate Change to compile scientifically robust and impartial information on the physical impacts of climate change for more than 20 countries. This was done using a consistent set of scenarios and as a pilot to a more comprehensive study of climate impacts. A report on the observations, projections and impacts of climate change has been prepared for each country. These provide up to date science on how the climate has already changed and the potential consequences of future changes. These reports complement those published by the IPCC as well as the more detailed climate change and impact studies published nationally.

Each report contains:

- A description of key features of national weather and climate, including an analysis of new data on extreme events.
- An assessment of the extent to which increases in greenhouse gases and aerosols in the atmosphere have altered the probability of particular seasonal temperatures compared to pre-industrial times, using a technique called 'fraction of attributable risk.'
- A prediction of future climate conditions, based on the climate model projections used in the Fourth Assessment Report from the IPCC.
- The potential impacts of climate change, based on results from the UK's Avoiding Dangerous Climate Change programme (AVOID) and supporting literature. For details visit: http://www.avoid.uk.net

The assessment of impacts at the national level, both for the AVOID programme results and the cited supporting literature, were mostly based on global studies. This was to ensure consistency, whilst recognising that this might not always provide enough focus on impacts of most relevance to a particular country. Although time available for the project was short, generally all the material available to the researchers in the project was used, unless there were good scientific reasons for not doing so. For example, some impacts areas were omitted, such as many of those associated with human health. In this case, these impacts are strongly dependant on local factors and do not easily lend themselves to the globally consistent framework used. No attempt was made to include the effect of future adaptation actions in the assessment of potential impacts. Typically, some, but not all, of the impacts are avoided by limiting global average warming to no more than 2 °C.

The Met Office Hadley Centre gratefully acknowledges the input that organisations and individuals from these countries have contributed to this study. Many nations contributed references to the literature analysis component of the project and helped to review earlier versions of these reports.

We welcome feedback and expect these reports to evolve over time. For the latest version of this report, details of how to reference it, and to provide feedback to the project team, please see the website at www.metoffice.gov.uk/climate-change/policy-relevant/obs-projections-impacts

In the longer term, we would welcome the opportunity to explore with other countries and organisations options for taking forward assessments of national level climate change impacts through international cooperation.

Summary

Climate observations

- A widespread warming trend has been recorded over the USA since 1960.
- There has been a widespread reduction in the number of cool nights across the whole of the contiguous US, with stronger decreases observed towards the coasts along with a widespread increase in the number of warm nights.
- There has been a general increase in summer and winter temperatures averaged over the country as a result of human influence on climate, making the occurrence of warm summer and winter temperatures more frequent and cold summer and winter temperatures less frequent.
- Since 1960 there has been a positive trend in precipitation on the north eastern seaboard but for the remainder of the country, there is no significant trend.

Climate change projections

- For the A1B emissions scenario projected temperature increases over the USA are generally higher in central, southwest and northern regions, up to around 4-4.5°C. The agreement between the CMIP3 ensemble is higher in southern and eastern parts of the country compared to the north.
- The USA shows a north-south division in projected precipitation changes, with the highest decreases, of up to around 20%, in the southwest, and increases of up to 10% in the northeast. However, the agreement across the CMIP3 ensemble is moderate to low. Much of this uncertainty arises from the USA being located in the transition zone between strong increases in precipitation over Canada, and decreases over Central America and the Caribbean.

Climate change impacts projections

Crop yields

- The majority of global- and regional-scale studies included here project declines in the yields of maize, soybean and wheat, three of the USA's major crops, as a consequence of climate change.

- Research by the AVOID programme looked at how present day agricultural land may change in suitability under climate change. This indicated that for the USA a reasonable proportion of cultivated areas could see a decline in suitability for production, with only small areas experiencing increasing in agricultural suitability.

Food security

- The USA is currently a country with extremely low levels of undernourishment. Several studies suggest that the USA could remain food secure under climate change scenarios over the next 40 years, largely due to its high adaptive capacity associated with an ability to import food.

- Research by the AVOID programme projects that the USA may avoid major food security issues under climate change by implementing structural adjustments, such as diverting food away from exports and animal feed.

Water stress and drought

- There is consensus among global-scale studies that much of the USA's population is currently exposed to water stress.

- Several recent assessments support the IPCC AR4 conclusion that annual mean precipitation could decrease in the southwest USA with climate change, and project that droughts could become more frequent and severe in this region with climate change.

- Projections of water stress with climate change indicate that water stress may increase moderately in the USA.

- Simulations from the AVOID programme are consistent in projecting a moderate increase in water stress, presenting a median increase of around 7% of the population of the USA being exposed to water stress increases by 2100 under the

SRES A1B emission scenario. This is lower under an aggressive mitigation scenario, at around 5%.

Pluvial flooding and rainfall

- The IPCC AR4 noted that under climate change scenarios, the largest precipitation increases were projected to be in the northeast USA.

- Studies since then have also pointed to increasing mean and extreme precipitation in the northeast USA, which is suggested in observational analyses and projected in 21st century simulations.

Fluvial flooding

- Recent studies demonstrate large uncertainties in estimating fluvial flooding under climate change scenarios across the USA. At least one global modelling study has projected a strong increase in flood frequency in parts of Southern USA, the East Coast states and the Pacific Northwest, but a decrease in other parts of the country.

- Results from the AVOID programme, based on climate projections from 21 GCMs, show that for the USA as a whole the model projections are evenly balanced between increasing and decreasing flood risk in the early 21st century. However, later in the century the models show a greater tendency towards increasing flood risk, especially in the A1B scenario.

Tropical cyclones

- There remains large uncertainty in the current understanding of how tropical cyclones might be affected by climate change. To this end, caution should be applied in interpreting model-based results, even where the models are in agreement.

- However, most global- and regional-scale studies reviewed here suggest that the frequency of tropical cyclones in the North Atlantic could decrease with climate change, which may result in fewer cyclones striking the eastern USA and the Gulf Coast. However, complex sub-basin-scale changes in cyclone frequency could lead to increasing cyclone counts in some coastal regions and decreases in others.

- The impact of climate change on cyclones near Hawaii is highly uncertain, due to the lack of model agreement on the sign of the change in cyclone frequency in the East Pacific.

- The majority of studies reviewed here project that tropical cyclone intensities and cyclone rainfall could increase in both the North Atlantic and the East Pacific, particularly for the most intense cyclones. These stronger storms could potentially cause an increase in cyclone damages in the USA due to climate change.

Coastal regions

- Studies published after the IPCC AR4 suggests that the USA is highly vulnerable to sea level rise (SLR). This supports conclusions from the IPCC AR4.

- One study shows that by the 2070s, the number of people exposed to SLR with climate change could reach 12.9 million under A1B emissions; an aggressive mitigation policy could reduce this by around 0.5 million.

Table of Contents

Chapter 1 – Climate Observations

Rationale

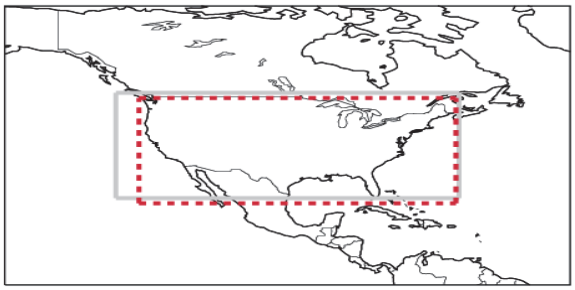

Figure 1. *Location of boxes for the regional average time series (red dashed box) in Figures 3, 6 and 7 and the attribution region (grey box) in Figures 4 and 5.*

Present day weather and climate play a fundamental role in the day to day running of society. Seasonal phenomena may be advantageous and depended upon for sectors such as farming or tourism. Other events, especially extreme ones, can sometimes have serious negative impacts posing risks to life and infrastructure, and significant cost to the economy. Understanding the frequency and magnitude of these phenomena, when they pose risks or when they can be advantageous and for which sectors of society, can significantly improve societal resilience. In a changing climate it is highly valuable to understand possible future changes in both potentially hazardous events and those reoccurring seasonal events that are depended upon by sectors such as agriculture and tourism. However, in order to put potential future changes in context, the present day must first be well understood both in terms of common seasonal phenomena and extremes.

The purpose of this chapter is to summarise the weather and climate from 1960 to present day. This begins with a general climate overview including an up to date analysis of changes in surface mean temperature. These changes may be the result of a number of factors including climate change, natural variability and changes in land use. There is then a focus on extremes of temperature, precipitation and storms selected from 2000 onwards, reported in the World Meteorological Organization (WMO) Annual Statement on the Status of the Global Climate and/or the Bulletin of the American Meteorological Society (BAMS) State of the Climate reports. This is followed by a discussion of changes in moderate extremes from 1960 onwards using an updated version of the HadEX extremes database (Alexander et al., 2006) which categorises extremes of temperature and precipitation. These are core climate variables which have received significant effort from the climate research community in terms of data acquisition and processing and for which it is possible to produce long high quality records for monitoring. No new analysis is included for storms (see the methodology section that follows for background). For seasonal temperature extremes, an attribution analysis then puts the seasons with highlighted extreme events into context of the recent climate versus a hypothetical climate in the absence of anthropogenic emissions (Christidis

et al, 2011). It is important to note that we carry out our attribution analyses on seasonal mean temperatures over the entire country. Therefore these analyses do not attempt to attribute the changed likelihood of individual extreme events. The relationship between extreme events and the large scale mean temperature is likely to be complex, potentially being influenced by *inter alia* circulation changes, a greater expression of natural internal variability at smaller scales, and local processes and feedbacks. Attribution of individual extreme events is an area of developing science. The work presented here is the foundation of future plans to systematically address the region's present and projected future weather and climate and the associated impacts.

The methodology section that follows provides details of the data shown here and of the scientific analyses underlying the discussions of changes in the mean temperature and in temperature and precipitation extremes. It also explains the methods used to attribute the likelihood of occurrence of seasonal mean temperatures.

Climate overview

With the exception of Alaska which extends beyond the Arctic Circle, the entire USA lies between latitudes 50°N and 25°N. This wide range of latitudes, combined with the USA's inclusion of extensive continental interior, long coastlines and a major mountain chain along its entire western flank, results in a considerable range of climates. Annual mean temperature ranges from -3°C at Fairbanks (65°N, Central Alaska), to around 11°C at Seattle (near western seaboard at 47°N), New York (eastern seaboard at 41°N) and Denver (only 39°N but high on the interior Great Plain) and 24°C at Miami (26°N in Florida). The entire USA is sufficiently distant from the equator for marked seasonality, with contrasting winter and summer temperature seasons, most noticeable in the continental interior and sub-arctic regions. The sea-bound Florida Peninsula has the smallest annual variation in monthly mean temperature of only ±5°C about the annual mean. This contrasts with ±11°C at Denver and ±20°C at Fairbanks.

Over much of the USA there is a general west to east progress of weather systems, so that the Rocky Mountain chain along the western seaboard greatly reduces precipitation to the east across the western Great Plains (e.g. Denver only 390 mm per year). However, this block to westerly winds also allows easier penetration into the Great Plains of cold northerly winds from the Arctic and warm, humid southerly winds from the Gulf of Mexico. The meeting of these contrasting air masses makes the central Great Plains (or "mid-west") the most tornado-prone region in the world, spring being the peak season. The northward penetration of moisture-laden air from the Gulf of Mexico makes a large swath of south-eastern USA one of the wettest regions (Miami 1400 mm and New York 1056 mm per year). The other main zone of high precipitation is the north-western coastal belt, where precipitation-bearing Pacific weather systems meet the mountain barrier, intensifying the precipitation (Seattle 940 mm per year but much more on adjacent mountains where winter snow accumulations are among the highest measured in the world). Towards the south of the USA the westerly winds lose their dominance, especially in summer, as the sub-tropical belt of relatively high pressure is approached. Hence precipitation decreases southwards along the west coast towards California and much of the south-west is desert (e.g. Phoenix, Arizona <200 mm per year).

The high sea temperatures of the Caribbean and Gulf of Mexico trigger tropical storms hurricanes, notably in late summer and early autumn. These threaten, particularly, the Gulf States, but northward-curving decaying storms can also bring torrential rains and strong winds to the entire Atlantic seaboard.

Analysis of long-term features in the mean temperature

CRUTEM3 data (Brohan et al., 2006) have been used to provide an analysis of mean temperatures from 1960 to 2010 over the USA using the median of pairwise slopes method to fit the trend (Sen, 1968; Lanzante, 1996). The methods are fully described in the methodology section. In agreement with increasing global average temperatures (Sánchez-Lugo et al., 2011), there is a spatially consistent signal of warming in mean temperature over the contiguous US (Figure 2), as shown in previous research (Field et al., 2007). Grid boxes in which the 5th to 95th percentiles of the slopes are of the same sign can be more confidently regarded as showing this signal: they are geographically widespread for both summer (June to August) and winter (December to February). Regionally averaged trends (over grid boxes included in the red dashed box in Figure 1) show clear warming trends, greater in winter at 0.27 ^{o}C per decade (5th to 95th percentile of slopes: 0.13 to 0.43 ^{o}C per decade) than in summer at 0.16 ^{o}C per decade (5th to 95th percentile of slopes: 0.10 to 0.22 ^{o}C per decade).

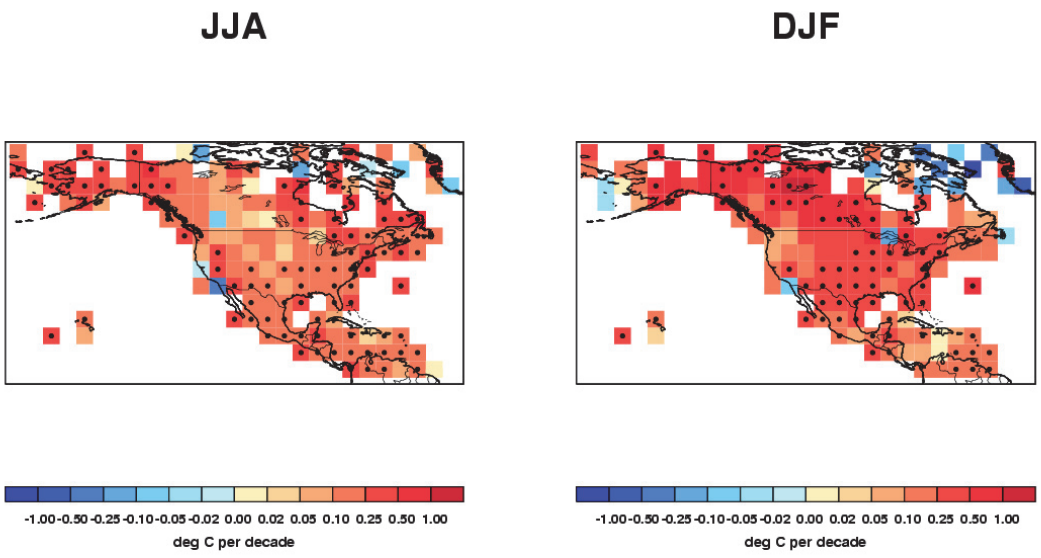

Figure 2. *Decadal trends in seasonally averaged temperatures for the US and surrounding regions over the period 1960 to 2010. Monthly mean anomalies from CRUTEM3 (Brohan et al., 2006) are averaged over each 3 month season (June-July-August – JJA and December-January-February – DJF). Trends are fitted using the median of pairwise slopes method (Sen, 1968; Lanzante, 1996). There is higher confidence in the trends shown if the 5th to 95th percentiles of the pairwise slopes do not encompass zero because here the trend is considered to be significantly different from a zero trend (no change). This is shown by a black dot in the centre of the respective grid box.*

Temperature extremes

Both hot and cold temperature extremes can place many demands on society. While seasonal changes in temperature are normal and indeed important for a number of societal sectors (e.g. tourism, farming etc.), extreme heat or cold can have serious negative impacts. Importantly, what is 'normal' for one region may be extreme for another region that is less well adapted to such temperatures.

Table 1 shows selected extreme events since 2000 that are reported in WMO Statements on Status of the Global Climate and/or BAMS State of the Climate reports. Two events, the cold November-December 2000 and the heat wave in July-August 2006 are highlighted below as examples of extreme temperature events for the USA.

Year	Month	Event	Details	Source
2000	Jul-Sept	Hot/dry	Hot and dry in West and Southwest. Significant wildfire events – 92,000 fires consumed 7.4 million acres nationwide.	BAMS (Lawrimore et al., 2001)
2000	Nov-Dec	Cold	Coldest November/December on record.	BAMS (Lawrimore et al., 2001)
2002	Summer	Heat	Many temperature records broken. Death Valley, California, tied its highest daily mean temperature on record, 45.3°C, in July.	BAMS (Douglas et al., 2003)
2005	Jul	Heat wave	Many daily records were reached in western US	WMO (2006)
2006	Jul - Aug	Heat wave	California and Central USA experienced a heat wave. Over 140 deaths and record wildfire season.	WMO (2007)
2007	Aug	Heat wave	Over 50 deaths attributed to the heat.	WMO (2008)

Table 1: *Selected extreme temperature events reported in WMO Statements on Status of the Global Climate and/or BAMS State of the Climate reports since 2000.*

Recent extreme temperature events

Extreme cold, November-December 2000

In November 2000, cold Arctic air stretching from Canada to the Gulf Coast was associated with a deep trough that had developed over much of the United States. Approximately 50% of the USA experienced very cold November-December temperatures, the coldest such 2-month period on record. A very strong surface pressure ridge extended from the central United States to northern Siberia, and persisted for several weeks, bringing bitterly cold air from northern Siberia which continued to flow into Canada and the central and eastern United States (Lawrimore et al., 2001).This was in marked contrast to the previous ten months which was the warmest January to October period on record (WMO, 2001).

Heat wave, July-August 2006

Many temperature records were broken across the USA as an intense and long-lasting heat wave developed in mid-July in the northern plains and upper Midwest. In the last 2 weeks of July more than 2,300 daily temperature records were broken. July 2006 was the second hottest month in the 112-year record, averaging 25.1°C, and 0.24°C cooler than July 1936. From the West Coast to the central plains many places broke records for the most days above 32.2°C (90°F) and 37.8°C (100°F) (Heim Jr. et al., 2007). Over 140 deaths in California were attributed to the July heat wave (WMO, 2007). The heat wave spread to the East Coast by the first week of August (Heim Jr. et al., 2007).

Analysis of long-term features in moderate temperature extremes

GHCND data (Durre et al., 2010) have been used to update the HadEX extremes analysis for the USA from 1960 to 2010 using daily maximum and minimum temperatures. Here we discuss changes in the frequency of cool days and nights and warm days and nights which are moderate extremes. Cool days/nights are defined as being below the 10^{th} percentile of daily maximum/minimum temperature and warm days/nights are defined as being above the 90^{th} percentile of the daily maximum/minimum temperature. The methods are fully described in the methodology section.

The trend in the number of cool nights clearly shows a decrease across the whole of the contiguous US (Figure 3), especially in the west and southeast. This is also seen, but to a lesser extent, in the trend for the number of warm nights, which shows a clear increase throughout. Recent studies have found that average night-time temperatures have seen a larger rise than daytime. Spring and autumn have experienced a greater warming than summer and winter (Field et al., 2007).

There is lower confidence generally in the trends for the frequency of cool and warm days. Although the central parts of the US appear to show an increase in cool days, there is low confidence in this signal. However the decrease in the number of cool days and the increase in the number of warm days are prominent on the west cost and in the Rocky Mountains. In the far south of Texas there is higher confidence in a decrease in the number of warm days

The time series in Figure 3 show the large annual variability in occurrence of warm nights and days and cool nights and days. For cool and warm days, no clear trend is observed, corroborating the maps, but for cool and warm nights there is higher confidence that the trends are respectively negative and positive.

a)

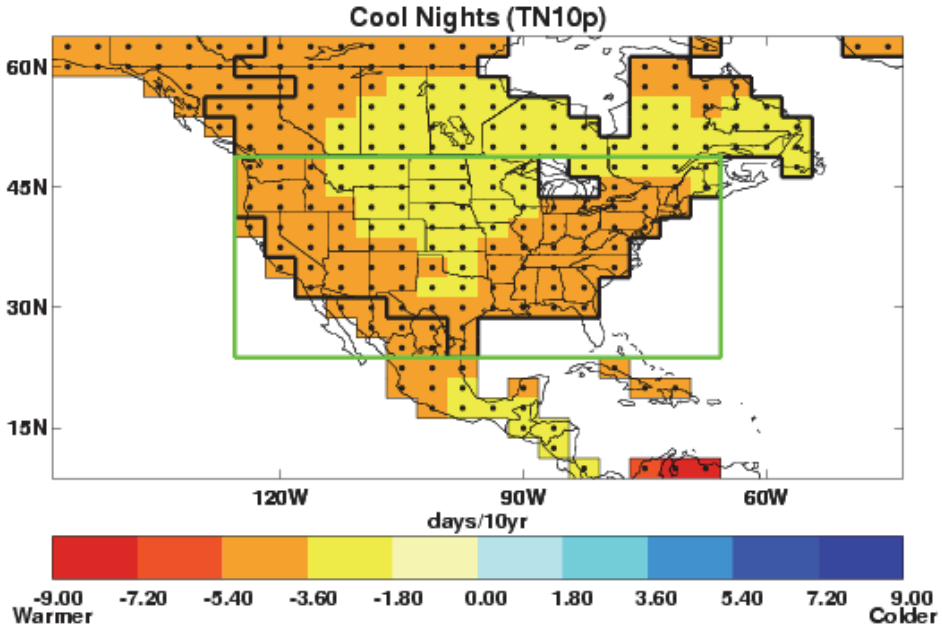

b)

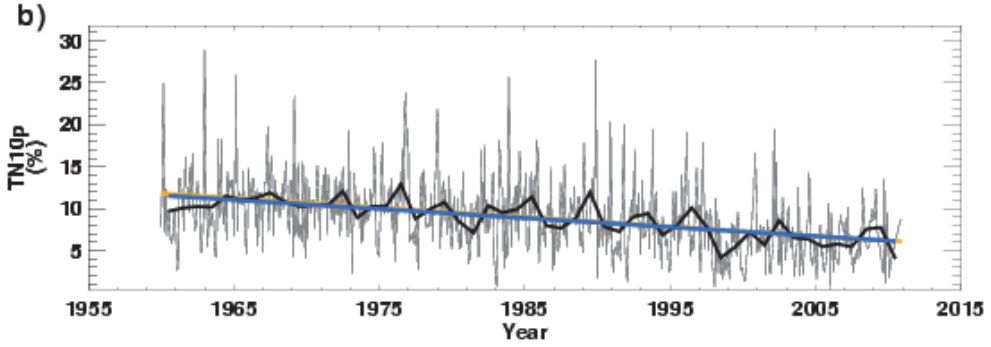

Monthly: -1.13% per decade (-1.35 to -0.92)
Total change of -5.65% from 1960 to 2010 (-6.74% to -4.61%)

Annual: -1.08% per decade (-1.37 to -0.83)
Total change of -5.41% from 1960 to 2010 (-6.84% to -4.13%)

c)

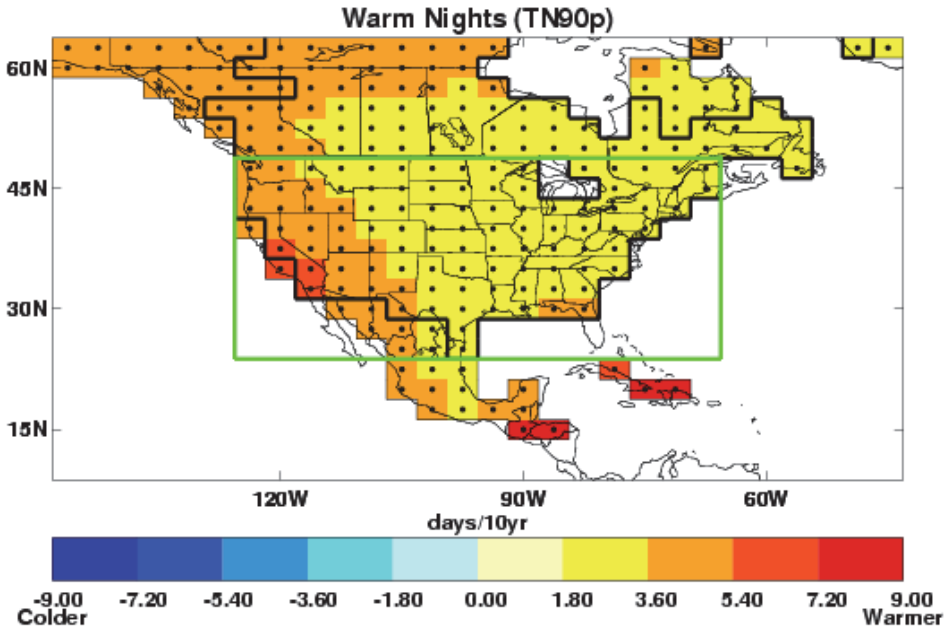

d)

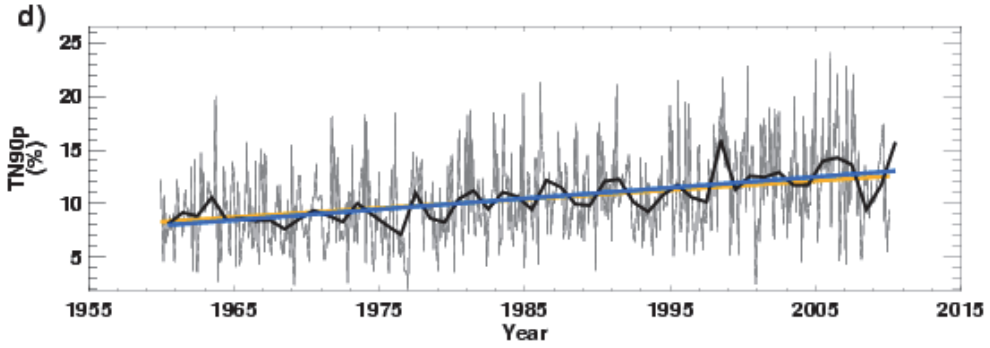

Monthly: 0.86% per decade (0.64 to 1.07)
Total change of 4.28% from 1960 to 2010 (3.22% to 5.36%)

Annual: 1.01% per decade (0.71 to 1.26)
Total change of 5.05% from 1960 to 2010 (3.55% to 6.31%)

e)

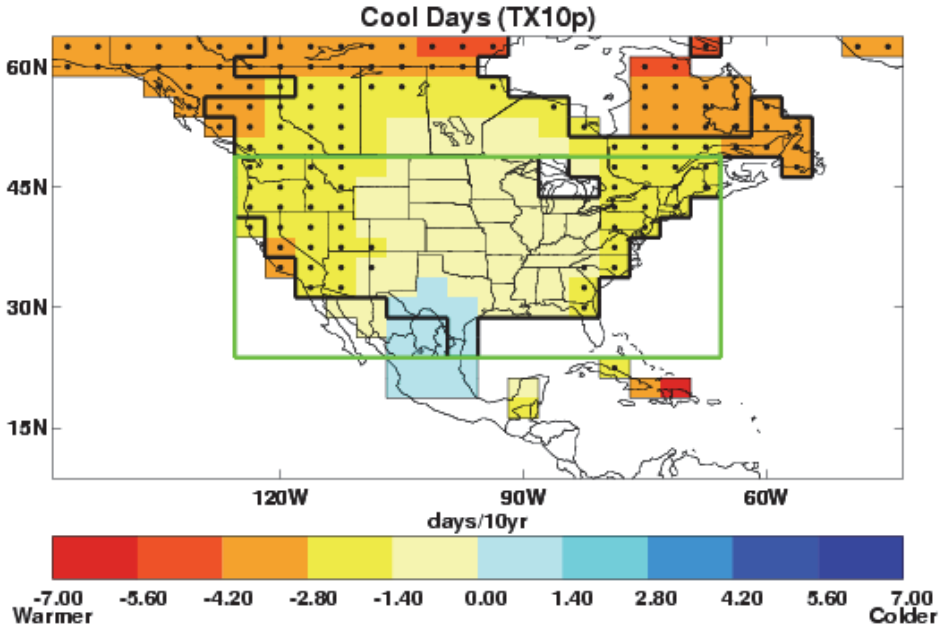

f)

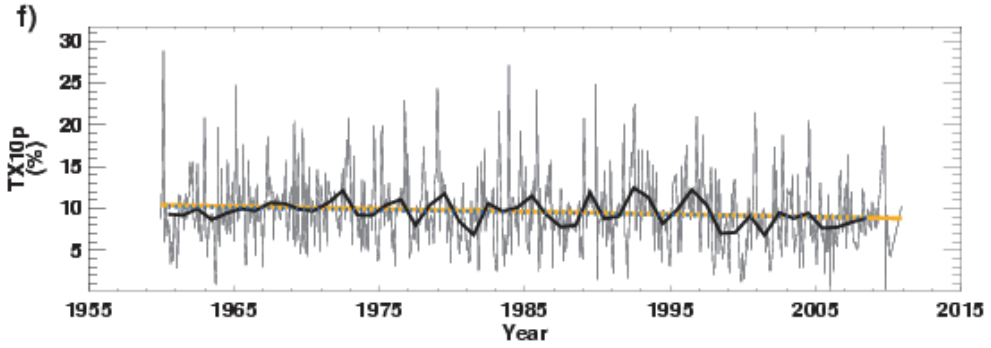

Monthly: -0.31% per decade (-0.53 to -0.09)
Total change of -1.57% from 1960 to 2010 (-2.67% to -0.46%)

Annual: -0.28% per decade (-0.55 to 0.02)
Total change of -1.11% from 1960 to 2008 (-2.21% to 0.07%)

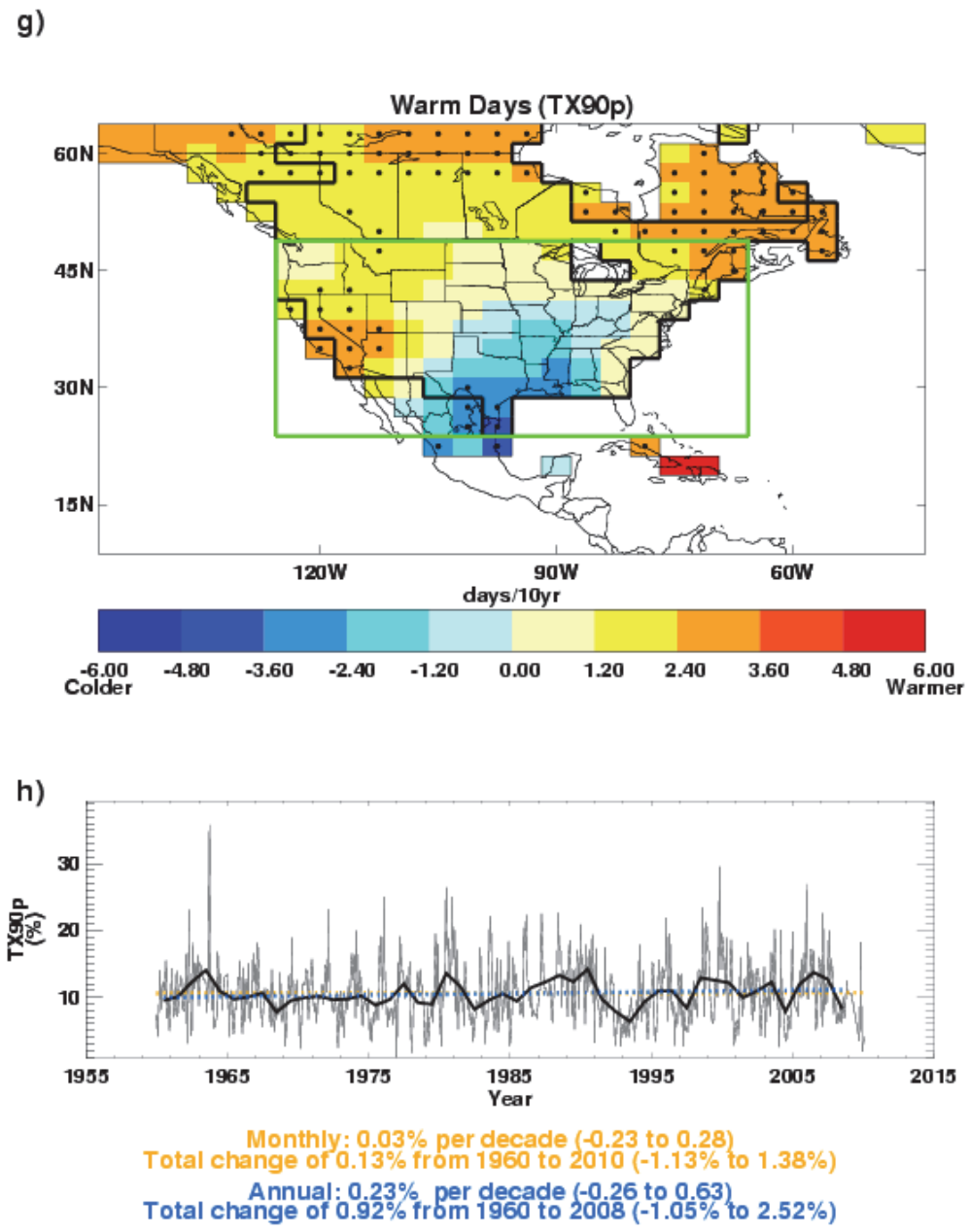

Figure 3. *Change in cool nights (a,b), warm nights (c,d), cool days (e,f) and warm days (g,h) for the US over the period 1960 to 2010 relative to 1961-1990 from the GHCND dataset (Durre et al., 2010). a,c,e,g) Grid box decadal trends. Grid boxes outlined in solid black contain at least 3 stations and so are likely to be more representative of the wider grid box. Trends are fitted using the median of pairwise slopes method (Sen, 1968; Lanzante, 1996). Higher confidence in a long-term trend is shown by a black dot if the 5th to 95th percentile slopes are of the same sign. Differences in spatial coverage occur because each index has its own decorrelation length scale (see methodology section). b,d,f,h) Area averaged annual time series for 125.625° to 65.625° W and 23.75° to 48.75° N as shown by the green box on the map and red box in Figure 1. Thin and thick black lines show the monthly and annual variation respectively. Monthly (orange) and annual (blue) trends are fitted as described above. The decadal trend and its 5th to 95th percentile pairwise slopes are stated along with the change over the period for which there are data available. Higher confidence in the trends, as denoted above, is shown by a solid line as opposed to a dotted one.*

Attribution of changes in likelihood of occurrence of seasonal mean temperatures

Today's climate covers a range of likely extremes. Recent research has shown that the temperature distribution of seasonal means would likely be different in the absence of anthropogenic emissions (Christidis et al., 2011). Here we discuss the seasonal means, within which the highlighted extreme temperature events occur, in the context of recent climate and the influence of anthropogenic emissions on that climate. The methods are fully described in the methodology section.

Winter 2000/01

The distributions of the December-January-February (DJF) mean regional temperature in recent years in the presence and absence of anthropogenic forcings are shown in Figure 4. Analyses with both models suggest that human influences on the climate have shifted the distribution to higher temperatures. Considering the average over the entire region, the 2000/01 winter is cold, as shown in Figure 4, as it lies near the cold tail of the seasonal temperature distribution for the climate influenced by anthropogenic forcings (distributions plotted in red). It is considerably warmer than the winter of 1978/79, the coldest in the CRUTEM3 dataset. In the absence of human influences on the climate (green distributions) the season lies in the central sector of the temperature distribution and would therefore be more common. It should be noted that the attribution results shown here refer to temperature anomalies over the entire region and over an entire season whereas the cold extreme event had a shorter duration; it started in late autumn and affected a smaller region.

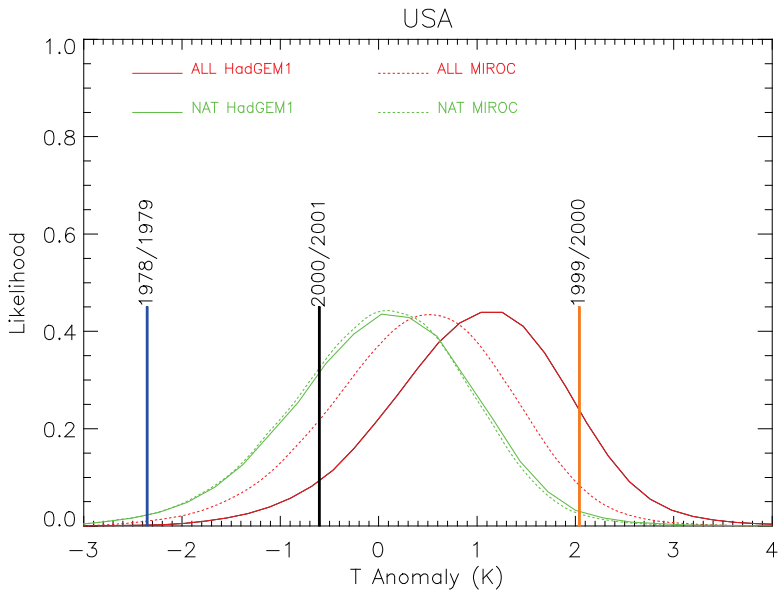

Figure 4. *Distributions of the December-January-February mean temperature anomalies (relative to 1961-1990) averaged over the US region (130-65W, 25-50N – shown in Figure 1) including (red lines) and excluding (green lines) the influence of anthropogenic forcings. The distributions describe the seasonal mean temperatures expected in recent years (2000-2009) and are based on analyses with the HadGEM1 (solid lines) and MIROC (dotted lines) models. The vertical black line marks the observed anomaly in 2000/01 and the vertical orange and blue lines correspond to the maximum and minimum anomaly in the CRUTEM3 dataset since 1900 respectively.*

Summer 2006

The distribution of the June-July-August (JJA) mean regional temperature in recent years in the presence and absence of anthropogenic forcings are shown in Figure 5. Analyses with both models suggest that human influences on the climate have shifted the distribution to higher temperatures. Considering the average over the entire region, the 2006 summer is average/warm, as it lies in the central sector and towards the warm tail of the temperature distributions for the climate influenced by anthropogenic forcings (red distributions), and it is also the hottest since 1900 in the CRUTEM3 dataset. The warmest season would be expected to lie further into the warm tails of the distributions plotted in red. Possible reasons why this is not the case could be that the limited number of observations in recent years does not adequately sample the distribution, or that the models have a warm bias in the region. In the absence of human influences on the climate (green distributions), the season would be exceptionally warm, as it lies further into the tail of the distributions plotted in green. It should be noted that the attribution results shown here refer to temperature anomalies over the entire region and over an entire season, whereas the actual extreme event had a shorter duration and affected a smaller region.

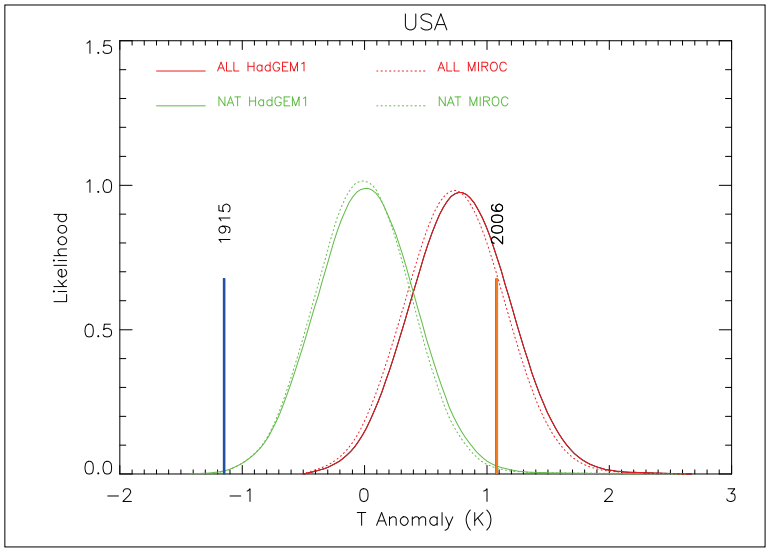

Figure 5. *Distributions of the June-July-August mean temperature anomalies (relative to 1961-1990) averaged over the US region (130-65W, 25-50N – shown in Figure 1) including (red lines) and excluding (green lines) the influence of anthropogenic forcings. The distributions describe the seasonal mean temperatures expected in recent years (2000-2009) and are based on analyses with the HadGEM1 (solid lines) and MIROC (dotted lines) models. The vertical orange and blue lines correspond to the maximum and minimum anomaly in the CRUTEM3 dataset since 1900 respectively.*

Precipitation extremes

Precipitation extremes, either excess or deficit, can be hazardous to human health, societal infrastructure, and livestock and agriculture. While seasonal fluctuations in precipitation are normal and indeed important for a number of societal sectors (e.g. tourism, farming etc.), flooding or drought can have serious negative impacts. These are complex phenomena and often the result of accumulated excesses or deficits or other compounding factors such as spring snow-melt, high tides/storm surges or changes in land use. The analysis section below deals purely with precipitation amounts.

Table 2 shows selected extreme events since 2000 that are reported in WMO Statements on Status of the Global Climate and/or BAMS State of the Climate reports. Two events, the September drought of 2007 and floods during June 2008 are highlighted below as examples of extreme precipitation events for the USA.

Year	Month	Event	Details	Source
1998-2000	May '98-Dec '00	Drought	Long-term drought persists. By August 2000, 36% of USA in severe/extreme drought.	WMO (2001); BAMS (Lawrimore et al., 2001)
2000	Nov	Rainfall	Record rainfall in early November. Hilo International Airport recorded highest 24-hour total of 27.24 inches.	BAMS (Lawrimore et al., 2001)
2002	Jul	Drought	Ongoing drought peaked to 39% of USA land area.	BAMS (Douglas et al., 2003)
2005	Dec-Feb	Drought	Severe winter drought in NW USA	WMO (2006)
2005	Jun-Aug	Drought	Severe summer drought extends into central US.	WMO (2006)
2005	Oct	Flooding	Record wet October (Northeast USA)	WMO (2006)
2006	Feb	Snow	Record snowfall in New York	WMO (2007)
2006	Jun-Aug	Wet	Wettest summer on record in New Hampshire, New York and Rhode Island.	BAMS (Heim Jr. et al., 2007)
2006	Oct	Snow	Record snowfall in Buffalo	WMO (2007)
2006	Nov	Flooding	Heavy rain and flooding in North West.	WMO (2007)
2007		Drought	Persistent severe to exceptional drought	WMO (2008)
2008	Jun	Flooding	Flooding across Midwest - worst floods since 1993	WMO (2009)
2008	Jul	Drought	Most of south-eastern US classed as in moderate to exceptional drought.	WMO (2009)
2008	Sept	Storms	Hurricane Ike. Third most destructive hurricane in US history. Maximum winds of 230 km/hour.	WMO (2009)
2009	Mar/Oct	Flooding	March saw record flooding on Red River in the northern plains region. For the USA as a whole it was the wettest October for 115 years.	WMO (2010)
2010	Dec-Feb	Snow	Heavy snowfall in eastern cities. Washington D.C. had a record total amount for the season.	WMO (2011)

***Table 2**: Selected extreme precipitation events reported in WMO Statements on Status of the Global Climate and/or BAMS State of the Climate reports since 2000.*

Recent extreme precipitation events

Drought, 2007

Approximately 43% of the United States was classed as being in moderate to extreme drought by the end of September 2007, with many areas experiencing record drought conditions. One of the major impacts of the drought was on the energy industry. Drought in the southeast lowered rivers in Alabama to the point where there was insufficient stream flow to meet the demand of industry, agriculture, municipalities, and natural evaporation. Alabama Power, the state's largest utility, was forced to operate some of its coal plants at significantly reduced levels to avoid raising water temperatures in the Coosa, Black Warrior and Mobile rivers, and the Tennessee Valley Authority shut down a nuclear power plant due to inadequate stream flow (NOAA, 2007).

This drought also coincided with heat wave conditions across much of western, southern and eastern North America (see Table 1).

Flooding, June 2008

Significant flooding affected a number of states, including Illinois, Indiana, Michigan, Minnesota, Missouri, and Wisconsin. The flooding arose owing to well above average precipitation from January to May, followed by significant rainfall in a 2-week period in June. Soil moisture levels preceding the flood were high. The atmospheric circulation during the main flood event was typical of other major floods, including the great Midwest floods of 1993 (Stephens et al., 2009).

Major rivers experienced record high flows, and in some locations peak river levels exceeded the 1 in 500 year level. Locally, flash flooding occurred with daily rainfall totals exceeding 127mm. More than 1,100 daily rainfall records were broken during the month (Stephens et al., 2009).

Analysis of long-term features in precipitation from 1960

GHCND data (Durre et al., 2010) have been used to update the HadEX extremes analysis for the USA from 1960 to 2010 for daily precipitation totals. Here we discuss changes in the annual total precipitation, and in the frequency of prolonged (greater than 6 days) wet and dry spells. The methods are fully described in the methodology section.

The trends in annual total precipitation (Figure 6) show an increase on the north eastern seaboard with higher confidence than elsewhere. For the remainder of the country, despite lower confidence in the trends, there nevertheless appears to be an overall increase in precipitation. For the numbers of continuous wet and dry days, there is no clear pattern in the trends and confidence is lower.

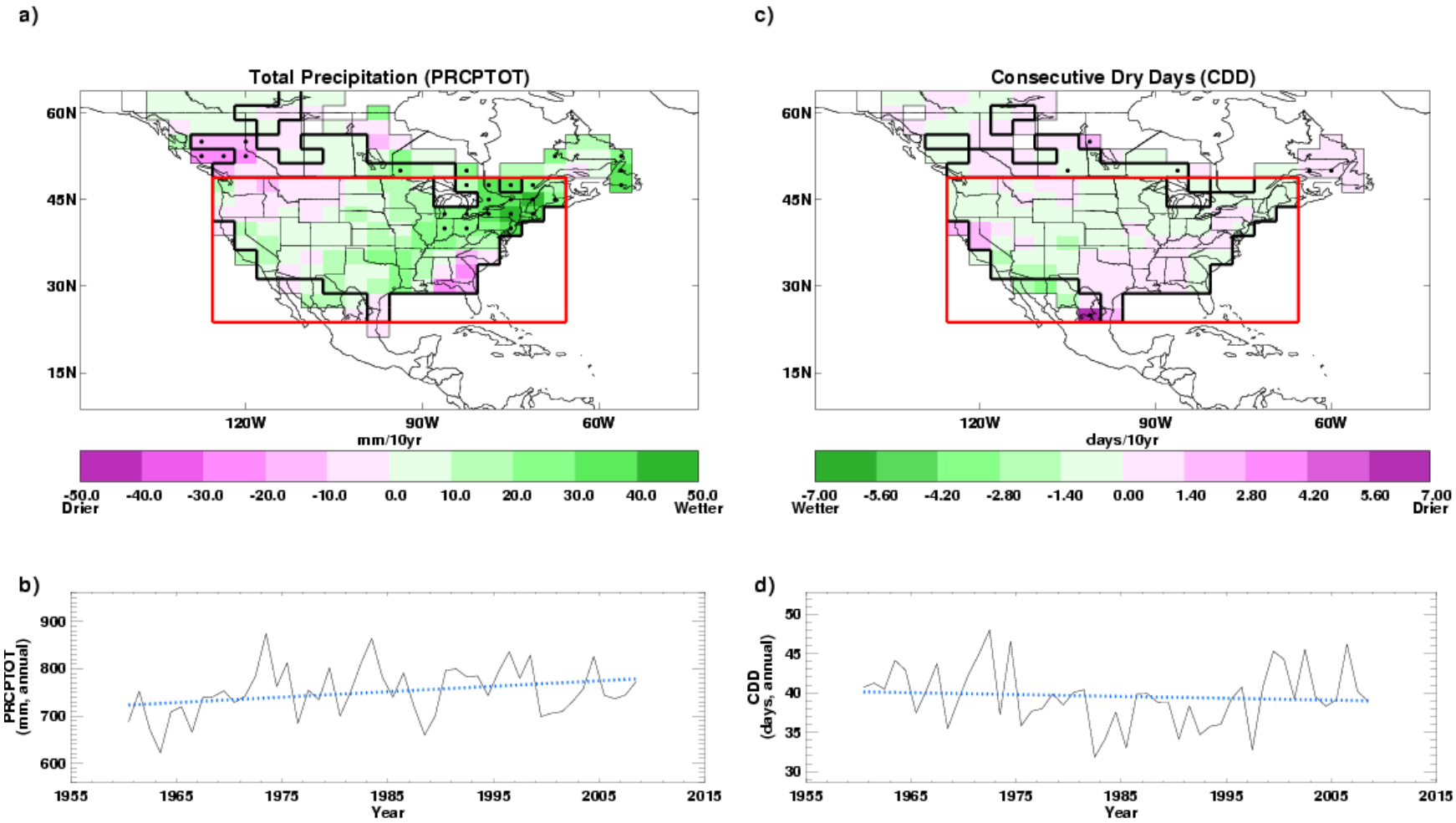

Annual: 11.52mm per decade (-0.56 to 23.03)
Total change of 46.08mm from 1960 to 2008 (-2.22mm to 92.12mm)

Annual: -0.24days per decade (-0.91 to 0.53)
Total change of -0.94days from 1960 to 2008 (-3.64days to 2.12days)

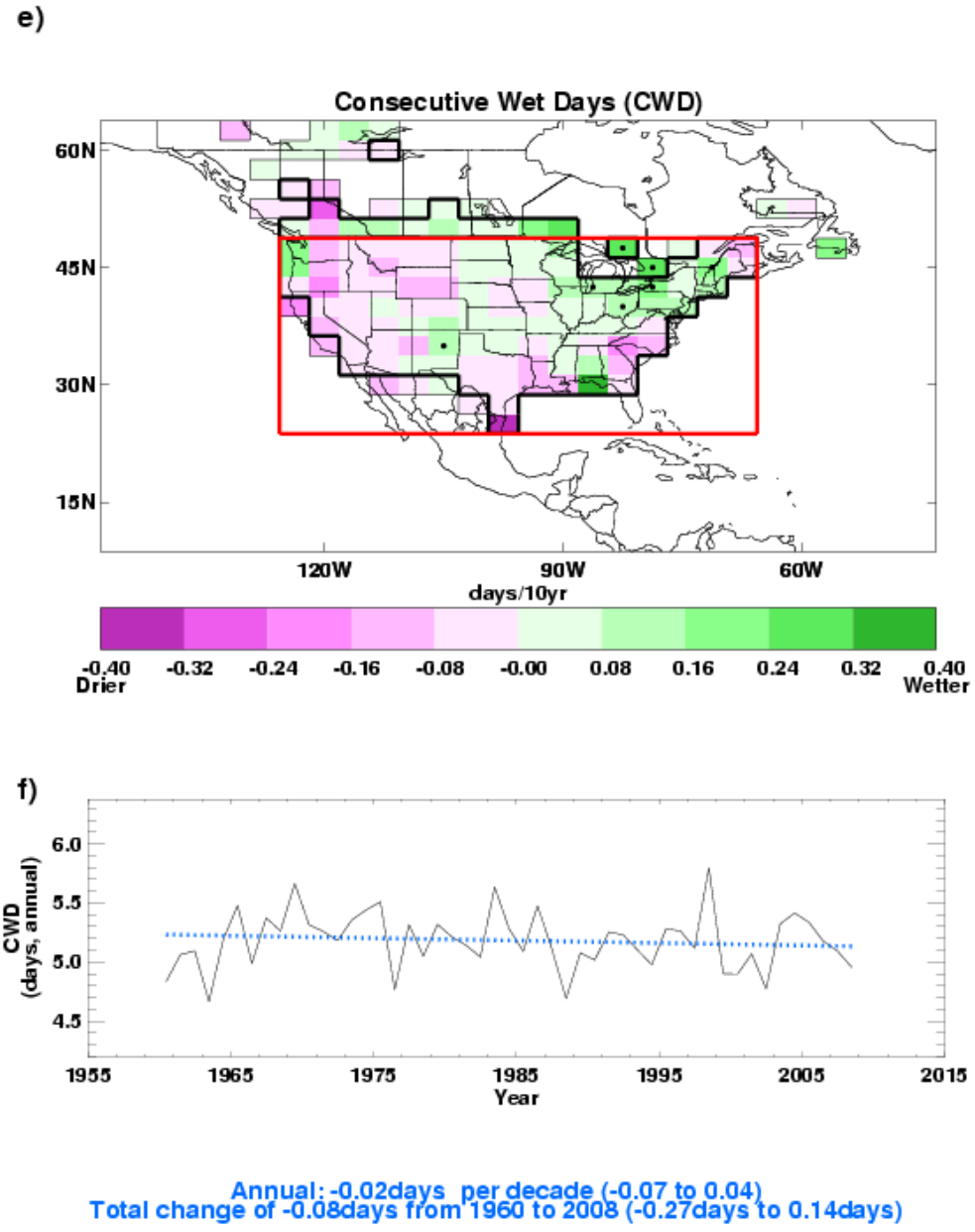

Figure 6. *The change in annual total rainfall (a,b), the annual number of continuous dry days (c,d) and annual number of continuous wet days (e,f) over the period 1960-2010. The maps and time series have been created in exactly the same way as Figure 3. Only annual regional averages are shown in b,d,f).*

The time series of annual total precipitation, also plotted in Figure 6, shows a large amount of annual variability and, although a linear best fit shows an increase, confidence is lower. In Figure 7 we focus on the south east of the US to highlight the drought which occurred there in 2007. The deficit in the total precipitation is clear; 2007 was the driest year since before 1960 in this region.

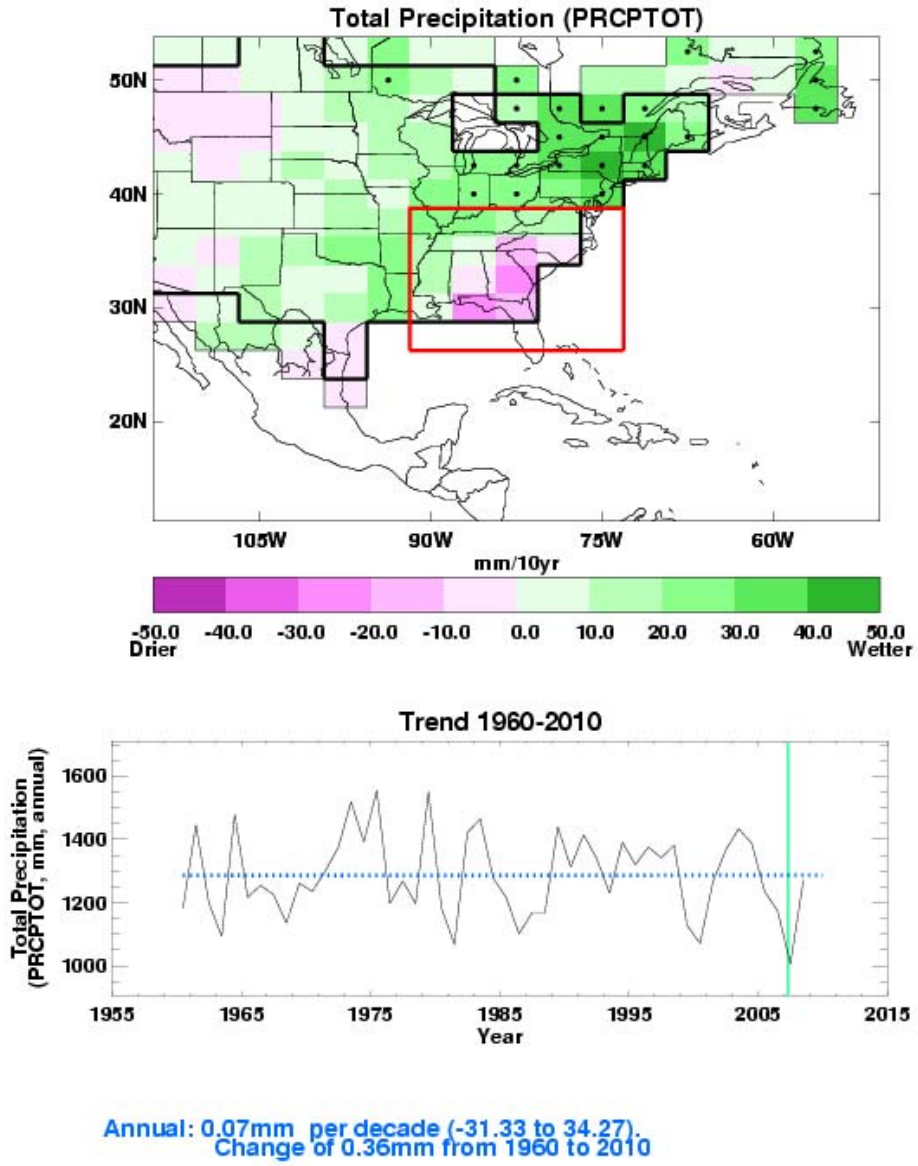

Figure 7. *Change in the annual total rainfall over the period 1960-2009. The map and time series have been created in exactly the same way as Figure 6. The green vertical line shows the drought of 2007.*

Storms

Storms can be very hazardous to all sectors of society. They can be small with localised impacts or spread across multiple states. There is no systematic observational analysis included for storms because, despite recent progress (Peterson et al., 2011; Cornes & Jones, 2011), wind data are not yet adequate for worldwide robust analysis (see methodology section). Further progress awaits studies of the more reliable barometric pressure data through the new 20th Century Reanalysis (Compo et al., 2011) and its planned successors.

Table 3 shows selected extreme events since 2000 that are reported in WMO Statements on Status of the Global Climate and/or BAMS State of the Climate reports. Hurricane Katrina in 2005 is highlighted below as an example of a storm event for the USA.

Year	Month	Event	Details	Source
2003		Storms	Very active storm season with 16 named storms. Hurricane Juan the worst hurricane to hit Halifax in modern history.	WMO (2004)
2005	Jan	Storm	Major winter storm - snowiest month on record for Boston	WMO (2006)
2005		Storms	Record number of named storms – 27 in total.	WMO (2006)
2005	Aug	Storm	Hurricane Katrina	WMO (2006)
2006	Dec	Storm	Storm along the Pacific northwest brought strong winds, heavy rainfall. Hurricane force gusts caused power outages in Washington and Oregon.	BAMS (Heim Jr. et al., 2007)
2007	Feb/Mar	Storm	Winter storm in North East. 300,000 people affected.	WMO (2008)
2008	Feb	Storm	Tornado outbreak in the southern US. 2192 recorded. 123 fatalities.	WMO (2009)
2008	Sept	Storms	Hurricane Ike. Third most destructive hurricane in US history. Maximum winds of 230 km/hour.	WMO (2009)

Table 3-

Recent storm events

Hurricane Katrina, August 2005

Hurricane Katrina was one of the worst natural disasters to hit the USA. It resulted in over 1,800 deaths, mainly in the southern states of Louisiana and Mississippi (Graumann et al., 2006). It was, according to Munich Re, the costliest storm on record (Shein, 2006).

Katrina formed over the Bahamas on August 23, 2005 and crossed southern Florida as a moderate Category 1 hurricane, causing some deaths and flooding there before strengthening rapidly in the Gulf of Mexico. The storm weakened before making its second landfall as a Category 3 storm in southeast Louisiana. It was one of the strongest storms to hit the USA, with sustained winds of 127 mph at landfall, equivalent to a Category 3 storm on the Saffir-Simpson scale. It had a minimum central pressure of 928 mb, the third lowest recorded (Graumann et al., 2006). The storm surge associated with the hurricane reached as high as 28 feet along the Mississippi coast, and penetrated six miles inland in many portions, and as much as 12 miles along bays and rivers. New Orleans suffered particularly badly from the hurricane, with many fatalities as defensive levees were breeched owing to the massive storm surge. Eighty percent of the city was flooded to depths of up to 20 feet in places (Graumann et al., 2006; Knabb et al., 2006).

Summary

The main features seen in observed climate over USA in this analysis are:

- There has been a widespread warming trend over the country since 1960.
- There has been a widespread reduction in the number of cool nights across the whole of the contiguous US (Figure 2), with stronger decreases observed towards the coasts. There has also been a widespread increase in the number of warm nights.
- There has been a general increase in summer and winter temperatures averaged over the country as a result of human influence on climate, making the occurrence of warm summer and winter temperatures more frequent and cold summer and winter temperatures less frequent.
- Since 1960 there has been a positive trend in precipitation on the north eastern seaboard but for the remainder of the country, there is no significant trend.

Methodology annex

Recent, notable extremes

In order to identify what is meant by ‘recent’ events the authors have used the period since 1994, when WMO Status of the Global Climate statements were available to the authors. However, where possible, the most notable events during the last 10 years have been chosen as these are most widely reported in the media, remain closest to the forefront of the memory of the country affected, and provide an example likely to be most relevant to today’s society. By ‘notable’ the authors mean any event which has had significant impact either in terms of cost to the economy, loss of life, or displacement and long term impact on the population. In most cases the events of largest impact on the population have been chosen, however this is not always the case.

Tables of recent, notable extreme events have been provided for each country. These have been compiled using data from the World Meteorological Organisation (WMO) Annual Statements on the Status of the Global Climate. This is a yearly report which includes contributions from all the member countries, and therefore represents a global overview of events that have had importance on a national scale. The report does not claim to capture all events of significance, and consistency across the years of records available is variable. However, this database provides a concise yet broad account of extreme events per country. This data is then supplemented with accounts from the monthly National Oceanic and Atmospheric Administration (NOAA) State of the Climate reports which outline global extreme events of meteorological significance.

We give detailed examples of heat, precipitation and storm extremes for each country where these have had significant impact. Where a country is primarily affected by precipitation or heat extremes this is where our focus has remained. An account of the impact on human life, property and the economy has been given, based largely on media reporting of events, and official reports from aid agencies, governments and meteorological organisations. Some data has also been acquired from the Centre for Research on Epidemiological Disasters (CRED) database on global extreme events. Although media reports are unlikely to be completely accurate, they do give an indication as to the perceived impact of an extreme event, and so are useful in highlighting the events which remain in the national psyche.

Our search for data has not been exhaustive given the number of countries and events included. Although there are a wide variety of sources available, for many events, an official account is not available. Therefore figures given are illustrative of the magnitude of impact only (references are included for further information on sources). It is also apparent that the reporting of extreme events varies widely by region, and we have, where possible, engaged with local scientists to better understand the impact of such events.

The aim of the narrative for each country is to provide a picture of the social and economic vulnerability to the current climate. Examples given may illustrate the impact that any given extreme event may have and the recovery of a country from such an event. This will be important when considering the current trends in climate extremes, and also when examining projected trends in climate over the next century.

Observational record

In this section we outline the data sources which were incorporated into the analysis, the quality control procedure used, and the choices made in the data presentation. As this report is global in scope, including 23 countries, it is important to maintain consistency of methodological approach across the board. For this reason, although detailed datasets of extreme temperatures, precipitation and storm events exist for various countries, it was not possible to obtain and incorporate such a varied mix of data within the timeframe of this project. Attempts were made to obtain regional daily temperature and precipitation data from known contacts within various countries with which to update existing global extremes databases. No analysis of changes in storminess is included as there is no robust historical analysis of global land surface winds or storminess currently available.

Analysis of seasonal mean temperature

Mean temperatures analysed are obtained from the CRUTEM3 global land-based surface-temperature data-product (Brohan et al., 2006), jointly created by the Met Office Hadley Centre and Climatic Research Unit at the University of East Anglia. CRUTEM3 comprises of more than 4000 weather station records from around the world. These have been averaged together to create 5° by 5° gridded fields with no interpolation over grid boxes that do not contain stations. Seasonal averages were calculated for each grid box for the 1960 to 2010 period and linear trends fitted using the median of pairwise slopes (Sen 1968; Lanzante 1996). This method finds the slopes for all possible pairs of points in the data, and takes

their median. This is a robust estimator of the slope which is not sensitive to outlying points. High confidence is assigned to any trend value for which the 5^{th} to 95^{th} percentiles of the pairwise slopes are of the same sign as the trend value and thus inconsistent with a zero trend.

Analysis of temperature and precipitation extremes using indices

In order to study extremes of climate a number of indices have been created to highlight different aspects of severe weather. The set of indices used are those from the World Climate Research Programme (WCRP) Climate Variability and Predictability (CLIVAR) Expert Team on Climate Change Detection and Indices (ETCCDI). These 27 indices use daily rainfall and maximum and minimum temperature data to find the annual (and for a subset of the indices, monthly) values for, e.g., the 'warm' days where daily maximum temperature exceeds the 90^{th} percentile maximum temperature as defined over a 1961 to 1990 base period. For a full list of the indices we refer to the website of the ETCCDI (http://cccma.seos.uvic.ca/ETCCDI/index.shtml).

Index	Description	Shortname	Notes
Cool night frequency	Daily minimum temperatures lower than the 10th percentile daily minimum temperature using the base reference period 1961-1990	TN10p	---
Warm night frequency	Daily minimum temperatures higher than the 90th percentile daily minimum temperature using the base reference period 1961-1990	TN90p	---
Cool day frequency	Daily maximum temperatures lower than the 10th percentile daily maximum temperature using the base reference period 1961-1990	TX10p	---
Warm day frequency	Daily maximum temperatures higher than the 90th percentile daily maximum temperature using the base reference period 1961-1990	TX90p	---
Dry spell duration	Maximum duration of continuous days within a year with rainfall <1mm	CDD	Lower data coverage due to the requirement for a 'dry spell' to be at least 6 days long resulting in intermittent temporal coverage
Wet spell duration	Maximum duration of continuous days with rainfall >1mm for a given year	CWD	Lower data coverage due to the requirement for a 'wet spell' to be at least 6 days long resulting in intermittent temporal coverage
Total annual precipitation	Total rainfall per year	PRCPTOT	---

Table 4. *Description of ETCCDI indices used in this document.*

A previous global study of the change in these indices, containing data from 1951-2003 can be found in Alexander et al. 2006, (HadEX; see http://www.metoffice.gov.uk/hadobs/hadex/). In this work we aimed to update this analysis to the present day where possible, using the most recently available data. A subset of the indices is used here because they are most easily related to extreme climate events (Table 4).

Use of HadEX for analysis of extremes

The HadEX dataset comprises all 27 ETCCDI indices calculated from station data and then smoothed and gridded onto a 2.5° x 3.75° grid, chosen to match the output from the Hadley Centre suite of climate models. To update the dataset to the present day, indices are calculated from the individual station data using the RClimDex/FClimDex software;

developed and maintained on behalf of the ETCCDI by the Climate Research Branch of the Meteorological Service of Canada. Given the timeframe of this project it was not possible to obtain sufficient station data to create updated HadEX indices to present day for a number of countries: Brazil; Egypt; Indonesia; Japan (precipitation only); South Africa; Saudi Arabia; Peru; Turkey; and Kenya. Indices from the original HadEX data-product are used here to show changes in extremes of temperature and precipitation from 1960 to 2003. In some cases the data end prior to 2003. Table 5 summarises the data used for each country. Below, we give a short summary of the methods used to create the HadEX dataset (for a full description see Alexander et al*.,* 2006).

To account for the uneven spatial coverage when creating the HadEX dataset, the indices for each station were gridded, and a land-sea mask from the HadCM3 model applied. The interpolation method used in the gridding process uses a decorrelation length scale (DLS) to determine which stations can influence the value of a given grid box. This DLS is calculated from the e-folding distance of the individual station correlations. The DLS is calculated separately for five latitude bands, and then linearly interpolated between the bands. There is a noticeable difference in spatial coverage between the indices due to these differences in decorrelation length scales. This means that there will be some grid-box data where in fact there are no stations underlying it. Here we apply black borders to grid-boxes where at least 3 stations are present to denote greater confidence in representation of the wider grid-box area there. The land-sea mask enables the dataset to be used directly for model comparison with output from HadCM3. It does mean, however, that some coastal regions and islands over which one may expect to find a grid-box are in fact empty because they have been treated as sea

Data sources used for updates to the HadEX analysis of extremes

We use a number of different data sources to provide sufficient coverage to update as many countries as possible to present day. These are summarised in Table 2. In building the new datasets we have tried to use exactly the same methodology as was used to create the original HadEX to retain consistency with a product that was created through substantial international effort and widely used, but there are some differences, which are described in the next section.

Wherever new data have been used, the geographical distributions of the trends were compared to those obtained from HadEX, using the same grid size, time span and fitting method. If the pattern of the trends in the temperature or precipitation indices did not match that from HadEX, we used the HadEX data despite its generally shorter time span.

Differences in the patterns of the trends in the indices can arise because the individual stations used to create the gridded results are different from those in HadEX, and the quality control procedures used are also very likely to be different. Countries where we decided to use HadEX data despite the existence of more recent data are Egypt and Turkey.

GHCND:

The Global Historical Climate Network Daily data has near-global coverage. However, to ensure consistency with the HadEX database, the GHCND stations were compared to those stations in HadEX. We selected those stations which are within 1500m of the stations used in the HadEX database and have a high correlation with the HadEX stations. We only took the precipitation data if its r>0.9 and the temperature data if one of its r-values >0.9. In addition, we required at least 5 years of data beyond 2000. These daily data were then converted to the indices using the *fclimdex* software.

ECA&D and SACA&D:

The European Climate Assessment and Dataset and the Southeast Asian Climate Assessment and Dataset data are pre-calculated indices comprising the core 27 indices from the ETCCDI as well as some extra ones. We kindly acknowledge the help of Albert Klein Tank, the KNMI[1] and the BMKG[2] for their assistance in obtaining these data.

Mexico:

The station data from Mexico has been kindly supplied by the SMN[3] and Jorge Vazquez. These daily data were then converted to the required indices using the *Fclimdex* software. There are a total of 5298 Mexican stations in the database. In order to select those which have sufficiently long data records and are likely to be the most reliable ones we performed a cross correlation between all stations. We selected those which had at least 20 years of data post 1960 and have a correlation with at least one other station with an *r*-value >0.95. This resulted in 237 stations being selected for further processing and analysis.

Indian Gridded:

The India Meteorological Department provided daily gridded data (precipitation 1951-2007, temperature 1969-2009) on a 1° x 1° grid. These are the only gridded daily data in our

[1] Koninklijk Nederlands Meteorologisch Instituut – The Royal Netherlands Meteorological Institute

[2] Badan Meteorologi, Klimatologi dan Geofisika – The Indonesian Meteorological, Climatological and Geophysical Agency

[3] Servicio Meteorológico Nacional de México – The Mexican National Meteorological Service

analysis. In order to process these in as similar a way as possible the values for each grid were assumed to be analogous to a station located at the centre of the grid. We keep these data separate from the rest of the study, which is particularly important when calculating the decorrelation length scale, which is on the whole larger for these gridded data.

Country	**Region box** (red dashed boxes in Fig. 1 and on each map at beginning of chapter)	**Data source** (T = temperature, P = precipitation)	**Period of data coverage** (T = temperature, P = precipitation)	**Indices included** (see Table 4 for details)	**Temporal resolution available**	**Notes**
Argentina	73.125 to 54.375 ^{o} W, 21.25 to 56.25 ^{o} S	Matilde Rusticucci (T,P)	1960-2010 (T,P)	TN10p, TN90p, TX10p, TX90p, PRCPTOT, CDD, CWD	annual	
Australia	114.375 to 155.625 ^{o} E, 11.25 to 43.75 ^{o} S	GHCND (T,P)	1960-2010 (T,P)	TN10p, TN90p, TX10p, TX90p, PRCPTOT, CDD, CWD	monthly, seasonal and annual	Land-sea mask has been adapted to include Tasmania and the area around Brisbane
Bangladesh	88.125 to 91.875 ^{o} E, 21.25 to 26.25 ^{o} N	Indian Gridded data (T,P)	1960-2007 (P), 1970-2009 (T)	TN10p, TN90p, TX10p, TX90p, PRCPTOT, CDD, CWD	monthly, seasonal and annual	Interpolated from Indian Gridded data
Brazil	73.125 to 31.875 ^{o} W, 6.25 ^{o} N to 33.75 ^{o} S	HadEX (T,P)	1960-2000 (P) 2002 (T)	TN10p, TN90p, TX10p, TX90p, PRCPTOT, CDD, CWD	annual	Spatial coverage is poor
China	73.125 to 133.125 ^{o} E, 21.25 to 53.75 ^{o} N	GHCND (T,P)	1960-1997 (P) 1960-2003 (T_{min}) 1960-2010 (T_{max})	TN10p, TN90p, TX10p, TX90p, PRCPTOT, CDD, CWD	monthly, seasonal and annual	Precipitation has very poor coverage beyond 1997 except in 2003-04, and no data at all in 2000-02, 2005-11
Egypt	24.375 to 35.625 ^{o} E, 21.25 to 31.25 ^{o} N	HadEX (T,P)	No data	TN10p, TN90p, TX10p, TX90p, PRCPTOT,	annual	There are no data for Egypt so all grid-box values have been interpolated from stations in Jordan, Israel, Libya and Sudan
France	5.625 ^{o} W to 9.375 ^{o} E, 41.25 to 51.25 ^{o} N	ECA&D (T,P)	1960-2010 (T,P)	TN10p, TN90p, TX10p, TX90p, PRCPTOT, CDD, CWD	monthly, seasonal and annual	

Germany	5.625 to 16.875 ^{o} E, 46.25 to 56.25 ^{o} N	ECA&D (T,P)	1960-2010 (T,P)	TN10p, TN90p, TX10p, TX90p, PRCPTOT, CDD, CWD	monthly, seasonal and annual	
India	69.375 to 99.375 ^{o} E, 6.25 to 36.25 ^{o} N	Indian Gridded data (T,P)	1960-2003 (P), 1970-2009 (T)	TN10p, TN90p, TX10p, TX90p, PRCPTOT, CDD, CWD	monthly, seasonal and annual	
Indonesia	95.625 to 140.625 ^{o} E, 6.25 ^{o} N to 11.25 ^{o} S	HadEX (T,P)	1968-2003 (T,P)	TN10p, TN90p, TX10p, TX90p, PRCPTOT,	annual	Spatial coverage is poor
Italy	5.625 to 16.875 ^{o} E, 36.25 to 46.25 ^{o} N	ECA&D (T,P)	1960-2010 (T,P)	TN10p, TN90p, TX10p, TX90p, PRCPTOT, CDD, CWD	monthly, seasonal and annual	Land-sea mask has been adapted to improve coverage of Italy
Japan	129.375 to 144.375 ^{o} E, 31.25 to 46.25 ^{o} N	HadEX (P) GHCND (T)	1960-2003 (P) 1960-2000 (T_{min}) 1960-2010 (T_{max})	TN10p, TN90p, TX10p, TX90p, PRCPTOT,	monthly, seasonal and annual (T), annual (P)	
Kenya	31.875 to 43.125 ^{o} E, 6.25 ^{o} N to 6.25 ^{o} S	HadEX (T,P)	1960-1999 (P)	TN10p, TN90p, TX10p, TX90p, PRCPTOT	annual	There are no temperature data for Kenya and so grid-box values have been interpolated from neighbouring Uganda and the United Republic of Tanzania. Regional averages include grid-boxes from outside Kenya that enable continuation to 2003
Mexico	118.125 to 88.125 ^{o} W, 13.75 to 33.75 ^{o} N	Raw station data from the Servicio Meteorológico Nacional (SMN) (T,P)	1960-2009 (T,P)	TN10p, TN90p, TX10p, TX90p, PRCPTOT, CDD, CWD	monthly, seasonal and annual	237/5298 stations selected. Non uniform spatial coverage. Drop in T and P coverage in 2009.
Peru	84.735 to 65.625 ^{o} W, 1.25 ^{o} N to 18.75 ^{o} S	HadEX (T,P)	1960-2002 (T,P)	TN10p, TN90p, TX10p, TX90p, PRCPTOT, CDD, CWD	annual	Intermittent coverage in TX90p, CDD and CWD

Russia	West Russia 28.125 to 106.875 ° E, 43.75 to 78.75 ° N, East Russia 103.125 to 189.375 ° E, 43.75 to 78.75 ° N	ECA&D (T,P)	1960-2010 (T,P)	TN10p, TN90p, TX10p, TX90p, PRCPTOT, CDD, CWD	monthly, seasonal and annual	Country split for presentation purposes only.
Saudi Arabia	31.875 to 54.375 ° E, 16.25 to 33.75 ° N	HadEX (T,P)	1960-2000 (T,P)	TN10p, TN90p, TX10p, TX90p, PRCPTOT	annual	Spatial coverage is poor
South Africa	13.125 to 35.625 ° W, 21.25 to 36.25 ° S	HadEX (T,P)	1960-2000 (T,P)	TN10p, TN90p, TX10p, TX90p, PRCPTOT, CDD, CWD	annual	---
Republic of Korea	125.625 to 129.375 ° E, 33.75 to 38.75 ° N	HadEX (T,P)	1960-2003 (T,P)	TN10p, TN90p, TX10p, TX90p, PRCPTOT, CDD	annual	There are too few data points for CWD to calculate trends or regional timeseries
Spain	9.375 ° W to 1.875 ° E, 36.25 to 43.75 ° N	ECA&D (T,P)	1960-2010 (T,P)	TN10p, TN90p, TX10p, TX90p, PRCPTOT, CDD, CWD	monthly, seasonal and annual	
Turkey	24.375 to 46.875 ° E, 36.25 to 43.75 ° N	HadEX (T,P)	1960-2003 (T,P)	TN10p, TN90p, TX10p, TX90p, PRCPTOT, CDD, CWD	annual	Intermittent coverage in CWD and CDD with no regional average beyond 2000
United Kingdom	9.375 ° W to 1.875 ° E, 51.25 to 58.75 ° N	ECA&D (T,P)	1960-2010 (T,P)	TN10p, TN90p, TX10p, TX90p, PRCPTOT, CDD, CWD	monthly, seasonal and annual	
United States of America	125.625 to 65.625 ° W, 23.75 to 48.75 ° N	GHCND (T,P)	1960-2010 (T,P)	TN10p, TN90p, TX10p, TX90p, PRCPTOT, CDD, CWD	monthly, seasonal and annual	

Table 5. *Summary of data used for each country*

Quality control and gridding procedure used for updates to the HadEX analysis of extremes

In order to perform some basic quality control checks on the index data, we used a two-step process on the indices. Firstly, internal checks were carried out, to remove cases where the 5 day rainfall value is less than the 1 day rainfall value, the minimum T_min is greater than the minimum T_max and the maximum T_min is greater than the maximum T_max. Although these are physically impossible, they could arise from transcription errors when creating the daily dataset, for example, a misplaced minus sign, an extra digit appearing in the record or a column transposition during digitisation. During these tests we also require that there are at least 20 years of data in the period of record for the index for that station, and that some data is found in each decade between 1961 and 1990, to allow a reasonable estimation of the climatology over that period.

Weather conditions are often similar over many tens of kilometres and the indices calculated in this work are even more coherent. The correlation coefficient between each station-pair combination in all the data obtained is calculated for each index (and month where appropriate), and plotted as a function of the separation. An exponential decay curve is fitted to the data, and the distance at which this curve has fallen by a factor $1/e$ is taken as the decorrelation length scale (DLS). A DLS is calculated for each dataset separately. For the GHCND, a separate DLS is calculated for each hemisphere. We do not force the fitted decay curve to show perfect correlation at zero distance, which is different to the method employed when creating HadEX. For some of the indices in some countries, no clear decay pattern was observed in some data sets or the decay was so slow that no value for the DLS could be determined. In these cases a default value of 200km was used.

We then perform external checks on the index data by comparing the value for each station with that of its neighbours. As the station values are correlated, it is therefore likely that if one station measures a high value for an index for a given month, its neighbours will also be measuring high. We exploit this coherence to find further bad values or stations as follows. Although raw precipitation data shows a high degree of localisation, using indices which have monthly or annual resolution improves the coherence across wider areas and so this neighbour checking technique is a valid method of finding anomalous stations.

We calculate a climatology for each station (and month if appropriate) using the mean value for each index over the period 1961-1990. The values for each station are then anomalised using this climatology by subtracting this mean value from the true values, so that it is clear if the station values are higher or lower than normal. This means that we do not need to take

differences in elevation or topography into account when comparing neighbours, as we are not comparing actual values, but rather deviations from the mean value.

All stations which are within the DLS distance are investigated and their anomalised values noted. We then calculate the weighted median value from these stations to take into account the decay in the correlation with increasing distance. We use the median to reduce the sensitivity to outliers.

If the station value is greater than 7.5 median-absolute-deviations away from the weighted median value (this corresponds to about 5 standard deviations if the distribution is Gaussian, but is a robust measure of the spread of the distribution), then there is low confidence in the veracity of this value and so it is removed from the data.

To present the data, the individual stations are gridded on a 3.75^{o} x 2.5^{o} grid, matching the output from HadCM3. To determine the value of each grid box, the DLS is used to calculate which stations can reasonably contribute to the value. The value of each station is then weighted using the DLS to obtain a final grid box value. At least three stations need to have valid data and be near enough (within 1 DLS of the gridbox centre) to contribute in order for a value to be calculated for the grid point. As for the original HadEX, the HadCM3 land-sea mask is used. However, in three cases the mask has been adjusted as there are data over Tasmania, eastern Australia and Italy that would not be included otherwise (Figure 8).

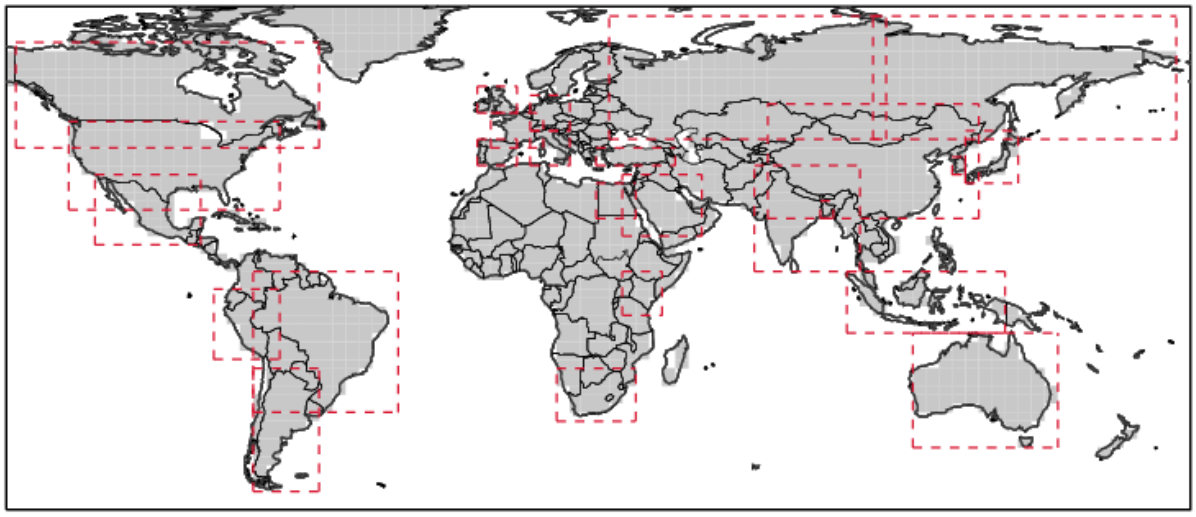

Figure 8. *Land-sea mask used for gridding the station data and regional areas allocated to each country as described in Table 5.*

Presentation of extremes of temperature and precipitation

Indices are displayed as regional gridded maps of decadal trends and regional average time-series with decadal trends where appropriate. Trends are fitted using the median of pairwise slopes method (Sen 1968, Lanzante 1996). Trends are considered to be significantly different from a zero trend if the 5th to 95th percentiles of the pairwise slopes do not encompass zero. This is shown by a black dot in the centre of the grid-box or by a solid line on time-series plots. This infers that there is high confidence in the sign (positive or negative) of the sign. Confidence in the trend magnitude can be inferred by the spread of the 5th to 95th percentiles of the pairwise slopes which is given for the regional average decadal trends. Trends are only calculated when there are data present for at least 50% of years in the period of record and for the updated data (not HadEX) there must be at least one year in each decade.

Due to the practice of data-interpolation during the gridding stage (using the DLS) there are values for some grid boxes when no actually station lies within the grid box. There is more confidence in grid boxes for which there are underlying data. For this reason, we identify those grid boxes which contain at least 3 stations by a black contour line on the maps. The DLS differs with region, season and index which leads to large differences in the spatial coverage. The indices, by their nature of being largely threshold driven, can be intermittent over time which also effects spatial and temporal coverage (see Table 4).

Each index (and each month for the indices for which there is monthly data) has a different DLS, and so the coverage between different indices and datasets can be different. The restrictions on having at least 20 years of data present for each input station, at least 50% of years in the period of record and at least one year in each decade for the trending calculation, combined with the DLS, can restrict the coverage to only those regions with a dense station network reporting reliably.

Each country has a rectangular region assigned as shown by the red dashed box on the map in Figure 1 and listed in Table 2, which is used for the creation of the regional average. This is sometimes identical to the attribution region shown in grey on the map in Figure 1. This region is again shown on the maps accompanying the time series of the regional averages as a reminder of the region and grid boxes used in the calculation. Regional averages are created by weighting grid box values by the cosine of their grid box centre latitude. To ensure consistency over time a regional average is only calculated when there are a sufficient number of grid boxes present. The full-period median number of grid-boxes present is calculated. For regions with a median of more than six grid-boxes there must be at

least 80% of the median number of grid boxes present for any one year to calculate a regional average. For regions with six or fewer median grid boxes this is relaxed to 50%. These limitations ensure that a single station or grid box which has a longer period of record than its neighbours cannot skew the timeseries trend. So sometimes there may be grid-boxes present but no regional average time series. The trends for the regional averages are calculated in the same way as for the individual grid boxes, using the median of pairwise slopes method (Sen 1968, Lanzante 1996). Confidence in the trend is also determined if the 5^{th} to 95^{th} percentiles of the pairwise slopes are of the same sign and thus inconsistent with a zero trend. As well as the trend in quantity per decade, we also show the full change in the quantity from 1960 to 2010 that this fitted linear trend implies.

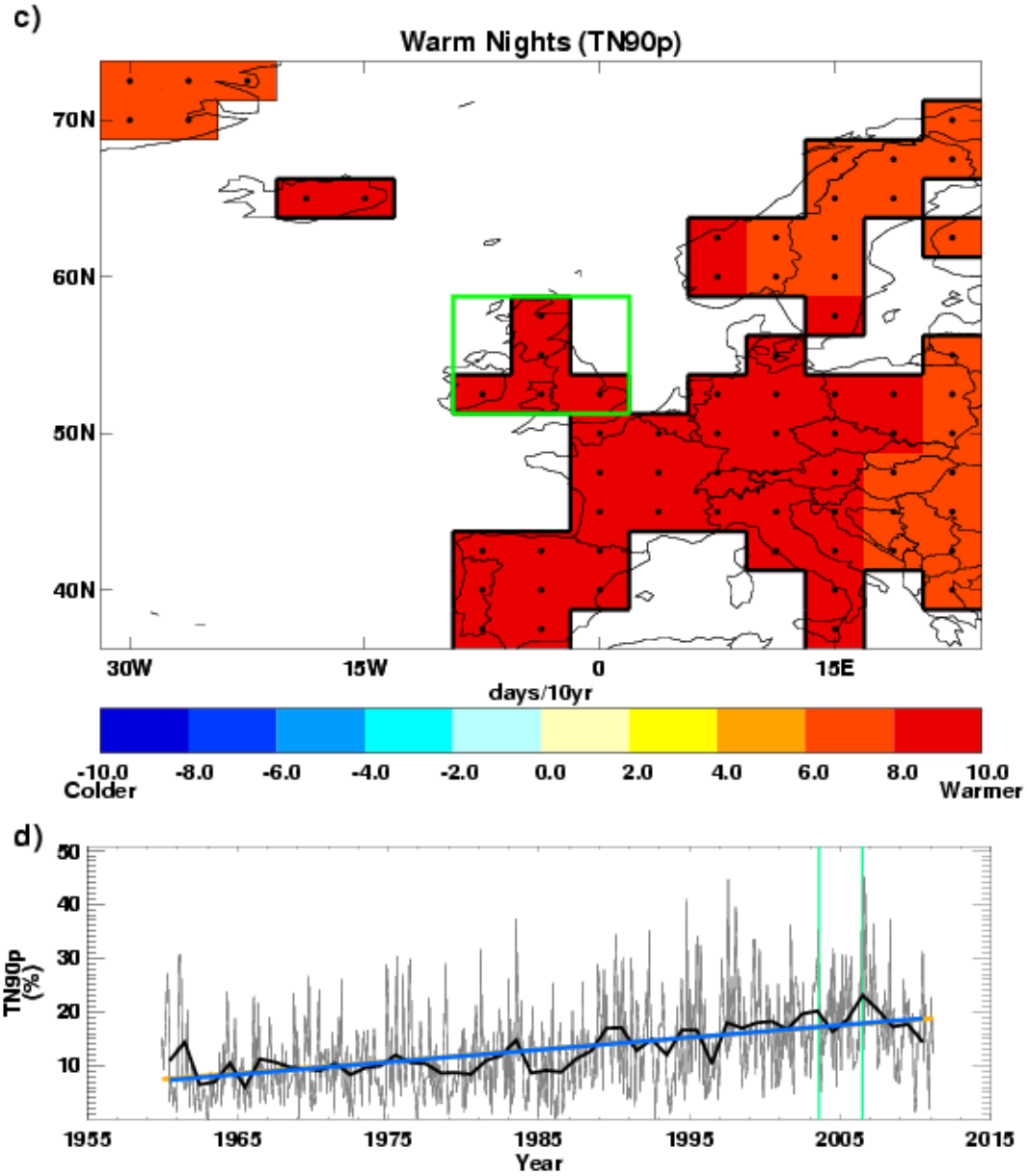
c)
Warm Nights (TN90p)
70N
60N
50N
40N
30W
15W
0
15E
days/10yr
-10.0
Colder
-8.0
-6.0
-4.0
-2.0
0.0
2.0
4.0
6.0
8.0
10.0
Warmer
d)
TN90p (%)
50
40
30
20
10
1955
1965
1975
1985
1995
2005
2015
Year
Monthly: 2.20% per decade (1.80 to 2.61)
Total change of 11.02% from 1960 to 2011 (9.00% to 13.06%)
Annual: 2.28% per decade (1.69 to 2.86)
Total change of 11.41% from 1960 to 2010 (8.43% to 14.28%)

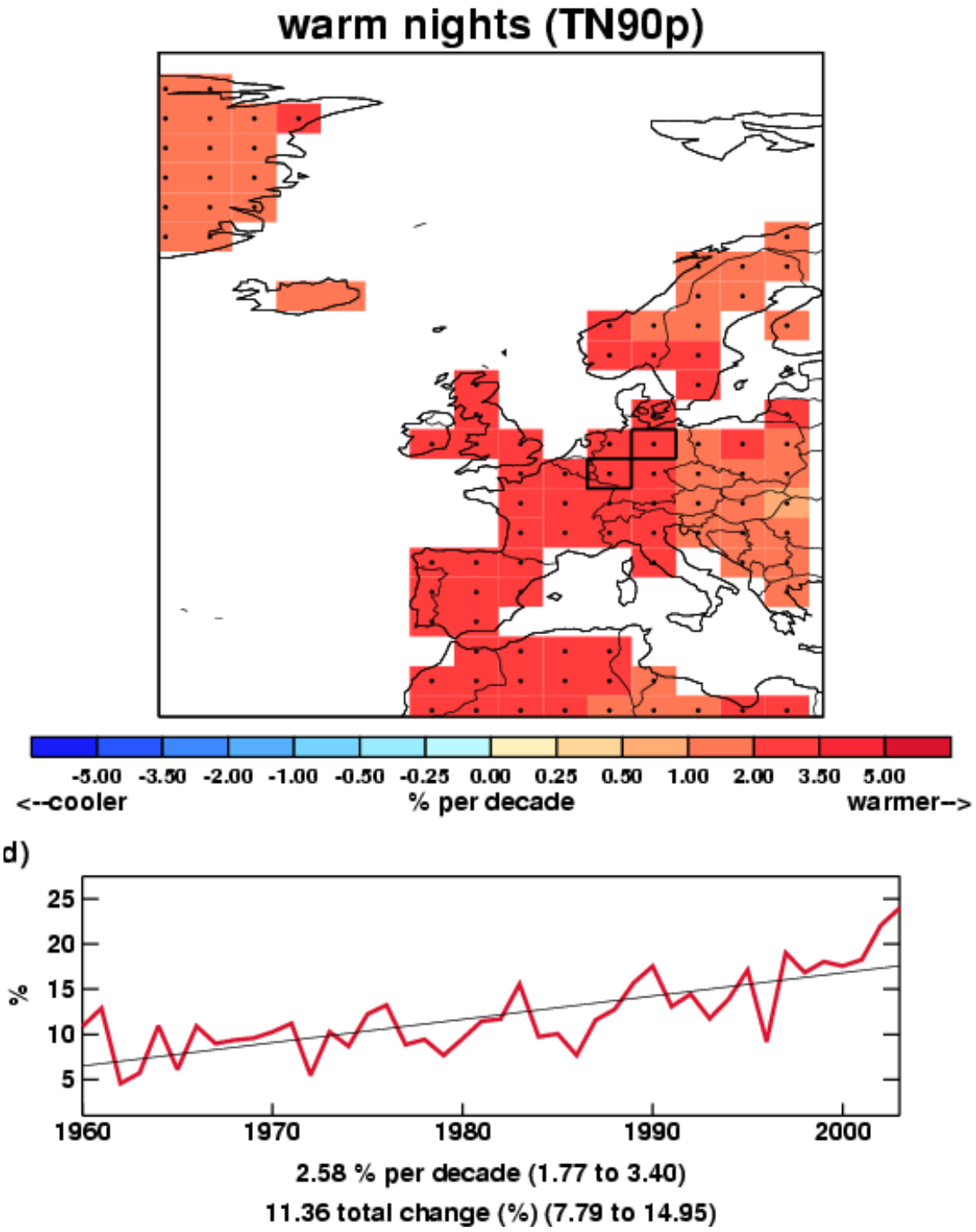

Figure 9. *Examples of the plots shown in the data section. Left: From ECA&D data between 1960-2010 for the number of warm nights, and Right: from HadEX data (1960-2003) for the total precipitation. A full explanation of the plots is given in the text below.*

The results are presented in the form of a map and a time series for each country and index. The map shows the grid box decadal trend in the index over the period for which there are data. High confidence, as determined above, is shown by a black dot in the grid box centre. To show the variation over time, the values for each year (and month if available) are shown in a time series for a regional average. The values of the indices have been normalised to a

base period of 1961-1990 (except the Indian gridded data which use a 1971 to 1990 period), both in HadEX and in the new data acquired for this project. Therefore, for example, the percentage of nights exceeding the 90th percentile for a temperature is 10% for that period.

There are two influences on whether a grid box contains a value or not – the land-sea mask, and the decorrelation length scale. The land-sea mask is shown in Figure 8. There are grid boxes which contain some land but are mostly sea and so are not considered. The decorrelation length scale sets the maximum distance a grid box can be from stations before no value is assigned to it. Grid boxes containing three or more stations are highlighted by a thick border. This indicates regions where the value shown is likely to be more representative of the grid box area mean as opposed to a single station location.

On the maps for the new data there is a box indicating which grid boxes have been extracted to calculate the area average for the time series. This box is the same as shown in Figure 1 at the beginning of each country's document. These selected grid boxes are combined using area (cosine) weighting to calculate the regional average (both annual [thick lines] and monthly [thin lines] where available). Monthly (orange) and annual (blue) trends are fitted to these time series using the method described above. The decadal trend and total change over the period where there are data are shown with 5th to 95th percentile confidence intervals in parentheses. High confidence, as determined above, is shown by a solid line as opposed to a dotted one. The green vertical lines on the time series show the dates of some of the notable events outlined in each section.

Attribution

Regional distributions of seasonal mean temperatures in the 2000s are computed with and without the effect of anthropogenic influences on the climate. The analysis considers temperatures averaged over the regions shown in Figure 10. These are also identified as grey boxes on the maps in Figure 1. The coordinates of the regions are given in Table 6. The methodology combines information from observations and model simulations using the approach originally introduced in Christidis et al., 2010 and later extended in Christidis et al., 2011, where more details can be found. The analysis requires spatial scales greater than about 2,500 km and for that reason the selected regions (Fig.10 and Table 6) are often larger than individual countries, or include several smaller countries in a single region (for example UK, Germany and France are grouped in one region).

Observations of land temperature come from the CRUTEM3 gridded dataset (Brohan et al., 2006) and model simulations from two coupled GCMs, namely the Hadley Centre HadGEM1 model (Martin et al., 2006) and version 3.2 of the MIROC model (K-1 Developers, 2004). The use of two GCMs helps investigate the sensitivity of the results to the model used in the analysis. Ensembles of model simulations from two types of experiments are used to partition the temperature response to external forcings between its anthropogenic and natural components. The first experiment (ALL) simulates the combined effect of natural and anthropogenic forcings on the climate system and the second (ANTHRO) includes anthropogenic forcings only. The difference of the two gives an estimate of the effect of the natural forcings (NAT). Estimates of the effect of internal climate variability are derived from long control simulations of the unforced climate. Distributions of the regional summer mean temperature are computed as follows:

a) A global optimal fingerprinting analysis (Allen and Tett, 1999; Allen and Stott, 2003) is first carried out that scales the global simulated patterns (fingerprints) of climate change attributed to different combinations of external forcings to best match them to the observations. The uncertainty in the scaling that originates from internal variability leads to samples of the scaled fingerprints, i.e. several realisations that are plausibly consistent with the observations. The 2000-2009 decade is then extracted from the scaled patterns and two samples of the decadal mean temperature averaged over the reference region are then computed with and without human influences, which provide the Probability Density Functions (PDFs) of the decadal mean temperature attributable to ALL and NAT forcings.

b) Model-derived estimates of noise are added to the distributions to take into account the uncertainty in the simulated fingerprints.

c) In the same way, additional noise from control model simulations is introduced to the distributions to represent the effect of internal variability in the annual values of the seasonal mean temperatures. The result is a pair of estimated distributions of the annual values of the seasonal mean temperature in the region with and without the effect of human activity on the climate. The temperatures throughout the analysis are expressed as anomalies relative to period 1961-1990.

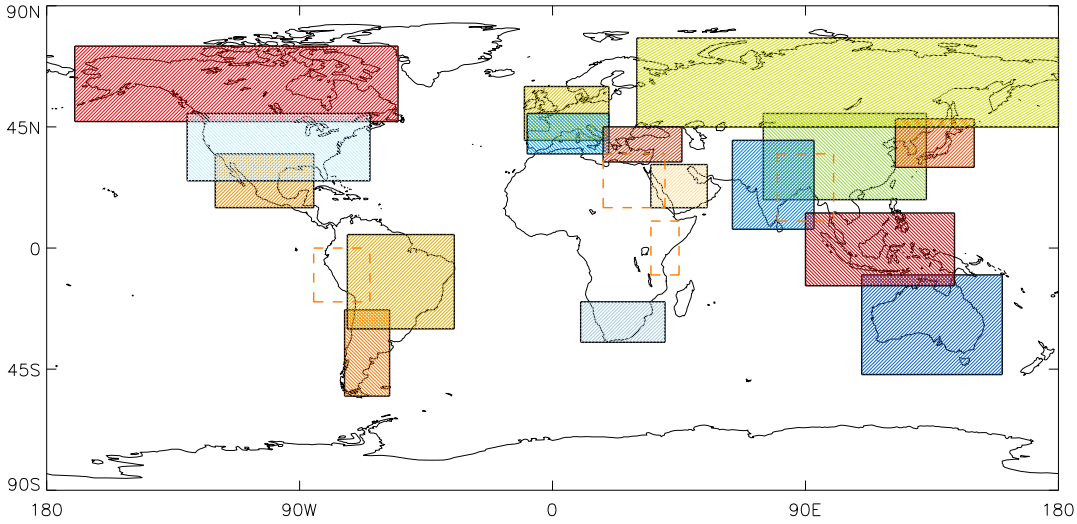

Figure 10. The regions used in the attribution analysis. Regions marked with dashed orange boundaries correspond to non-G20 countries that were also included in the analysis.

Region	Region Coordinates
Argentina	74-58W, 55-23S
Australia	110-160E, 47-10S
Bangladesh	80-100E, 10-35N
Brazil	73-35W, 30S-5N
Canada-Alaska	170-55W, 47-75N
China	75-133E, 18-50N
Egypt	18-40E, 15-35N
France-Germany-UK	10W-20E, 40-60N
India	64-93E, 7-40N
Indonesia	90-143E, 14S-13N
Italy-Spain	9W-20E, 35-50N
Japan-Republic of Korea	122-150E, 30-48N
Kenya	35-45E, 10S-10N
Mexico	120-85W, 15-35N
Peru	85-65W, 20-0S
Russia	30-185E, 45-78N
Saudi Arabia	35-55E, 15-31N
South Africa	10-40E, 35-20S
Turkey	18-46E, 32-45N

Table 6. *The coordinates of the regions used in the attribution analysis.*

References

ALEXANDER, L. V., ZHANG. X., PETERSON, T. C., CAESAR, J., GLEASON, B., KLEIN TANK, A. M. G., HAYLOCK, M., COLLINS, D., TREWIN, B., RAHIMZADEH, F., TAGIPOUR, A., RUPA KUMAR, K., REVADEKAR, J., GRIFFITHS, G., VINCENT, L., STEPHENSON, D. B., BURN, J., AGUILAR, E., BRUNET, M., TAYLOR, M., NEW, M., ZHAI, P., RUSTICUCCI, M. AND VAZQUEZ-AGUIRRE, J. L. 2006. Global observed changes in daily climate extremes of temperature and precipitation. *J. Geophys. Res*. 111, D05109. doi:10.1029/2005JD006290.

ALLEN, M. R., TETT S. F. B. 1999. Checking for model consistency in optimal fingerprinting. Clim Dyn 15: 419-434.

ALLEN M. R., STOTT P. A. 2003. Estimating signal amplitudes in optimal fingerprinting, part I: theory. Clim Dyn 21: 477-491.

BROHAN, P., KENNEDY, J.J., HARRIS, I., TETT, S.F.B. AND JONES, P.D. 2006. Uncertainty estimates in regional and global observed temperature changes: a new dataset from 1850. *J. Geophys. Res*. 111, D12106. doi:10.1029/2005JD006548.

CHRISTIDIS N., STOTT. P A., ZWIERS, F. W., SHIOGAMA, H., NOZAWA, T. 2010. Probabilistic estimates of recent changes in temperature: a multi-scale attribution analysis. Clim Dyn 34: 1139-1156.

CHRISTIDIS, N., STOTT, P. A., ZWIERS, F. W., SHIOGAMA, H., NOZAWA, T. 2011. The contribution of anthropogenic forcings to regional changes in temperature during the last decade. *Climate Dynamics* in press.

COMPO, G. P., J.S. WHITAKER, P.D. SARDESHMUKH, N. MATSUI, R.J. ALLAN, X. YIN, B.E. GLEASON, R.S. VOSE, G. RUTLEDGE, P. BESSEMOULIN, S. BRÖNNIMANN, M. BRUNET, R.I. CROUTHAMEL, A.N. GRANT, P.Y. GROISMAN, P.D. JONES, M.C. KRUK, A.C. KRUGER, G.J. MARSHALL, M. MAUGERI, H.Y. MOK, Ø. NORDLI, T.F. ROSS, R.M. TRIGO, X.L. WANG, S.D. WOODRUFF AND S.J. WORLEY. 2011. The Twentieth Century Reanalysis Project, *Q. J. R.Met.Soc. 137*, 1-28, doi: 10.1002/qj.776.

CORNES, R. C., AND P. D. JONES. 2011. An examination of storm activity in the northeast Atlantic region over the 1851–2003 period using the EMULATE gridded MSLP data series, *J. Geophys. Res*. 116, D16110, doi:10.1029/2011JD016007.

DOUGLAS, A., K. GLEASON, D. PHILLIPS AND A. M. WAPLE. 2003. North America in State of the Climate 2002. *Bulletin of the American Meteorological Society*, 84, S35-36.

DURRE, I, MENNE, MJ, GLEASON, BE, HOUSTON, TG, VOSE, RS, 2010. Comprehensive Automated Quality Assurance of Daily Surface Observations*, Journal of Applied Meteorology and Climatology*, 49, 8, 1615-1633.

FIELD, C.B., MORTSCH, L.D., BRKLACICH, M., FORBES, D.L., KOVACS, P., PATZ, J.A., RUNNING, S.W. AND SCOTT, M.J. 2007. North America. *Climate Change 2007: Impacts, Adaptation and Vulnerability. Contribution of Working Group II to the Fourth Assessment Report of the Intergovernmental Panel on Climate Change*, M.L. Parry, O.F. Canziani, J.P. Palutikof, P.J. van der Linden and C.E. Hanson, Eds., Cambridge University Press, Cambridge, UK, 617-652.

GRAUMANN, A., T. HOUSTON, J. LAWRIMORE, D. LEVINSON, N. LOTT, S. MCCOWN, S. STEPHENS AND D. WUERTZ. 2006. Hurricane Katrina, A Climatological Perspective. NOAA's National Climatic Data Centre. Available online: http://www.ncdc.noaa.gov/oa/reports/tech-report-200501z.pdf accessed 13 October 2011.

HEIM JR., R. R., D. H. LEVINSON, N. B. GUTTMAN, AND A. M. SANCHEZ-LUGO. 2007. United States in State of the Climate 2006. *Bulletin of the American Meteorological Society*, 87, S84-87.

K-1 MODEL DEVELOPERS (2004) K-1 coupled GCM (MIROC) description, K-1 Tech Rep, H Hasumi and S Emori (eds), Centre for Clim Sys Res, Univ of Tokyo.

KNABB, R.D., J.R. RHOME, D.P. BROWN. 2005 revised 2006. Tropical Cyclone Report: Hurricane Katrina: 23–30 August 2005. National Hurricane Center. Available online: http://www.nhc.noaa.gov/pdf/TCR-AL122005_Katrina.pdf accessed 13 October 2011.

LANZANTE, J. R. 1996. Resistant, robust and non-parametric techniques for the analysis of climate data: theory and examples, including applications to historical radiosonde station data. *Int. J. Clim*. 16, 1197–226.

LAWRIMORE, J.H., M.S. HALPERT, G.D. BELL, M.J. MENNE, B. LYON, R.C. SCHNELL, K.L. GLEASON, D.R. EASTERLING, W. THIAW, W.J. WRIGHT, R.R. HEIM JR., D.A. ROBINSON AND L. ALEXANDER. 2001. State of the Climate 2000. *Bulletin of the American Meteorological Society*, 82, S18-20.

MARTIN G.M., RINGER. M. A., POPE V. D., JONES, A., DEARDEN, C., HINTON, T. 2006. The physical properties of the atmosphere in the new Hadley Centre Global Environmental Model (HadGEM1). Part I: Model description and global climatology. J Clim 19: 1274-1301.

NOAA (NATIONAL OCEANIC AND ATMOSPHERIC ADMINISTRATION). 2007. *State of the Climate: Drought September 2007*. Available online: http://www.ncdc.noaa.gov/sotc/drought/2007/9 accessed 30 September 2011.

PETERSON, T.C., VAUTARD, R., McVICAR, T.R., THÉPAUT, J-N. AND BERRISFORD, P. 2011. [Global Climate] Surface Winds over Land in State of the Climate 2010. *Bulletin of the American Meteorological Society* 92 (6), S57.

SANCHEZ-LUGO, A., KENNEDY, J.J. AND BERRISFORD, P. 2011. [Global Climate] Surface Temperatures in State of the Climate 2010. *Bulletin of the American Meteorological Society* 92 (6), S36-S37.

SEN, P. K. 1968. Estimates of the regression coefficient based on Kendall's tau. *J. Am. Stat. Assoc*. 63, 1379–89.

SHEIN, K. A. 2006. Introduction in State of the Climate 2005. *Bulletin of the American Meteorological Society* 86, S7.

STEPHENS, S. E., R. R. HEIM, JR., K. L. GLEASON, C. FENIMORE, G. D. BELL, M. SHULSKI, AND R. A. BALLARD. 2009. United States in State of the Climate 2008. *Bulletin of the American Meteorological Society* 89, S126.

WMO WORLD METEOROLOGICAL ORGANIZATION. 2001, 2004, 2007, 2008, 2009, 2010, 2011. Statement on Status of the Global Climate in 2000, WMO-No. 920. http://www.wmo.int/pages/prog/wcp/wcdmp/statement/wmostatement_en.html

Acknowledgements

Data for this work were taken from the GHCND database (Durre et al., 2010). We thank Lisa Alexander and Markus Donat (University of New South Wales) for their help and advice. We also thank reviewers from the United States for their valuable input and advice.

Chapter 2 – Climate Change Projections

Introduction

Climate models are used to understand how the climate will evolve over time and typically represent the atmosphere, ocean, land surface, cryosphere, and biogeochemical processes, and solve the equations governing their evolution on a geographical grid covering the globe. Some processes are represented explicitly within climate models, large-scale circulations for instance, while others are represented by simplified parameterisations. The use of these parameterisations is sometimes due to processes taking place on scales smaller than the typical grid size of a climate model (a Global Climate Model (GCM) has a typical horizontal resolution of between 250 and 600km) or sometimes to the current limited understanding of these processes. Different climate modelling institutions use different plausible representations of the climate system, which is why climate projections for a single greenhouse gas emissions scenario differ between modelling institutes. This gives rise to "climate model structural uncertainty".

In response to a proposed activity of the World Climate Research Programme's (WCRP's; http://www.wcrp-climate.org/) Working Group on Coupled Modelling (WGCM), the Program for Climate Model Diagnosis and Intercomparison (PCMDI; http://www-pcmdi.llnl.gov/) volunteered to collect model output contributed by leading climate modelling centres around the world. Climate model output from simulations of the past, present and future climate was collected by PCMDI mostly during the years 2005 and 2006, and this archived data constitutes phase 3 of the Coupled Model Intercomparison Project (CMIP3). In part, the WGCM organised this activity to enable those outside the major modelling centres to perform research of relevance to climate scientists preparing the IPCC Fourth Assessment Report (AR4). This unprecedented collection of recent model output is commonly known as the "CMIP3 multi-model dataset". The GCMs included in this dataset are referred to regularly throughout this review, although not exclusively.

The CMIP3 multi-model ensemble has been widely used in studies of regional climate change and associated impacts. Each of the constituent models was subject to extensive testing by the contributing institute, and the ensemble has the advantage of having been constructed from a large pool of alternative model components, therefore sampling alternative structural assumptions in how best to represent the physical climate system. Being assembled on an opportunity basis, however, the CMIP3 ensemble was not designed to represent model uncertainties in a systematic manner, so it does not, in isolation, support robust estimates of the risk of different levels of future climate change, especially at a regional level.

Since CMIP3, a new (CMIP5) generation of coupled ocean-atmosphere models has been developed, which is only just beginning to be available and is being used for new projections for the IPCC Fifth Assessment Report (AR5).

These newer models typically feature higher spatial resolution than their CMIP3 counterparts, including in some models a more realistic representation of stratosphere-troposphere interactions. The CMIP5 models also benefit from several years of development in their parameterisations of small scale processes, which, together with resolution increases, are expected to result in a general improvement in the accuracy of their simulations of historical climate, and in the credibility of their projections of future changes. The CMIP5 programme also includes a number of comprehensive Earth System Models (ESMs) which explicitly simulate the earth's carbon cycle and key aspects of atmospheric chemistry, and also contain more sophisticated representations of aerosols compared to CMIP3 models.

The CMIP3 results should be interpreted as a useful interim set of plausible outcomes. However, their neglect of uncertainties, for instance in carbon cycle feedbacks, implies that higher levels of warming outside the CMIP3 envelope cannot be ruled out. In future, CMIP5 coupled model and ESM projections can be expected to produce improved advice on future regional changes. In particular, ensembles of ESM projections will be needed to provide a more comprehensive survey of possible future changes and their relative likelihoods of occurrence. This is likely to require analysis of the CMIP5 multi-model ESM projections, augmented by larger ensembles of ESM simulations in which uncertainties in physical and biogeochemical feedback processes can be explored more systematically, for example via ensembles of model runs in which key aspects of the climate model are slightly adjusted. Note that such an exercise might lead to the specification of wider rather than narrower uncertainties compared to CMIP3 results, if the effects of representing a wider range of earth system processes outweigh the effects of refinements in the simulation of physical atmosphere-ocean processes already included in the CMIP3 models.

Climate projections

The Met Office Hadley Centre is currently producing perturbed parameter ensembles of a single model configuration known as HadCM3C, to explore uncertainties in physical and biogeochemical feedback processes. The results of this analysis will become available in the next year and will supplement the CMIP5 multi-model ESM projections, providing a more comprehensive set of data to help progress understanding of future climate change. However, many of the studies covered in the chapter on climate impacts have used CMIP3 model output. For this reason, and because it is still the most widely used set of projections available, the CMIP3 ensemble output for temperature and precipitation, for the A1B emission scenario, for the USA and the surrounding region is shown below.

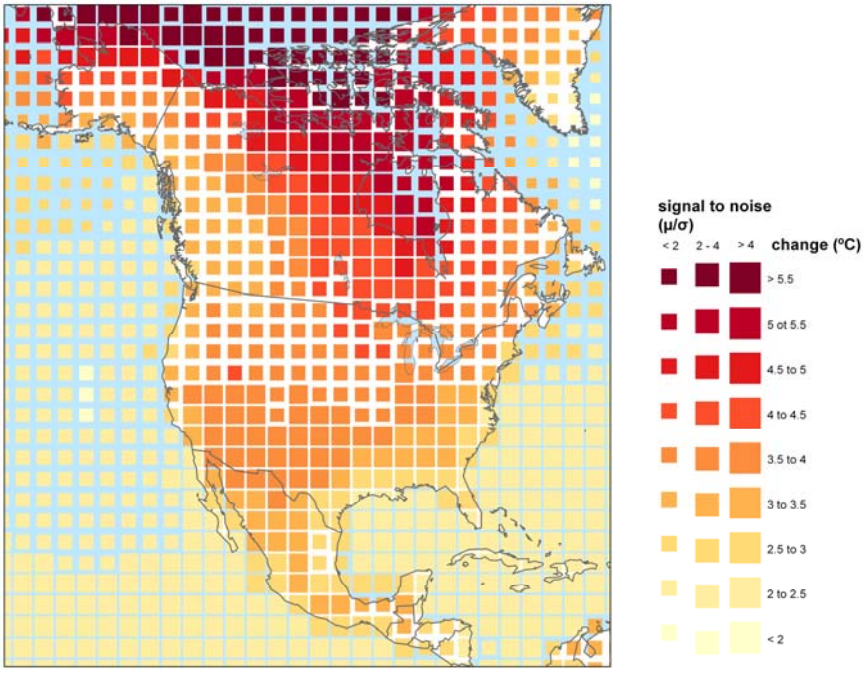

Figure 1. *Percentage change in average annual temperature by 2100 from 1960-1990 baseline climate, averaged over 21 CMIP3 models. The size of each pixel represents the level of agreement between models on the magnitude of the change.*

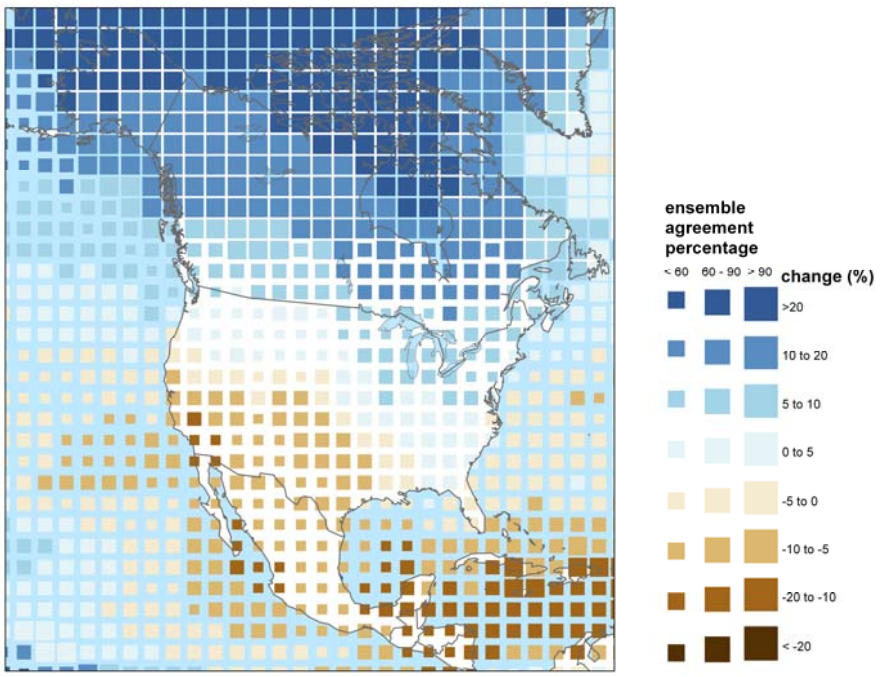

***Figure 2**. Percentage change in average annual precipitation by 2100 from 1960-1990 baseline climate, averaged over 21 CMIP3 models. The size of each pixel represents the level of agreement between models on the sign of the change.*

Summary of temperature change in the USA

Figure 1 shows the percentage change in average annual temperature by 2100 from 1960-1990 baseline climate, averaged over 21 CMIP3 models. All of the models in the CMIP3 ensemble project increased temperatures in the future, but the size of each pixel indicates how well the models agree over the magnitude of the increase.

Projected temperature increases over the USA are generally higher in central, southwest and northern regions, up to around 4-4.5°C. The agreement between the models is higher in southern and eastern parts of the country compared to the north.

Summary of precipitation change in the USA

Figure 2 shows the percentage change in average annual precipitation by 2100 from 1960-1990 baseline climate, averaged over 21 CMIP3 models. Unlike for temperature, the models sometimes disagree over whether precipitation is increasing or decreasing over a region, so

in this case the size of each pixel indicates the percentage of the models in the ensemble that agree on the sign of the change in precipitation.

The USA shows a north-south division in projected precipitation changes, with the highest decreases, of up to around 20%, in the southwest, and increases of up to 10% in the northeast. The ensemble agreement is moderate to low. The USA is located in the transition zone between strong increases in precipitation over Canada, and decreases over Central America and the Caribbean.

Chapter 3 – Climate Change Impact Projections

Introduction

Aims and approach

This chapter looks at research on a range of projected climate change impacts, with focus on results for the USA. It includes projections taken from the AVOID programme, for some of the impact sectors.

The aim of this work is to take a 'top down' approach to assessing global impacts studies, both from the literature and from new research undertaken by the AVOID programme. This project covers 23 countries, with summaries from global studies provided for each of these. This global approach allows some level of comparison between countries, whilst presenting information on a scale most meaningful to inform international policy.

The literature covered in this chapter focuses on research published since the Fourth Assessment Report (AR4) of the Intergovernmental Panel on Climate Change (IPCC) and should be read in conjunction with IPCC AR4 WG1 and WG2 reports. For some sectors considered, an absence of research developments since the IPCC AR4, means earlier work is cited as this helps describe the current level of scientific understanding. This report focuses on assessing scientific research about climate change impacts within sectors; it does not present an integrated analysis of climate change adaptation policies.

Some national and sub-national scale literature is reported to a limited extent to provide some regional context.

Impact sectors considered and methods

This report reviews the evidence for the impact of climate change on a number of sectors, for the USA. The following sectors are considered in turn in this report:

- Crop yields
- Food security
- Water stress and drought
- Pluvial flooding and rainfall
- Fluvial flooding

- Tropical cyclones (where applicable)
- Coastal regions

Supporting literature

Literature searches were conducted for each sector with the Thomson Reuters Web of Science (WoS., 2011) and Google Scholar academic search engines respectively. Furthermore, climate change impact experts from each of the 23 countries reviewed were contacted. These experts were selected through a combination of government nomination and from experts known to the Met Office. They were asked to provide literature that they felt would be of relevance to this review. Where appropriate, such evidence has been included. A wide range of evidence was considered, including; research from international peer-reviewed journal papers; reports from governments, non-governmental organisations, and private businesses (e.g. reinsurance companies), and research papers published in national journals.

For each impact sector, results from assessments that include a global- or regional-scale perspective are considered separately from research that has been conducted at the national- or sub-national-scale. The consideration of global- and regional-scale studies facilitates a comparison of impacts across different countries, because such studies apply a consistent methodology for each country. While results from national- and sub-national-scale studies are not easily comparable between countries, they can provide a level of detail that is not always possible with larger-scale studies. However, the national- and sub-national scale literature included in this project does not represent a comprehensive coverage of regional-based research and cannot, and should not, replace individual, detailed impacts studies in countries. The review aims to present an up-to-date assessment of the impact of climate change on each of the sectors considered.

AVOID programme results

Much of the work in this report is drawn from modelling results and analyses coming out of the AVOID programme. The AVOID programme is a research consortium funded by DECC and Defra and led by the UK Met Office and also comprises the Walker Institute at the University of Reading, the Tyndall Centre represented through the University of East Anglia,

and the Grantham Institute for Climate Change at Imperial College. The expertise in the AVOID programme includes climate change research and modelling, climate change impacts in natural and human systems, socio-economic sciences, mitigation and technology. The unique expertise of the programme is in bringing these research areas together to produce integrated and policy-relevant results. The experts who work within the programme were also well suited to review the literature assessment part of this report. In this report the modelling of sea level rise impacts was carried out for the AVOID programme by the University of Southampton.

The AVOID programme uses the same emissions scenarios across the different impact sectors studied. These are a business as usual (IPCC SRES A1B) and an aggressive mitigation (the AVOID A1B-2016-5-L) scenario. Model output for both scenarios was taken from more than 20 GCMs and averaged for use in the impact models. The impact models are sector specific, and frequently employ further analytical techniques such as pattern scaling and downscaling in the crop yield models.

Data and analysis from AVOID programme research is provided for the following impact sectors:

- Crop yields
- Water stress and drought
- Fluvial flooding
- Coastal regions

Uncertainty in climate change impact assessment

There are many uncertainties in future projections of climate change and its impacts. Several of these are well-recognised, but some are not. One category of uncertainty arises because we don’t yet know how mankind will alter the climate in the future. For instance, uncertainties in future greenhouse gas emissions depends on the future socio-economic pathway, which, in turn, depends on factors such as population, economic growth, technology development, energy demand and methods of supply, and land use. The usual approach to dealing with this is to consider a range of possible future scenarios.

Another category of uncertainties relate to our incomplete understanding of the climate system, or an inability to adequately model some aspects of the system. This includes:

- Uncertainties in translating emissions of greenhouse gases into atmospheric concentrations and radiative forcing. Atmospheric CO_2 concentrations are currently rising at approximately 50% of the rate of anthropogenic emissions, with the remaining 50% being offset by a net uptake of CO_2 into the oceans and land biosphere. However, this rate of uptake itself probably depends on climate, and evidence suggests it may weaken under a warming climate, causing more CO_2 to remain in the atmosphere, warming climate further. The extent of this feedback is highly uncertain, but it not considered in most studies. The phase 3 of the Coupled Model Intercomparison Project (CMIP3), which provided the future climate projections for the IPCC Fourth Assessment Report (AR4), used a single estimate of CO_2 concentration rise for each emissions scenario, so the CMIP3 projections (which were used in most studies presented here, including AVOID) do not account for this uncertainty.

- Uncertainty in climate response to the forcing by greenhouse gases and aerosols. One aspect of this is the response of global mean temperature ("climate sensitivity"), but a more relevant aspect for impacts studies is the response of regional climates, including temperature, precipitation and other meteorological variables. Different climate models can give very different results in some regions, while giving similar results in other regions. Confidence in regional projections requires more than just agreement between models: physical understanding of the relevant atmospheric, ocean and land surface processes is also important, to establish whether the models are likely to be realistic.

- Additional forcings of regional climate. Greenhouse gas changes are not the only anthropogenic driver of climate change; atmospheric aerosols and land cover change are also important, and unlike greenhouse gases, the strength of their influence varies significantly from place to place. The CMIP3 models used in most impacts studies generally account for aerosols but not land cover change.

- Uncertainty in impacts processes. The consequences of a given changes in weather or climatic conditions for biophysical impacts such as river flows, drought, flooding, crop yield or ecosystem distribution and functioning depend on many other processes which are often poorly-understood, especially at large scales. In particular, the extent to which different biophysical impacts interact with each other has been hardly studied, but may be crucial; for example, impacts of climate change on crop

yield may depend not only on local climate changes affecting rain-fed crops, but also remote climate changes affecting river flows providing water for irrigation.

- Uncertainties in non-climate effects of some greenhouse gases. As well as being a greenhouse gas, CO_2 exerts physiological influences on plants, affecting photosynthesis and transpiration. Under higher CO_2 concentrations, and with no other limiting factors, photosynthesis can increase, while the requirements of water for transpiration can decrease. However, while this has been extensively studied under experimental conditions, including in some cases in the free atmosphere, the extent to which the ongoing rise in ambient CO_2 affects crop yields and natural vegetation functioning remains uncertain and controversial. Many impacts projections assume CO_2 physiological effects to be significant, while others assume it to be non-existent. Studies of climate change impacts on crops and ecosystems should therefore be examined with care to establish which assumptions have been made.

In addition to these uncertainties, the climate varies significantly through natural processes from year-to-year and also decade-to-decade, and this variability can be significant in comparison to anthropogenic forcings on shorter timescales (the next few decades) particularly at regional scales. Whilst we can characterise the natural variability it will not be possible to give a precise forecast for a particular year decades into the future.

A further category of uncertainty in projections arises as a result of using different methods to correct for uncertainties and limitations in climate models. Despite being painstakingly developed in order to represent current climate as closely as possible, current climate models are nevertheless subject to systematic errors such as simulating too little or too much rainfall in some regions. In order to reduce the impact of these, '*bias correction*' techniques are often employed, in which the climate model is a source of information on the *change* in climate which is then applied to the observed present-day climate state (rather than using the model's own simulation of the present-day state). However, these bias-corrections typically introduce their own uncertainties and errors, and can lead to inconsistencies between the projected impacts and the driving climate change (such as river flows changing by an amount which is not matched by the original change in precipitation). Currently, this source of uncertainty is rarely considered

When climate change projections from climate models are applied to climate change impact models (e.g. a global hydrological model), the climate model structural uncertainty carries through to the impact estimates. Additional uncertainties include changes in future emissions

and population, as well as parameterisations within the impact models (this is rarely considered). Figure 1 highlights the importance of considering climate model structural uncertainty in climate change impacts assessment. Figure 1 shows that for 2°C prescribed global-mean warming, the magnitude of, and sign of change in average annual runoff from present, simulated by an impacts model, can differ depending upon the GCM that provides the climate change projections that drive the impact model. This example also shows that the choice of impact model, in this case a global hydrological model (GHM) or catchment-scale hydrological model (CHM), can affect the magnitude of impact and sign of change from present (e.g. see IPSL CM4 and MPI ECHAM5 simulations for the Xiangxi). To this end, throughout this review, the number of climate models applied in each study reviewed, and the other sources of uncertainty (e.g. emissions scenarios) are noted. Very few studies consider the application of multiple impacts models and it is recommended that future studies address this.

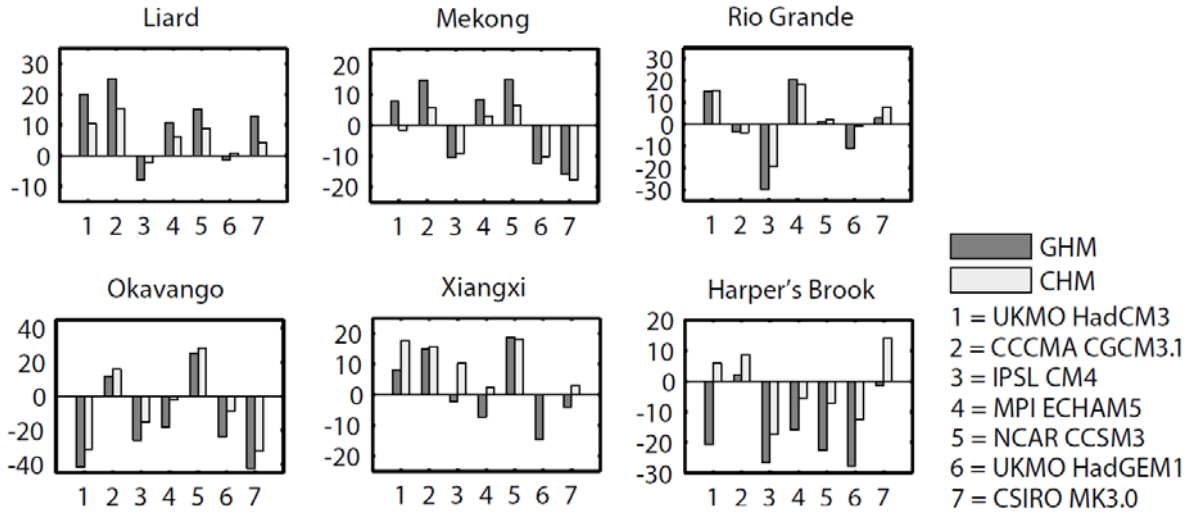

Figure 1. *Change in average annual runoff relative to present (vertical axis; %), when a global hydrological model (GHM) and a catchment-scale hydrological model (CHM) are driven with climate change projections from 7 GCMs (horizontal axis), under a 2°C prescribed global-mean warming scenario, for six river catchments. The figure is from Gosling et al. (2011).*

Uncertainties in the large scale climate relevant to the USA include changes in the El Niño-Southern Oscillation (ENSO) which could undergo rapid change with climate change. This could have a serious impact on large-scale atmospheric circulation, rainfall and seasonality in many parts of the world. Latif and Keenlyside (2009) concluded that, at this stage of understanding, it is not known how climate change could affect the tropical Pacific climate system. None of the global climate models (GCMs) they analysed showed rapid changes in behaviour. However, a threshold of abrupt change cannot be ruled out because whilst the

GCMs that Latif and Keenlyside (2009) analysed (the IPCC AR4 GCMs) are better than the previous generation of models (Reichler and Kim, 2008), these same models all show large biases in simulating the contemporary tropical Pacific, with no consensus on the sign of change in ENSO-like response.

Summary of findings for each sector

Crop yields

- Quantitative crop yield projections under climate change scenarios for the USA vary across studies due to the application of different models, assumptions and emissions scenarios.
- However, a number, but not all, of global- and regional-scale studies included here project declines in the yields of maize, soybean and wheat, three of the USA's major crops, as a consequence of climate change.
- Important knowledge gaps and key uncertainties include the quantification of yield increases due to CO_2 fertilisation, the quantification of yield reductions due to ozone damage and the extent to which crop diseases might affect crop yields with climate change.

Food security

- The USA is currently a country of extremely low undernourishment. Several studies suggest that the USA could remain food secure under climate change scenarios over the next 40 years, largely due to its high adaptive capacity associated with an ability to import food.
- Research by the AVOID programme projects that the USA may avoid major food security issues under climate change by implementing structural adjustments, such as diverting food away from exports and animal feed.
- One study projects that the national economy of the USA presents a very low vulnerability to climate change impacts on fisheries by the 2050s. Fish catches might reduce slightly across much of the USA with climate change but they could increase significantly in Alaska.

Water stress and drought

- There is consensus among global-scale studies that much of the USA's population is currently exposed to water stress.
- Several assessments included here confirm reports from the IPCC AR4 that annual mean precipitation could decrease in the southwest USA with climate change, and project that droughts could become more frequent and severe in this region in particular with climate change.
- Projections of water stress with climate change from studies that consider some of the inherent uncertainties in such projections indicate that water stress may increase moderately in the USA.
- Simulations from the AVOID programme are consistent in projecting a moderate increase in water stress, presenting a median increase of around 7% of the USA's population to be exposed to water stress increases by 2100 under SRES A1B. This is lower under an aggressive mitigation scenario, at around 5%.

Pluvial flooding and rainfall

- The IPCC AR4 noted that under climate change scenarios, the largest precipitation increases were projected to be in the northeast USA.
- Studies since then have also pointed to increasing mean and extreme precipitation in the northeast USA, which is suggested in observational analyses and projected in 21st century simulations.
- Mean precipitation could decrease in the southwest USA with smaller changes to extreme precipitation events.

Fluvial flooding

- Recent studies demonstrate large uncertainties in estimating fluvial flooding under climate change scenarios across the USA. At least one global modelling study has

projected a strong increase in flood frequency in parts of southern USA, the east coast states and the Pacific Northwest, but a decrease in other parts of the country.

- Results from the AVOID programme, based on climate projections from 21 GCMs, show that for the USA as a whole the model projections are evenly balanced between increasing and decreasing flood risk in the early 21st century, but later in the century the models show a greater tendency towards increasing flood risk, especially in the A1B scenario.

Tropical cyclones

- There remains large uncertainty in the current understanding of how tropical cyclones might be affected by climate change, including in the North Atlantic and East Pacific, as conclusions are based upon a limited number of studies whose projections are from either coarse-resolution global models or from statistical or dynamical downscaling techniques. To this end, caution should be applied in interpreting model-based results, even where the models are in agreement.

- However, most global- and regional-scale studies reviewed here suggest that the frequency of tropical cyclones in the North Atlantic could decrease with climate change, which may result in fewer cyclones striking the eastern USA and the Gulf coast. However, complex sub-basin-scale changes in cyclone frequency could lead to increasing cyclone counts in some coastal regions and decreases in others.

- The impact of climate change on cyclones near Hawaii is highly uncertain, due to the lack of model agreement on the sign of the change in cyclone frequency in the East Pacific.

- The majority of studies reviewed here project that tropical cyclone intensities and cyclone rainfall could increase in both the North Atlantic and the East Pacific, particularly for the most intense cyclones. These stronger storms could potentially cause an increase in cyclone damages in the USA due to climate change.

Coastal regions

- Studies published after the IPCC AR4 suggests that the USA is highly vulnerable to sea level rise (SLR). This supports conclusions from the IPCC AR4.
- One study shows that by the 2070s, the number of people exposed to SLR with climate change could increase from 6.7 million in present to 12.9 million under A1B emissions; an aggressive mitigation scenario could reduce this by around 0.5 million.

Crop yields

Headline

Crop yield projections under climate change scenarios for the USA vary across studies due to the application of different models, assumptions and emissions scenarios. However, the majority of studies show yield declines with climate change for the three major crops; maize, soybean and wheat.

Results from the AVOID programme for the USA indicate that the areas of current croplands becoming less suitable for cultivation are projected to be smaller under the mitigation scenario than the A1B scenario, and under both scenarios the area of declining suitability is larger than that of increasing suitability (which remains small over the 21st century in both scenarios).

Supporting literature

Introduction

The impacts of climate change on crop productivity are highly uncertain due to the complexity of the processes involved. Most current studies are limited in their ability to capture the uncertainty in regional climate projections, and often omit potentially important aspects such as extreme events and changes in pests and diseases. Importantly, there is a lack of clarity on how climate change impacts on drought are best quantified from an agricultural perspective, with different metrics giving very different impressions of future risk. The dependence of some regional agriculture on remote rainfall, snowmelt and glaciers adds to the complexity - these factors are rarely taken into account, and most studies focus solely on the impacts of local climate change on rain-fed agriculture. However, irrigated agricultural land produces approximately 40-45 % of the world's food (Doll and Siebert 2002), and the water for irrigation is often extracted from rivers which can depend on climatic conditions far from the point of extraction. Hence, impacts of climate change on crop productivity often need to take account of remote as well as local climate changes. Indirect impacts via sea-level rise, storms and diseases have also not been quantified. Perhaps most seriously, there is high uncertainty in the extent to which the direct effects of CO_2 rise on plant physiology will

interact with climate change in affecting productivity. Therefore, at present, the aggregate impacts of climate change on large-scale agricultural productivity cannot be reliably quantified (Gornall et al, 2010). This section summarises findings from a range of post IPCC AR4 assessments to inform and contextualise the analysis performed by AVOID programme for this project. The results from the AVOID work are discussed in the next section.

Maize, soybeans and wheat are the most important food crops in the USA in terms of harvested area, quantity as well as value (see Table 1) (FAO, 2008).

Harvested area (ha)		**Quantity (Metric ton)**		**Value ($1000)**	
Maize	31700000	Maize	307000000	Maize	23600000
Soybeans	30200000	Soybeans	80700000	Soybeans	16800000
Wheat	22500000	Wheat	68000000	Wheat	9300000
Seed cotton	3060000	Sugar cane	25000000	Cotton lint	4140000
Sorghum	2940000	Sugar beet	24300000	Tomatoes	4010000
Barley	1520000	Potatoes	18800000	Grapes	3080000
Rice, paddy	1200000	Tomatoes	13700000	Potatoes	2560000

Table 1. *The top 7 crops by harvested area, quantity and value according to the FAO (2008) in the USA. Crops that feature in all lists are shaded green; crops that feature in two top 7 lists are shaded amber. Data is from FAO (2008) and has been rounded down to three significant figures.*

A number of impact model studies looking at crop yield which include results for some of the main crops in the USA have been conducted. They apply a variety of methodological approaches, including using different climate model inputs and treatment of other factors that might affect yield, such as impact of increased CO_2 in the atmosphere on plant growth and adaption of agricultural practises to changing climate conditions. These different models, assumptions and emissions scenarios mean that there are a range of crop yield projections for the USA.

Important knowledge gaps and key uncertainties which are applicable to the USA as well as at the global-scale, include; the quantification of yield increases due to CO_2 fertilisation and yield reductions due to ozone damage (Ainsworth and McGrath, 2010, Iglesias et al., 2009), and the extent crop diseases could affect crop yields with climate change (Luck et al., 2011)

Most crop simulation models do not include the direct effect of extreme temperatures on crop development and growth, thus only changes in mean climate conditions are considered to affect crop yields for the studies included here.

Assessments that include a global or regional perspective

Recent past

In order to assess the impact of recent climate change (1980-2008) on wheat, maize, rice and soybean, Lobell et al. (2011) looked at how the overall yield trend in these crops changed in response to changes in climate over the period studied. The study was conducted at the global-scale but national estimates for the USA were also calculated. Lobell et all. (2011) divided the climate-induced yield trend by the overall yield trend for 1980–2008, to produce a simple metric of the importance of climate relative to all other factors. The ratio produced indicates the influence of climate on the productivity trend overall. So for example a value of –0.1 represents a 10% reduction in yield gain due to climate change, compared to the increase that could have been achieved without climate change, but with technology and other gains. This can also be expressed as 10 years of climate trend being equivalent to the loss of roughly 1 year of technology gains. For the USA, no significant positive or negative effects on crop yield were estimated relative to what could have been achieved without the climate trends (see Table 2).

Crop	Trend
Maize	-0.1 to 0.0
Rice	n/a
Wheat	0.0 to 0.1
Soybean	-0.1 to 0.0

Table 2. *The estimated net impact of climate trends for 1980-2008 on crop yields. Climate-induced yield trend divided by overall yield trend. 'n/a' infers zero or insignificant crop production or unavailability of data. Data is from Lobell et al. (2011).*

Climate change studies

Global studies on changes in crop yield due to climate change covered in this report are derived mainly from applying Global Climate Model (GCM) output to crop models. The results for the USA are presented.

Included in this report are recent studies have applied climate projections from GCMs to crop yield models to assess the global-scale impact of climate change on crop yields, and which include impact estimates at the national-scale for the USA (Iglesias and Rosenzweig, 2009, Arnell et al., 2010a, Arnell et al., 2010b). The process of CO_2 fertilisation of some crops is usually included in most climate impact studies of yields. However, other gases can influence crop yield and are not always included in impacts models. An example of this is

ozone (O_3) and so a study which attempts to quantify the potential impact on crop yield of changes in ozone in the atmosphere is also included (Avnery et al. 2011). In addition to these studies, the AVOID programme analysed the patterns of climate change for 21 GCMs, to establish an index of 'climate suitability' of agricultural land. Climate suitability is not directly equivalent to crop yields, but is a means of looking at a standard metric across all the countries included in this project, and of assessing the level of agreement on variables that affect crop production, between all 21 GCMs.

Iglesias and Rosenzweig (2009) repeated an earlier study presented by Parry et al. (2004) by applying climate projections from the HadCM3 GCM (instead of HadCM2, which was applied by Parry et al. (2004)), under seven SRES emissions scenarios and for three future time periods. This study used consistent crop simulation methodology and climate change scenarios globally, and weighted the model site results by their contribution to regional and national, and rain-fed and irrigated production. The study also applied a quantitative estimation of physiological CO_2 effects on crop yields and considered the affect of adaptation by assessing the country or regional potential for reaching optimal crop yield. The results from the study are presented in Table 3 and Table 4. The simulations showed wheat yield gains under all emissions scenarios by 2020 and for five emission scenarios by 2050 and 2080 respectively. The impact of climate change on rice yield depended upon the emission scenario; the B1 and B2 emissions scenarios were associated with more pessimistic yield changes than under the A1FI and A2 scenarios. Maize yield was simulated to increase above baseline with climate change by 2020 but declined below baseline levels for time horizons thereafter.

Scenario	Year	Wheat	Rice	Maize
	2020	4.08	2.08	0.62
	2050	-0.37	-1.37	-5.01
A1FI	2080	2.00	1.00	-8.00
	2020	4.63	2.63	1.37
	2050	4.60	2.60	-1.78
A2a	2080	3.13	2.13	-6.11
	2020	2.25	0.25	1.20
	2050	2.78	0.78	-1.96
A2b	2080	2.00	1.00	-6.70
	2020	3.47	1.47	0.20
	2050	3.11	1.11	-1.72
A2c	2080	2.81	1.81	-8.40
	2020	1.05	-0.95	-0.32
	2050	-0.17	-1.17	-3.61
B1a	2080	-0.14	-3.14	-5.76
	2020	1.46	-0.54	-0.61
	2050	0.94	-0.06	-3.24
B2a	2080	2.68	1.68	-2.52
	2020	1.86	-0.14	0.21
	2050	0.98	-0.02	-2.79
B2b	2080	-1.23	-2.23	-4.39

Table 3. *Rice and maize yield changes (%) relative to baseline scenario (1970-2000) for different emission scenarios and future time periods. Some emissions scenarios were run in an ensemble simulation (e.g. A2a, A2b, A2c). Data is from Iglesias and Rosenzweig (2009).*

	Wheat		Rice		Maize	
	Up	Down	Up	Down	Up	Down
Baseline to 2020	7	0	4	3	5	2
Baseline to 2050	5	2	3	4	0	7
Baseline to 2080	5	2	5	2	0	7
2020 to 2050	1	6	3	4	0	7
2050 to 2080	2	5	3	4	1	6

Table 4*. The number of emission scenarios that predict yield gains ("Up") or yield losses ("Down") for rice and maize between two points in time. Data is from Iglesias and Rosenzweig (2009).*

A comprehensive assessment of climate change over the USA was undertaken by Karl et al. (2009). The summary of this meta-analysis, in terms of projected future crop yield in the country, is that although many crops showed positive responses to low levels of warming and elevated CO_2, higher levels of warming often negatively affected growth and yield. The meta-analysis comments that the findings of Hatfield et al (2008) of relatively low optimal temperatures for development of grain and soybean mean that that they will increasingly begin to experience failure as warming proceeds.

Arnell et al. (2010a) used 5 GCMs to assess the effects of climate scenarios on crop productivity. Specifically, the crop simulation model GLAM-maize was used to simulate the effect of climate change on maize productivity. The model includes a simulation of the affect of CO_2 fertilisation on crop yield. For the USA a loss of between approximately 40% and 52% of yield was projected, relative to the baseline (1961-1990) by 2050 in the absence of adaptation and mitigation strategies, under A1B emissions. Implementing the mitigation strategy A1B-2016-5-L (a 5%/year reduction in emissions from 2016 onwards to a low emissions floor) reduced the negative impact by approximately 20% and 30% in 2050 and 2100 respectively.

Arnell et al. (2010b) applied the same crops model used by Arnell et al. (2010a) to assess the potential impacts on water and food security of a set of defined climate policies. One of the metrics of impact included was the regional change of yield. For wheat, only changes at the global-scale were reported but for soybean projected yield changes at the region or country level were published as bar charts. The results showed all models projected a decrease in yield throughout the 21st century under the SRES A1B emission scenario. When the mitigation scenarios of 2-5% reduction in CO_2 per year were applied to two of the models, the decrease in yield was reduced by between 7-15% depending on the model and the mitigation scenario, demonstrated the potential for mitigation action to reduce the impact of climate change. The detailed results for USA are displayed in Table 5.

	2050	**2085**	**2100**
No mitigation	-30 to -20	-48 to -34	-57 to -40
2050 IPSL	7 to 13	n/a	n/a
2050 CGCM31	9 to 15	n/a	n/a

Table 5. *Range of yield change (%) at three different times in the future as estimated by five GCMs under the SRES A1B emission scenario (Row 1; values show range across the 5 GCMs) and avoided impact on regional soybean production (expressed as % of A1B impact) by 2050 for several mitigation scenarios as simulated with two GCMs (Row 2 and 3). The mitigations scenarios included reductions in emissions from 2016 or 2030 onwards, at rates of 2-5%/year. Data is from Arnell et al. (2010b).*

Elsewhere, recent studies have assessed the impact of climate change on a global-scale and include impact estimates for North America as a whole (Fischer, 2009, Tatsumi et al., 2011). Whilst these studies provide a useful indicator of crop yields under climate change for the North America *region*, it should be noted that the crop yields presented in such cases are

not definitive *national* estimates for the USA only. This is because the yields are averaged over the entire region, which includes other countries as well as the USA.

Fischer (2009) projected global 'production potential' changes for 2050 using the GAEZ (Global Agro-Ecological Zones) crops model with climate change scenarios from the HadCM3 and CSIRO GCMs respectively, under SRES A2 emissions. The impact of future climate on crop yields of rain-fed cereals are presented in Table 6 (relative to yield realised under current climate) for North America. It can be seen that increased CO_2 levels were of benefit to all crops simulated.

	CO_2 fert.	2020s		2050s		2080s	
		CSIRO	HADCM3	CSIRO	HADCM3	CSIRO	HADCM3
Rain-fed wheat	Yes	3	-1	10	-3	7	-2
	No	0	n/a	4	n/a	-3	n/a
Rain-fed maize	Yes	3	7	9	2	7	-1
	No	2	n/a	5	n/a	2	n/a
Rain-fed cereals	Yes	n/a	1	n/a	0	n/a	0
	No	n/a	n/a	n/a	n/a	n/a	n/a
Rain-fed sorghum	Yes	15	n/a	25	n/a	28	n/a
	No	12	n/a	20	n/a	21	n/a

Table 6. *Impacts of climate change on the production potential of rain-fed cereals in current cultivated land (% change with respect to yield realised under current climate), with two GCMs and with and without CO_2 fertilisation ("CO_2 fert.") under SRES A2 emissions. Data is from Fischer (2009).*

Tatsumi et al. (2011) applied an improved version of the GAEZ crop model (iGAEZ) to simulate crop yields on a global scale for wheat, potato, cassava, soybean, rice, sweet potato, maize, green beans. The impact of global warming on crop yields from the 1990s to 2090s was assessed by projecting five GCM outputs under the SRES A1B scenario and comparing the results for crop yields as calculated using the iGAEZ model for the period of 1990-1999. The results for North America are displayed in Table 7.

Wheat	Potato	Cassava	Soybean	Rice	Sweet potato	Maize	Green beans
-9.47	-10.12	-	-5.71	-26.41	-8.12	-6.09	-2.80

Table 7. *Average change in yield (%), during 1990s-2090s in North America. Data is from Tatsumi et al. (2011).*

In addition to the studies looking at the effect of changes in climate and CO_2 concentrations on crop yield, Avnery et al. (2011) investigated the effects of ozone surface exposure on

crop yield losses by 2030 for soybeans, maize and wheat under the SRES A2 and B1 scenarios respectively. Two metrics of ozone exposure were investigated; seasonal daytime (08:00-19:59) mean O_3 ("M12") and accumulated O_3 above a threshold of 40 ppbv ("AOT40"). The affect of the ozone exposure was considered in isolation from climate and other changes. The results for the USA are presented in Table 8.

	A2		B1	
	M12	**AOT40**	**M12**	**AOT40**
Soybeans	15-20	10-15	10-15	8-10
Maize	6-8	2-4	4-6	0-2
Wheat	4-6	15-20	2-4	8-10

Table 8. *National relative crop yield losses (%) for 2030 under A2 and B1 emission scenarios according to the M12 (seasonal daytime (08:00–19:59) mean) and AOT40 (accumulated O_3 above a threshold of 40 ppbv) metrics of O_3 exposure. Data is from Avnery et al. (2011).*

National-scale or sub-national scale assessments

Literature searches yielded no results for national-scale or sub-national scale studies for this impact sector.

AVOID programme results

To further quantify the impact of climate change on crops, the AVOID programme simulated the effect of climate change on the suitability of land for crop cultivation for all countries reviewed in this literature assessment based upon the patterns of climate change from 21 GCMs (Warren et al., 2010). This ensures a consistent methodological approach across all countries and takes consideration of climate modelling uncertainties.

Methodology

The effect of climate change on the suitability of land for crop cultivation is characterised here by an index which defines the percentage of cropland in a region with 1) a decrease in suitability or 2) an increase in suitability. A threshold change of 5% is applied here to characterise decrease or increase in suitability. The crop suitability index is calculated at a spatial resolution of 0.5°x0.5°, and is based on climate and soil properties (Ramankutty et al., 2002). The baseline crop suitability index, against which the future changes are measured, is

representative of conditions circa 2000. The key features of the climate for the crop suitability index are temperature and the availability of water for plants. Changes in these were derived from climate model projections of future changes in temperature and precipitation, with some further calculations then being used to estimate actual and potential evapotranspiration as an indicator of water availability. It should be noted that changes in atmospheric CO_2 concentrations can decrease evapotranspiration by increasing the efficiency of water use by plants (Ramankutty et al., 2002), but that aspect of the index was not included in the analysis here. Increased CO_2 can also increase photosynthesis and improve yield to a small extent, but again these effects are not included. Exclusion of these effects may lead to an overestimate of decreases in suitability.

The index here is calculated only for grid cells which contain cropland circa 2000, as defined in the global crop extent data set described by Ramankutty et al. (2008) which was derived from satellite measurements. It is assumed that crop extent does not change over time. The crop suitability index varies significantly for current croplands across the world (Ramankutty et al., 2002), with the suitability being low in some current cropland areas according to this index. Therefore, while climate change clearly has the potential to decrease suitability for cultivation if temperature and precipitation regimes become less favourable, there is also scope for climate change to increase suitability in some existing cropland areas if conditions become more favourable in areas where the suitability index is not at its maximum value of 1. It should be noted that some areas which are not currently croplands may already be suitable for cultivation or may become suitable as a result of future climate change, and may become used a croplands in the future either as part of climate change adaptation or changes in land use arising for other reasons. Such areas are not included in this analysis.

Results

Crop suitability was estimated under the pattern of climate change from 21 GCMs with two emissions scenarios; 1) SRES A1B and 2) an aggressive mitigation scenario where emissions follow A1B up to 2016 but then decline at a rate of 5% per year thereafter to a low emissions floor (denoted A1B-2016-5-L). The application of 21 GCMs is an attempt to quantify the uncertainty due to climate modelling, although it is acknowledged that only one crop suitability impacts model is applied. Simulations were performed for the years 2030, 2050, 2080 and 2100. The results for the USA are presented in Figure 2.

Under all the climate projections, some existing cropland areas in the USA become less suitable for cultivation while other existing cropland areas become more suitable. The areas of increased and decreased suitability differ considerably according to the climate model

used, but some common trends can be discerned. The areas experiencing declining suitability become larger through the 21st century in both the A1B and mitigation scenario, but the increase is larger in A1B. The difference between model projections of this quantity also becomes larger over time, and also becomes larger under A1B than the mitigation scenario.

However, the range of areas projected to experience increased suitability is relatively small at only 2%-15% in 2030 in both scenarios, with the upper projection rising to approximately 20% in both scenarios by 2100. Most models project improving suitability over less than 10% of current USA cropland areas throughout the 21st Century.

In 2030, the mean and spread of projected areas of declining suitability is the same both scenarios, with the mean being 31% and the spread being 7% to 53%. Over the 21st century, the projected area of declining suitability becomes larger in both scenarios, while the difference between model projections also becomes larger over time. The growth in area of declining suitability is greater in A1B than the mitigation scenario, rising to 18% to 94% by 2100 in A1B compared to 10% to 73% under the mitigation scenario.

So, for the USA, the areas of current croplands becoming less suitable for cultivation are projected to be smaller under the mitigation scenario than the A1B scenario, and under both scenarios the area of declining suitability is larger than that of increasing suitability (which remains small over the 21st century in both scenarios).

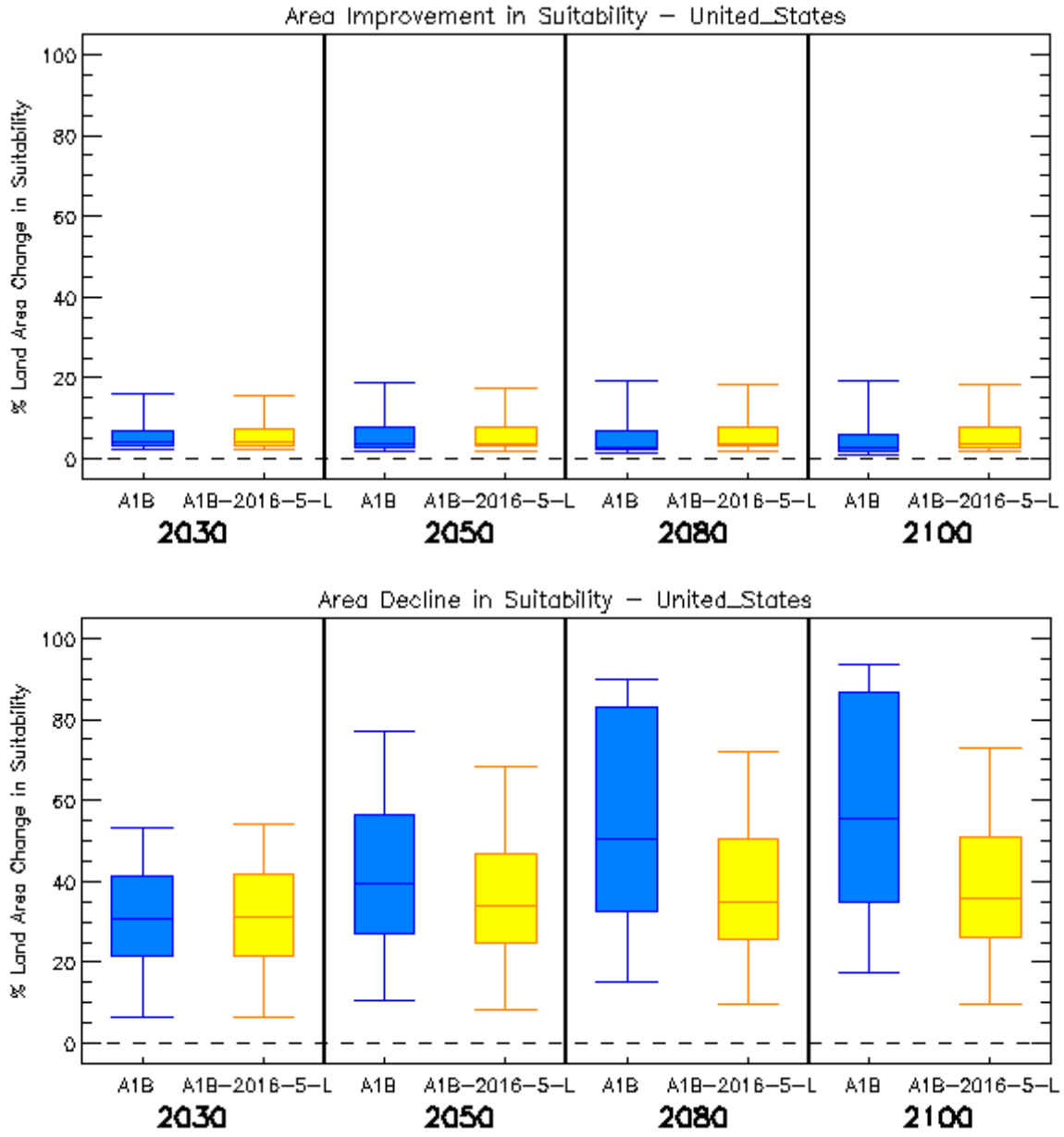

Figure 2. *Box and whisker plots for the impact of climate change on increased crop suitability (top panel) and decreased crop suitability (bottom panel) for the USA, from 21 GCMs under two emissions scenarios (A1B and A1B-2016-5-L), for four time horizons. The plots show the 25th, 50th, and 75th percentiles (represented by the boxes), and the maximum and minimum values (shown by the extent of the whiskers).*

Food security

Headline

Several studies suggest that the USA could remain food secure under climate change scenarios, largely due to its high adaptive capacity associated with an ability to import food. Research by the AVOID programme shows that the USA may avoid major food security issues under climate change by implementing structural adjustments, such as diverting food away from exports and animal feed.

New knowledge since the IPCC AR4 regards the response of marine capture fisheries to climate change for the USA. Recent studies suggest that the national economy of the USA presents a very low vulnerability to climate change impacts on fisheries, however further studies are required to increase confidence in this conclusion.

Supporting literature

Introduction

Food security is a concept that encompasses more than just crop production, but is a complex interaction between food availability and socio-economic, policy and health factors that influence access to food, utilisation and stability of food supplies. In 1996 the World Food Summit defined food security as existing 'when all people, at all times, have physical and economic access to sufficient, safe and nutritious food to meet their dietary needs, and their food preferences are met for an active and healthy life'. As such this section cannot be a comprehensive analysis of all the factors that are important in determining food security, but does attempt to assess a selection of the available literature on how climate change, combined with projections of global and regional population and policy responses, may influence food security.

Assessments that include a global or regional perspective

The USA is not a country of high concern in terms of food security, particularly in a global context. According to FAO statistics the USA has extremely low levels of undernourishment, (less than 5% of the population). Moreover, a number of global studies

suggest that the USA could remain food secure under climate change scenarios, largely due to its high adaptive capacity associated with an ability to import food (Wu et al., 2011) and/or to make food production related-structural adjustments (Arnell et al., 2010b).

A study on food security by Wu et al. (2011) simulated crop yields with the GIS-based Environmental Policy Integrated Climate (EPIC) model. This was combined with crop areas simulated by a crop choice decision model to calculate total food production and per capita food availability across the globe, which was used to represent the status of food availability and stability. The study focussed on the SRES A1 emission scenario and applied climate change simulations for the 2000s (1991–2000) and 2020s (2011–2020). The climate simulations were performed by MIROC (Model for Interdisciplinary Research on Climate) version 3.2., which means the effects of climate model uncertainty were not considered. Downscaled population and GDP data from the International Institute for Applied Systems Analysis (IIASA) were applied in the simulations. The conclusion of this study, based on crop model and crop decision information, was that whilst much of central and eastern USA become more vulnerable to food insecurity between 2000 and 2020, the population could still be food-secure because they rely less on subsistence agriculture than other countries and the USA also possesses a high capability of importing food due to the strong purchasing power and financial support. Moreover, the USA presents substantial adaptive capacity and proactive food management systems, which help offset potential increases in food insecurity.

A further study by Falkenmark et al. (2009), gave results which looked at projections of available water for crops suggested, somewhat contrary to the conclusions above, that the USA could be a food exporting country in 2050, because food production will be sufficient enough to not require food imports or shifts in agriculture. This was based upon a global analysis of food security under climate change scenarios that considered the importance of water availability for ensuring global food security. The study did not include analysis of potential changes in yield of major crops, due to changes in temperature or other climate and non-climate factors. The study presents an analysis of water constraints and opportunities for global food production on current croplands and assesses five main factors:

1) how far improved land and water management might go towards achieving global food security,

2) the water deficits that would remain in regions currently experiencing water scarcity and which are aiming at food self-sufficiency,

3) how the water deficits above may be met by importing food,

4) the cropland expansion required in low income countries without the needed purchasing power for such imports, and

5) the proportion of that expansion pressure which could remain unresolved due to potential lack of accessible land.

Similar to the study presented by Wu et al. (2011), there is no major treatment of modelling uncertainty; simulations were generated by only the LPJml dynamic global vegetation and water balance model (Gerten et al. 2004) with population growth and climate change under the SRES A2 emission scenario. Falkenmark et al. (2009) summarise the impacts of future improvements (or lack thereof) in water productivity for each country across the globe and show that this generates either a deficit or a surplus of water in relation to food water requirements in each country. These can be met either by trade or by horizontal expansion (by converting other terrestrial ecosystems to crop land).

Arnell et al. (2010b) demonstrate how important adaptation measures could be for the USA, if major food security issues are to be avoided under climate change. The study considered the impacts of global climate change and mitigation scenario on food security for eleven countries. The study applied climate change patterns from the HadCM3 GCM and explored food security under two emissions scenarios; a business as usual scenario (SRES A1B) and four mitigations scenarios where emissions peak in 2030 and subsequently reduce at 2% per year to a high emissions floor (referred to as 2030-2-H) or 5% per year to a low emissions floor (2030-5-L), or where they peak in 2016 and subsequently reduce at 2% per year to a high emissions floor (referred to as 2016-2-H) or 5% per year to a low emissions floor (2016-5-L). The study also considered a series of structural adjustments that could be made in the future to adapt to food security issues, including that 1) if there is a shortfall of any per-capita food availability due to crop yield and/or population changes, then original (baseline) food amounts are made up by reducing or removing export amounts; and 2) if, after the above adjustments, there is still a shortfall, then the amount of crops going to animal feed is reduced or removed to try to make up to the original (baseline) food amounts. The model simulations presented by Arnell et al. (2010b) characterise the numbers of people *exposed to undernourishment* in the absence of increased crop production and imports, not actual numbers of undernourished people. The results are presented in Figure 3. Arnell et al. (2010b) showed that under the A1B scenario, the USA population could increase by 40% by 2050, which, coupled with decreases in major crops yields of up to 26% and no structural adjustments, could result in 81% of the USA population being exposed to undernourishment. However, with structural adjustments incorporated into the simulations, Arnell et al. (2010b)

found that 8% of the USA population was exposed to undernourishment in 2100 under A1B, 4% under both 2016-2-H and 2030-5-L, and 2% under the 2016-5-L scenario.

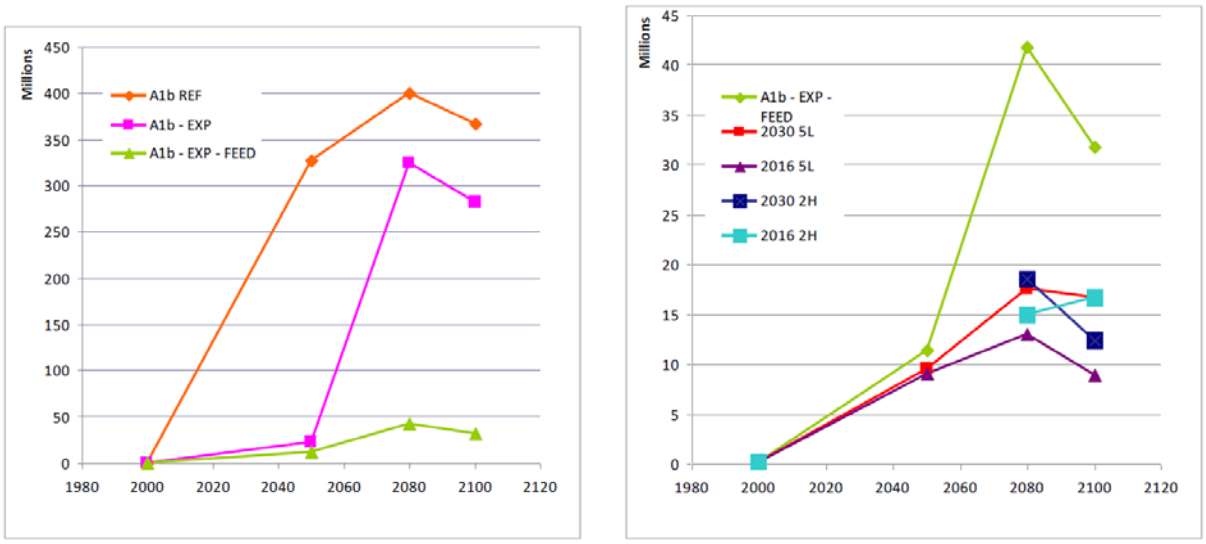

Figure 3. *Total projected population exposed to undernourishment in the USA. The left panel shows total exposure under the A1B emissions scenario ("A1b REF"), plus the A1B scenario with exports reduced or removed ("A1b–EXP") and the A1B scenario with exports removed and allocation to feed reduced or removed ("A1b–EXP–FEED"). The right panel shows the total exposure under the A1b–EXP–FEED and three mitigation scenarios. The figure is from Arnell et al. (2010b).*

The International Food Policy Research Institute (IFPRI) have produced a report and online tool that describes the possible impact of climate change on two major indicators of food security; 1) the number of children aged 0-5 malnourished, and 2) the average daily kilocalorie availability (Nelson et al., 2010, IFPRI, 2010)**.** The study considered three broad socio-economic scenarios; 1) a 'pessimistic' scenario, which is representative of the lowest of the four GDP growth rate scenarios from the Millennium Ecosystem Assessment GDP scenarios and equivalent to the UN high variant of future population change, 2) a 'baseline' scenario, which is based on future GDP rates estimated by the World Bank and a population change scenario equivalent to the UN medium variant, and 3) an 'optimistic' scenario that is representative of the highest of the four GDP growth rate scenarios from the Millennium Ecosystem Assessment GDP scenarios and equivalent to the UN low variant of future population change. Nelson et al. (2010) also considered climate modelling and emission uncertainty. The study applied two GCMs, the CSIRO GCM and the MIROC GCM, and forced each GCM with two SRES emissions scenarios (A1B and B1). They also considered a no climate change emissions scenario, which they called 'perfect mitigation' (note that in most other climate change impact studies that this is referred to as the baseline). IFPRI have not published projections for child malnourishment in the USA but information on average

daily kilocalorie availability has been made available. Table 9 displays the average daily kilocalorie availability simulated under different climate and socioeconomic scenarios for the USA and Figure 4 displays the effect of climate change, calculated by comparing the 'perfect mitigation' scenario with each baseline, optimistic and pessimistic scenario. Whilst by 2050 climate change is attributable for up to almost 8% decline in kilocalorie availability, the absolute value of available kilocalories remains high (above 3,000) under all scenarios, which suggests the USA may not face food security issues in 2050.

Scenario	2010	2050
Baseline CSI A1B	3589	3616
Baseline CSI B1	3594	3640
Baseline MIR A1B	3573	3544
Baseline MIR B1	3584	3598
Baseline Perfect Mitigation	3635	3829
Pessimistic CSI A1B	3650	3428
Pessimistic CSI B1	3655	3450
Pessimistic MIR A1B	3633	3358
Pessimistic MIR B1	3641	3394
Pessimistic Perfect Mitigation	3697	3625
Optimistic CSI A1B	3615	3796
Optimistic CSI B1	3620	3815
Optimistic MIR A1B	3598	3712
Optimistic MIR B1	3606	3750
Optimistic Perfect Mitigation	3661	4015

Table 9. *Average daily kilocalorie availability simulated under different climate and socioeconomic scenarios, for the USA (IFPRI, 2010).*

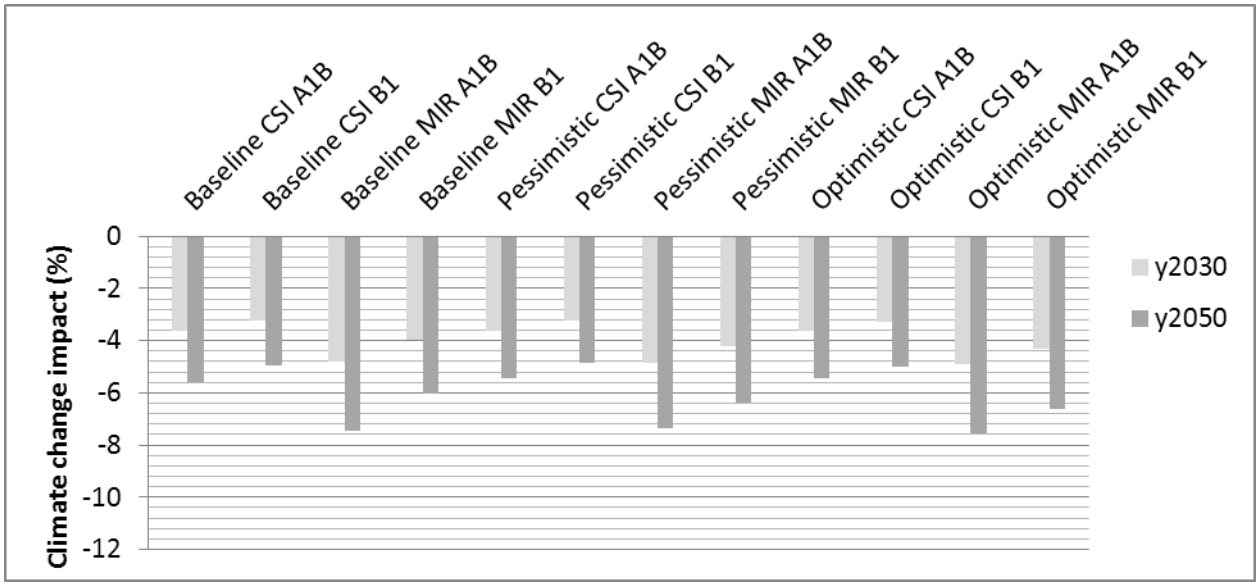

Figure 4*. The impact of climate change on average daily kilocalorie availability for the USA (IFPRI, 2010).*

It is important to note that up until recently, projections of climate change impacts on global food supply have tended to focus solely on production from terrestrial biomes, with the large contribution of animal protein from marine capture fisheries often ignored. However, recent studies that are applicable to the USA have attempted to address this knowledge gap (Allison et al., 2009, Cheung et al., 2010) In addition to the direct affects of climate change, changes in the acidity of the oceans, due to increases in CO_2 levels, could also have an impact of marine ecosystems, which could also affect fish stocks. However, this relationship is complex and not well understood, and studies today have not been able to begin to quantify the impact of ocean acidification on fish stocks.

Allison et al. (2009) present a global analysis that compares the vulnerability of 132 national economies to potential climate change impacts on their capture fisheries. The study considered a country's vulnerability to be a function of the combined effect of projected climate change, the relative importance of fisheries to national economies and diets, and the national societal capacity to adapt to potential impacts and opportunities. Climate change projections from a single GCM under two emissions scenarios (SRES A1FI and B2) were used in the analysis. Allison et al. (2009) concluded that the national economy of the USA presented a very low vulnerability to climate change impacts on fisheries, in similarity with much of western Europe (see Figure 5). It should be noted, however, that results from studies that have applied only a single climate model or climate change scenario should be interpreted with caution. This is because they do not consider other possible climate change

scenarios which could result in a different impact outcome, in terms of magnitude and in some cases sign of change.

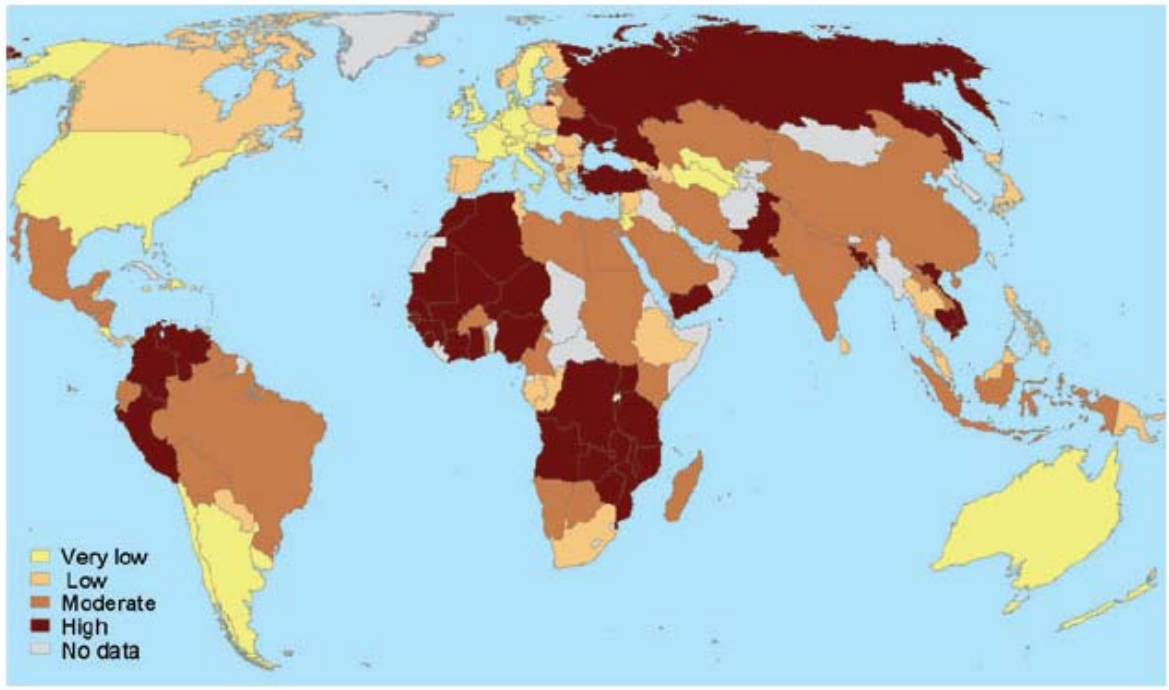

Figure 5. *Vulnerability of national economies to potential climate change impacts on fisheries under SRES B2 (Allison et al., 2009). Colours represent quartiles with dark brown for the upper quartile (highest index value), yellow for the lowest quartile, and grey where no data were available.*

Another study, presented by Cheung et al. (2010), highlights the importance of regional variations in fish food supply across the USA. The study projected changes in global catch potential for 1066 species of exploited marine fish and invertebrates from 2005 to 2055 under climate change scenarios. Cheung et al. (2010) found that climate change may lead to large-scale redistribution of global catch potential, with an average of 30–70% increase in high-latitude regions and a decline of up to 40% in the tropics. The simulations were based climate simulations from a single GCM (GFDL CM2.1) under a SRES A1B emissions scenario (CO_2 concentration at 720ppm in 2100) and a stable-2000 level scenario (CO_2 concentration maintains at year 2000 level of 365 ppm). The limitations of applying a single GCM have been mentioned previously. The projected change in the 10-year averaged maximum catch potential, for the USA (excluding Alaska and Hawaii), between 2005 to 2055 was around a 13% and 8% decrease under the A1B and stabilisation scenarios respectively. However, when Alaska was considered in isolation of the rest of the USA, the projected changes between 2005 and 2055 were around a 24% and 13% *increase* under the A1B and

stabilisation scenarios respectively. Figure 6 demonstrates how this compares with projected changes for other countries across the globe, which highlights that Alaska, is one of the regions that might experience the largest increases in catch potential under climate change.

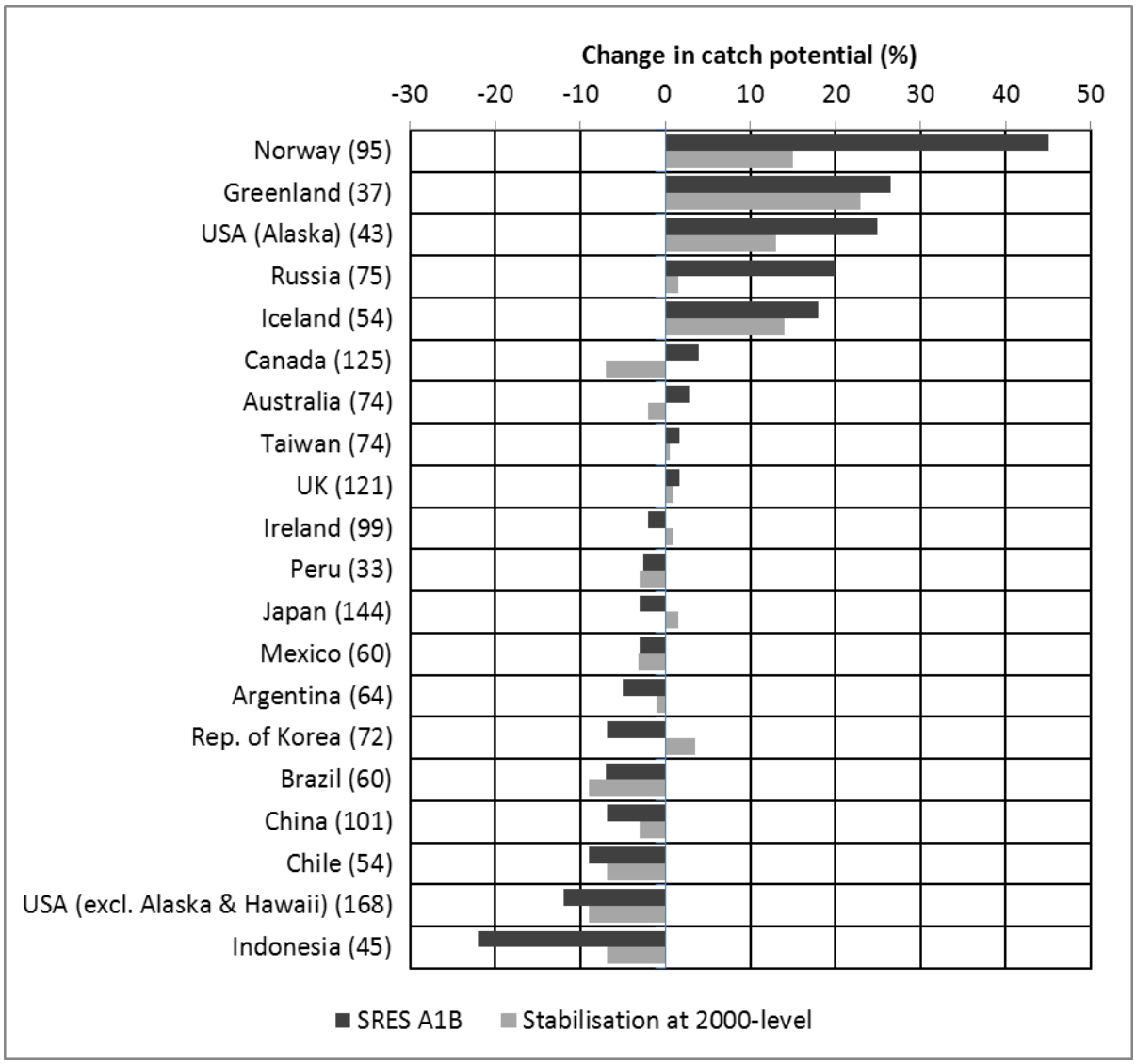

***Figure 6**. Projected changes in the 10-year averaged maximum catch potential from 2005 to 2055. The numbers in parentheses represent the numbers of exploited species included in the analysis. Adapted from Cheung et al. (2010).*

National-scale or sub-national scale assessments

Literature searches yielded no results for national-scale or sub-national scale studies for this impact sector.

Water stress and drought

Headline

Recent work confirms reports from the IPCC AR4 that annual mean precipitation could decrease in the southwest USA with climate change. Moreover, droughts could become more frequent and severe in this region. Recent assessments indicate that much of the USA's population is not currently exposed to a human water security threat, but that there are widespread limits to the amount of water made available for environmental water requirements. Projections of water stress with climate change from studies that consider some of the inherent uncertainties in producing such projections indicate that water stress could increase moderately in the USA. Recent simulations by the AVOID programme further confirm this. The north-west and south-east could exhibit the greatest increases in water stress, whilst some basins of mid-western USA could see a slight decrease in water stress with climate change, although there is uncertainty associated with this.

Supporting literature

Introduction

For the purposes of this report droughts are considered to be extreme events at the lower bound of climate variability; episodes of prolonged absence or marked deficiency of precipitation. Water stress is considered as the situation where water stores and fluxes (e.g. groundwater and river discharge) are not replenished at a sufficient rate to adequately meet water demand and consumption.

This section of the review considers droughts to be extreme events at the lower bound of climate variability; episodes of prolonged absence or marked deficiency of precipitation. Water stress is considered as the situation where water stores and fluxes (e.g. groundwater and river discharge) are not replenished at a sufficient rate to adequately meet water demand and consumption.

A number of impact model studies looking at water stress and drought for the present (recent past) and future (climate change scenario) have been conducted. These studies are conducted at global or national scale and include the application of global water 'availability' or 'stress' models driven by one or more climate change scenario from one or more GCM. The approaches variously include other factors and assumptions that might affect water availability, such as the impact of changing demographics and infrastructure investment, etc. These different models (hydrological and climate), assumptions and emissions scenarios mean that there are a range of water stress projections for the USA. This section summarises findings from these studies to inform and contextualise the analysis performed by the AVOID programme for this project. The results from the AVOID work and discussed in the next section.

Important knowledge gaps and key uncertainties which are applicable to the USA as well as at the global-scale, include; the appropriate coupling of surface water and groundwater in hydrological models, including the recharge process, improved soil moisture and evaporation dynamics, inclusion of water quality, inclusion of water management (Wood et al. 2011) and further refinement of the down-scaling methodologies used for the climate driving variables (Harding et al. 2011).

Assessments that include a global or regional perspective

Recent past

Recent research presented by Vörösmarty et al. (2010) describes the calculation of an '*Adjusted Human Water Security Threat'* (HWS) indicator. The indicator is a function of the cumulative impacts of 23 biophysical and chemical drivers simulated globally across 46,517 grid cells representing 99.2 million km^2. With a digital terrain model at its base, the calculations in each of the grid boxes of this model take account of the multiple pressures on the environment, and the way these combine with each other, as water flows in river basins. The level of investment in water infrastructure is also considered. This infrastructure measure (the *investment benefits factor*) is based on actual existing built infrastructure, rather than on the financial value of investments made in the water sector, which is a very unreliable and incomplete dataset. The analysis described by Vörösmarty et al. (2010) represents the current state-of-the-art in applied policy-focussed water resource assessment. In this measure of water security, the method reveals those areas where this is lacking, which is a representation of human water stress. One drawback of this method is that no analysis is provided in places where there is 'no appreciable flow', where rivers do not flow, or only do so for such short periods that they cannot be reliably measured. This method also

does not address places where water supplies depend wholly on groundwater or desalination, being piped in, or based on wastewater reuse. It is based on what is known from all verified peer reviewed sources about surface water resources as generated by natural ecosystem processes and modified by river and other hydraulic infrastructure (Vörösmarty et al., 2010).

Here, the method described by Vörösmarty et al. (2010), is used to estimate present day HWS for the USA to provide detailed national level information. The model applied operates at 50km resolution, so, larger countries appear to have smoother coverage than smaller countries, but all are mapped and calculated on the same scale, with the same data and model, and thus comparisons between places are legitimate. It is important to note that this analysis is a comparative one, where each place is assessed *relative* to the rest of the globe. In this way, this presents a realistic comparison of conditions across the globe. As a result of this, however, some places may seem to be less stressed than may be originally considered. One example is Australia, which is noted for its droughts and long dry spells, and while there are some densely populated cities in that country where water stress is a real issue, for most of the country, *relative to the rest of the world*, the measure suggests water stress (as measured by HWS defined by Vörösmarty et al., (2010)), is not a serious problem.

Figure 7 presents the results of this analysis for the USA. Large areas of the USA have significantly low levels of water security threat.

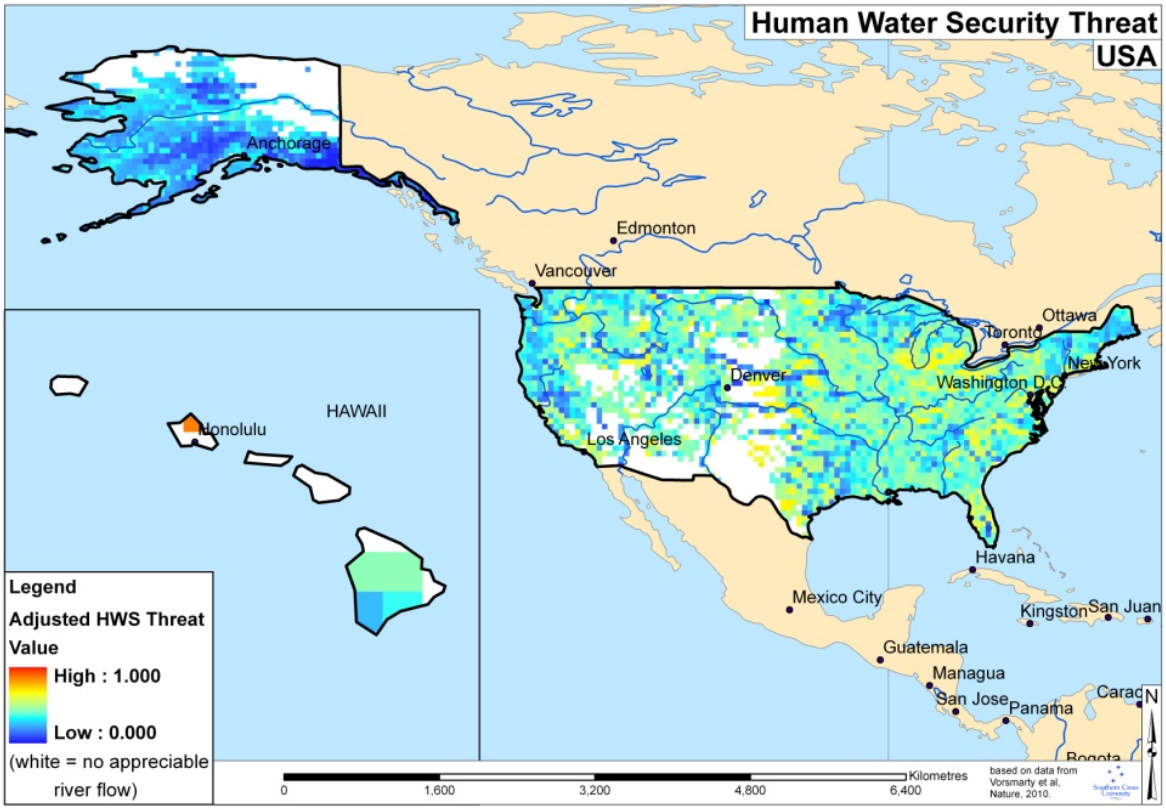

Figure 7. *Present Adjusted Human Water Security Threat (HWS) for the USA, calculated following the method described by Vörösmarty et al. (2010).*

Smakhtin et al. (2004) present a first attempt to estimate the volume of water required for the maintenance of freshwater-dependent ecosystems at the global scale. This total environmental water requirement (EWR) consists of ecologically relevant low-flow and high-flow components. The authors argue that the relationship between water availability, total use and the EWR may be described by the water stress indicator (WSI). If WSI exceeds 1.0, the basin is classified as “environmentally water scarce”. In such a basin, the discharge has already been reduced by total withdrawals to such levels that the amount of water left in the basin is less than EWR. Smaller index values indicate progressively lower water resources exploitation and lower risk of “environmental water scarcity.” Basins where WSI is greater than 0.6 but less than 1.0 are arbitrarily defined as heavily exploited or “environmentally water stressed” and basins where WSI is greater than 0.3 but less than 0.6 are defined as moderately exploited. In these basins, 0-40% and 40-70% of the utilizable water respectively is still available before water withdrawals come in conflict with the EWR. Environmentally “safe” basins are defined as those where WSI is less than 0.3. The global distribution of WSI for the 1961-1990 time horizon is shown in Figure 8. The results demonstrate that in the

west, and south-west of the USA, nearly all basins exhibit high water stress, when considering the EWR, with many catchments displaying a WSI greater than 1.

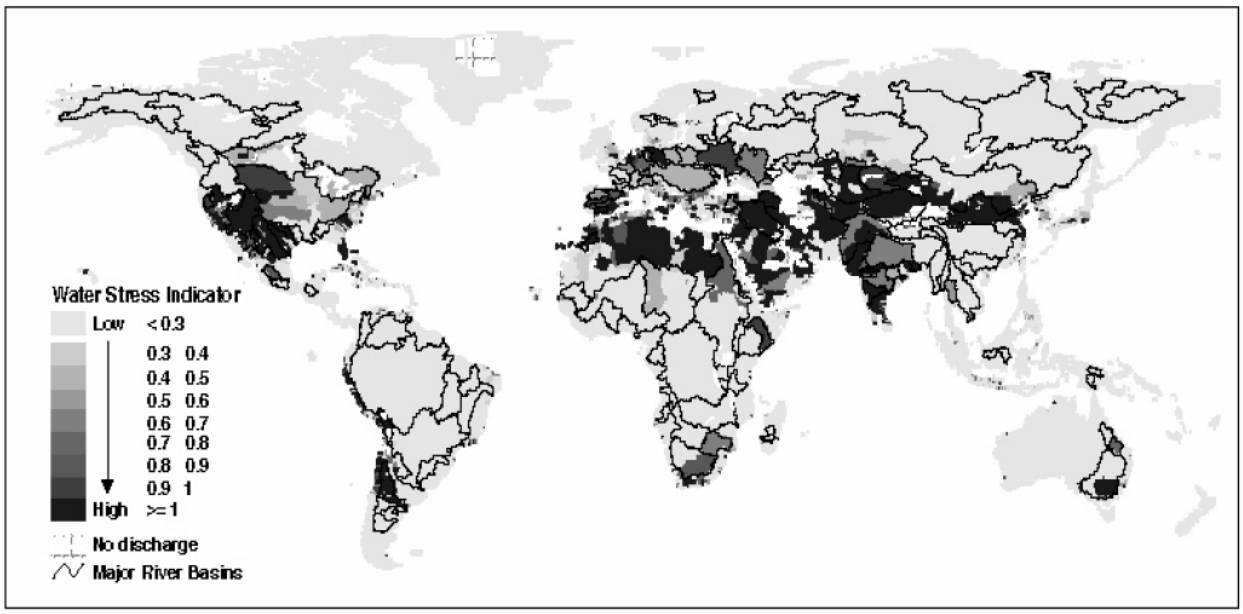

Figure 8. *A map of the major river basins across the globe and the water stress indicator (WSI) for the 1961-1990 time horizon. The figure is from Smakhtin et al. (2004).*

Climate change studies

The IPCC AR4 (2007a) stated that annual mean precipitation is likely to decrease in the southwest USA with climate change. This is confirmed by more recent work. Washington et al. (2009) investigated climate change projections from an aggressive mitigation scenario (CO_2 stabilisation in 2100 at around 450ppm) compared with a non-mitigation scenario (CO_2 concentrations around 740ppm in 2100).They found that that under the non-mitigation scenario, precipitation decreased by around 30-50% in south-western USA. Under the mitigation scenario, the projected values were about half that.

Rockstrom et al. (2009) applied the LPJml vegetation and water balance model (Gerten et al. 2004) to assess green-blue water (irrigation and infiltrated water) availability and requirements. The authors applied observed climate data from the CRU TS2.1 gridded dataset for a present-day simulation, and climate change projections from the HadCM2 GCM under the SRES A2 scenario to represent the climate change scenario for the year 2050. The study assumed that if water availability was less than 1,300m^3/capita/year, then the country was considered to demonstrate insufficient water availability for food self-sufficiency. The simulations presented by Rockstrom et al. (2009) should not be considered as definitive, however, because the study only applied one climate model, which means climate modelling

uncertainty was overlooked. The results from the two simulations are presented in Figure 9. Rockstrom et al. (2009) found that globally in 2050 and under the SRES A2 scenario, around 59% of the world's population could be exposed to "blue water shortage" (i.e. irrigation water shortage), and 36% exposed to "green water shortages" (i.e. infiltrated rain shortage). For the USA, Rockstrom et al. (2009) found that current per capita availability of green-blue water is over 10,000m^3/capita/year in the present climate, and while this is projected to decrease, the country is not expected to fall below the 1,300m^3/capita/year threshold that indicates insufficient water for food self-sufficiency . It should be noted, however, that results from studies that have applied only a single climate model or climate change scenario should be interpreted with caution. This is because they do not consider other possible climate change scenarios which could result in a different impact outcome, in terms of magnitude and in some cases sign of change.

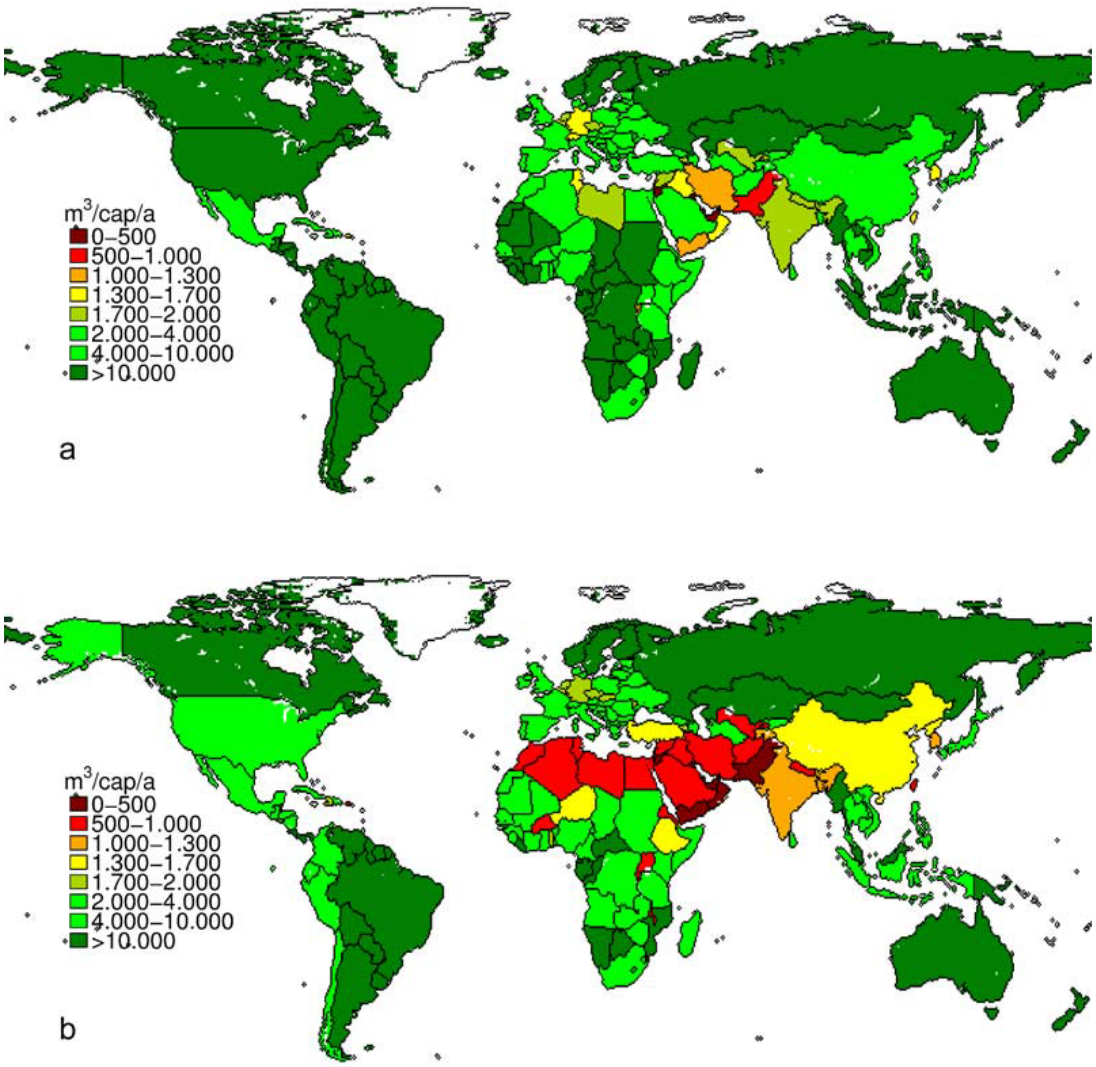

Figure 9. *Simulated blue-green water availability (m^3/capita/year) for present climate (top panel) and including both demographic and climate change under the SRES A2 scenario in 2050 (bottom panel). The study assumed that if water availability was less than 1,300m^3/capita/year, then the country was considered to present insufficient water for food self-sufficiency. The figure is from Rockstrom et al. (2009).*

Doll (2009) presents updated estimates of the impact of climate change on groundwater resources by applying a new version of the WaterGAP hydrological model. The study accounted for the number of people affected by changes in groundwater resources under climate change relative to a baseline period (1961-1990). To this end, the study provides an assessment of the vulnerability of humans to decreases in available groundwater resources (GWR). This indicator was termed the “Vulnerability Index” (VI), defined as; VI = -% change GWR * Sensitivity Index (SI). The SI component was a function of three specific sensitivity indicators that include: an indicator of water scarcity (calculated from the ratio between

consumptive water use to low flows), an indicator for the dependence upon groundwater supplies, and an indicator for the adaptive capacity of the human system. Doll (2009) applied climate projections from two GCMs (ECHAM4 and HadCM3) to WaterGAP, for two scenarios (SRES A2 and B2), for the 2050s. Figure 10 presents each of these four simulations respectively. Simulations with ECHAM4 indicate that areas of the north-west are highly vulnerable to decreases in groundwater, and to a lesser extent large areas of mid-west USA, whilst the HadCM3 simulations indicate that the south, midwest, and north-west are highly vulnerable to decreases in groundwater supplies.

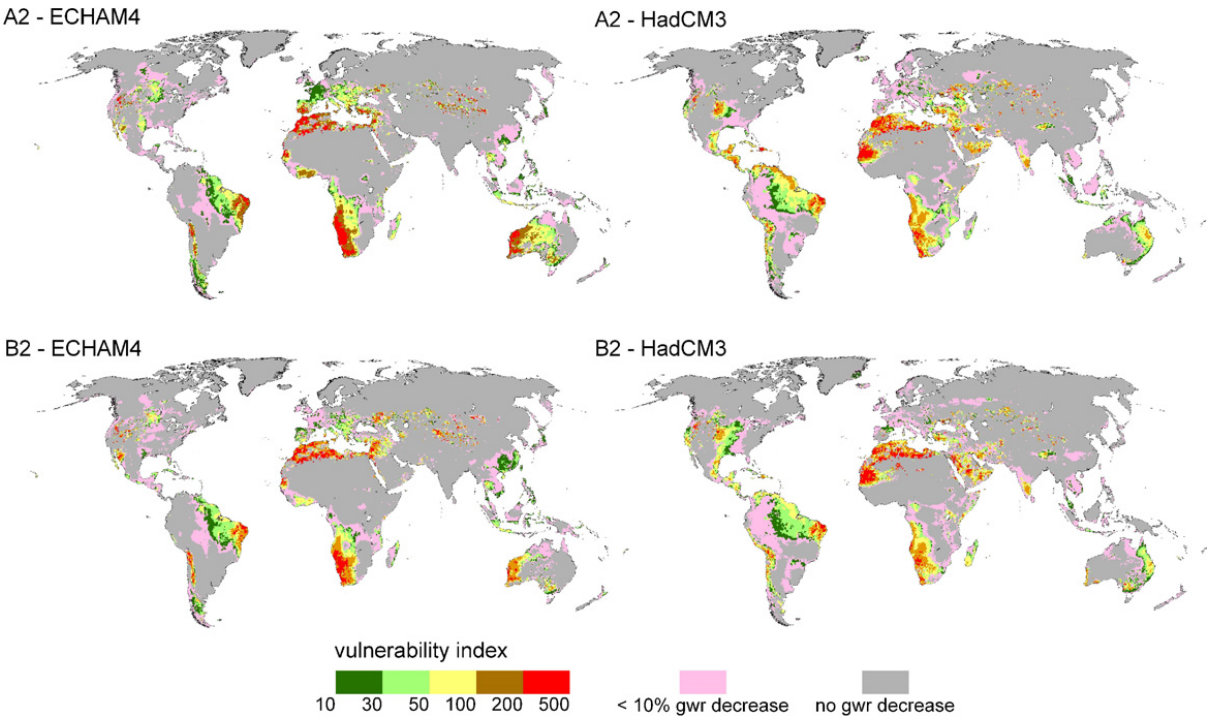

Figure 10. *Vulnerability index (VI) showing human vulnerability to climate change induced decreases of renewable groundwater resources (GWR) by the 2050s under two emissions scenarios for two GCMs. VI is only defined for areas with a GWR decrease of at least 10% relative tobaseline (1961-1990). The figure is from Doll (2009).*

Fung et al. (2011) applied climate change scenarios for prescribed global-mean warming of 2°C and 4°C respectively, from two ensembles; 1) an ensemble of 1518 (2°C world) and 399 (4°C) members from the ClimatePrediction.net (CPDN) experiments, and 2) an ensemble of climate projections from 22 CMIP3 GCMs. The climate projections were applied to the MacPDM global hydrological model (Gosling and Arnell, 2011) and population projections followed the UNPOP60 population scenario. Fung et al. (2011) calculated a water stress index (WSI) based upon resources per capita, similar to the method applied by Rockstrom et

al. (2009). Results from the simulations are presented in Figure 11. There was consensus across models that water stress increases with climate change across large parts of the north-west, central and seastern USA.

It should be noted that the estimates of drying across the globe that are presented by Fung et al. (2011) could be over-estimated slightly. This is because the MacPDM hydrological model is an offline model; i.e. it is not coupled to an ocean-atmosphere GCM. Therefore the dynamical effects of vegetation changes in response to water availability are not simulated. Recent work has highlighted that increased plant water use efficiency under higher CO_2 may ameliorate future increased drought to some extent, but not completely (Betts et al., 2007).

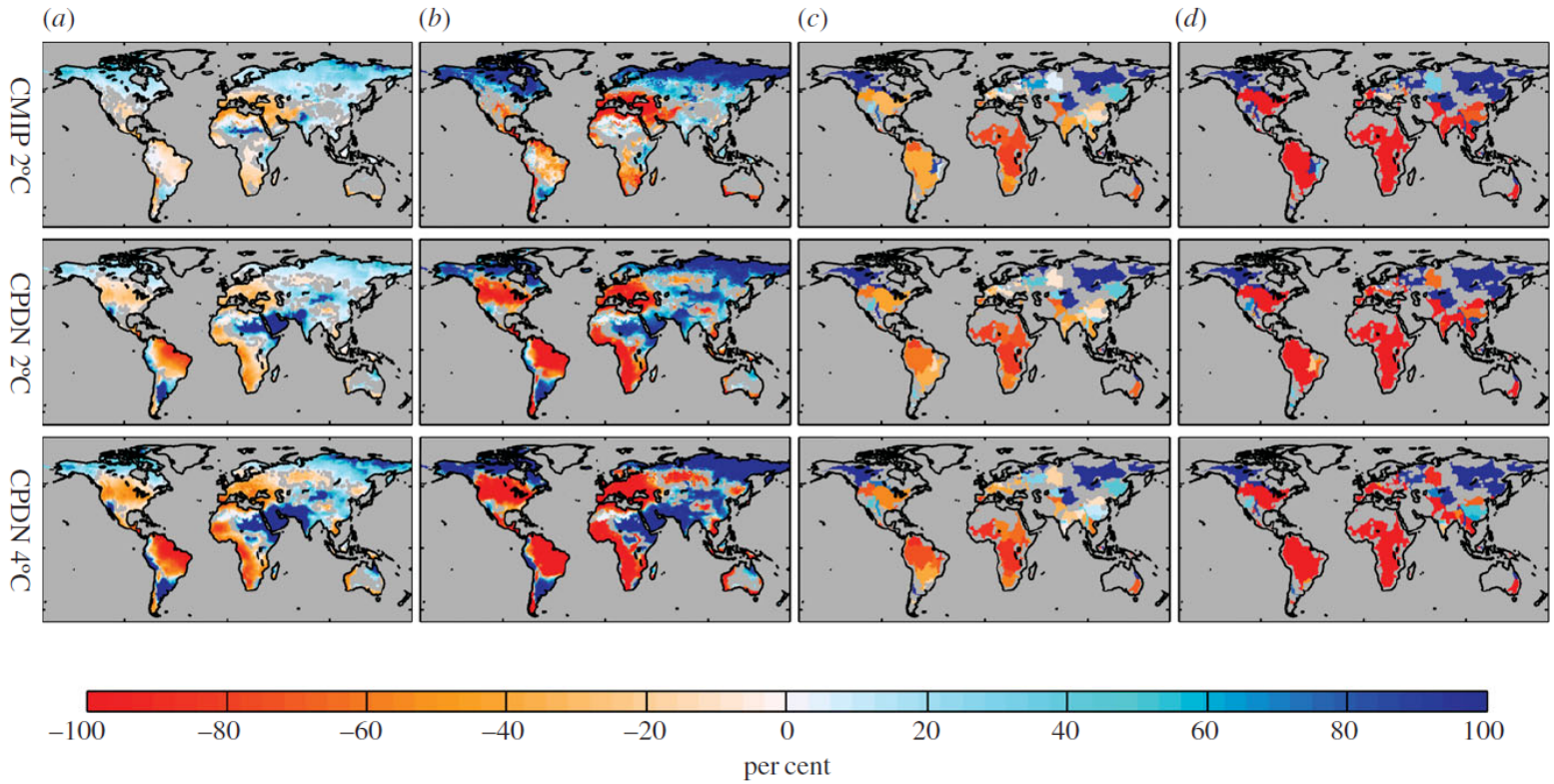

Figure 11. *For a 2°C and 4°C rise in temperature and UNPOP60 population scenario compared with the baseline period (1961-1990); (a) spatial pattern of ensemble-average changes in mean annual run-off (DMAR), (b) model consensus on direction of change in run-off, (c) ensemble-average change in water stress (DWSI) and (d) model consensus on the direction of change in water stress. For the model consensus, red and therefore negative values represent the percentage of models showing a negative change in the respective parameter and for blue, positive values, represent the percentage of models showing a positive change. For DMAR and DWSI, colour classification spans from −100% to greater than 100% (this means that high positive values of DMAR and DWSI are effectively filtered out in these plots), whereas for consensus, colour classification spans from −100% to 100%. For plots of DMAR and consensus for the direction of change in run-off, grey land areas represent where DMAR is less than natural variability. For DWSI and consensus for direction of change in water stress, only 112 major river basins are plotted (Greenland has been excluded from the analysis). The figure is from Fung et al. (2011).*

National-scale or sub-national scale assessments

National-scale studies support results from global-scale assessments (IPCC, 2007a, Washington et al., 2009) that annual mean precipitation could decrease in the south-west USA with climate change. For example, a comprehensive assessment of climate change over the USA was undertaken by Karl et al. (2009). The summary, in terms of future precipitation projections, is that northern areas could become wetter, and southern areas, particularly in the west, could become drier. Trends in drought had strong regional variations. With climate change, Karl et al. (2009) showed that droughts are could become more frequent and severe in some regions, in particular the Southwest. Water supplies could also be limited by early snowmelt in the western US. Both floods and droughts are could become more common and more intense as regional and seasonal precipitation patterns change (Karl et al., 2009).

Observations show that over the past several decades, extended dry periods have become more frequent in parts of the USA, although analyses differ as to whether change has been seen in the southwest. Longer periods between rainfalls, combined with higher air temperatures, dry soils and vegetation, cause drought. With climate change, precipitation intensity is projected to increase, but the number of dry days between precipitation events is also projected to increase, especially in more arid areas (Groisman and Knight, 2008). The authors note that mid-continental areas and the southwest are particularly threatened by future drought.

A study by Hayhoe et al. (2007) projected a general increase in drought frequency in the north-east USA with climate change, particularly under the A1FI emissions scenario where the frequency of short term droughts reaches 1 per year in parts of the north-east by the end of the 21st Century. The authors also found that medium-term drought frequencies increase considerably under A1FI but show only slight changes under the B1 emissions scenario. The maximum drought length, in western New York State, reached over 10 months by 2070-2099 under A1FI. Uncertainties were found in the model's ability to simulate historic severe droughts such as occurred during the 1960s, however. Supporting this, Strzepek et al. (2010) found that the frequency of meteorological drought based upon precipitation alone (measured by the Standardized Precipitation Index (SPI)) is projected to increase in parts of the USA, such as the south-western states, and decrease in others, based upon climate change projections from 22 GCMs under three emissions scenario (A2, A1B and B1); see Figure 12. The area of increasing drought frequency expands with climate change, and the region of lessening frequency contracts over time and with higher emissions. Moreover, the SPI drought measures showed increasing drought frequency under higher emissions for

areas that were prone to more drought, but decreasing frequency for areas that were getting wetter. Hydrological drought, based upon both precipitation and temperature (measured by the Palmer Drought Severity Index (PDSI)), was projected to increase across most of the country, with substantial increases in frequency by 2050; see Figure 12. The south-western USA and the Rocky Mountain states were projected to experience the largest increases in drought frequency. Increased temperatures results in higher rates of evapotranspiration, and reductions in soil moisture. Whilst the spatial pattern of projected precipitation changes varies over the USA, the near uniform increase in temperatures means that hydrological drought projections are likely to be more uniform than meteorological drought projections. There was greater uncertainty (dispersion across the 22 GCMs considered) under the higher emissions SRES scenarios for both drought measures.

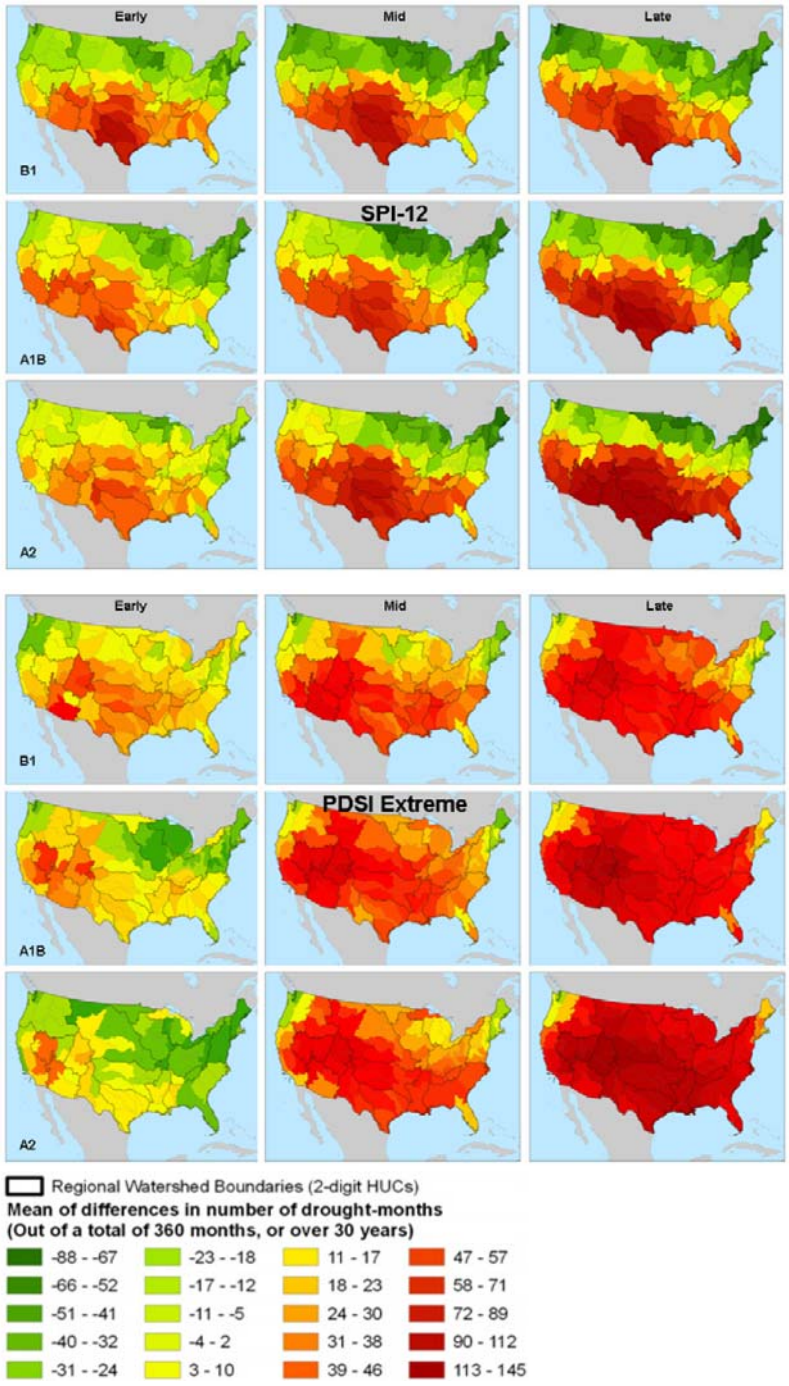

Figure 12. *Top panel shows mean changes across 22 GCMs in SPI drought frequency relative to the 20th century baseline across the SRES scenarios (the vertical axis) and 21st century time periods (the horizontal axis; early, middle, and late 21st century periods of 30 years (2006–35, 2036–65, and 2066–95)). Bottom panel shows mean changes across 22 GCMs in PDSI extreme drought months relative to the 20th century baseline. The figure is from Strzepek et al. (2010).*

Likewise, Wehner et al. (2011) present multi-model mean projections of the PDSI for North America at the end of the 21st Century under the SRES A1B emissions scenario. The authors show that what is currently considered to constitute severe to extreme drought conditions could be normal climatology in the future. Widespread drying was projected over

much of North America at the point in time when the global mean temperature increases by 2.5°C relative to 1900-1990. Moderate drought conditions were projected to be the normal state in the western USA. For continental USA and Mexico, about 35% of the region's climatology was classed as moderate drought and about 5% as extreme drought in this projection.

AVOID Programme Results

To further quantify the impact of climate change on water stress and the inherent uncertainties, the AVOID programme calculated water stress indices for all countries reviewed in this literature assessment based upon the patterns of climate change from 21 GCMs (Warren et al., 2010), following the method described by Gosling et al. (2010) and Arnell (2004). This ensures a consistent methodological approach across all countries and takes consideration of climate modelling uncertainties.

Methodology

The indicator of the effect of climate change on exposure to water resources stress has two components. The first is the number of people within a region with an *increase in exposure to stress*, calculated as the sum of 1) people living in water-stressed watersheds with a significant reduction in runoff due to climate change and 2) people living in watersheds which become water-stressed due to a reduction in runoff. The second is the number of people within a region with a *decrease in exposure to stress*, calculated as the sum of 1) people living in water-stressed watersheds with a significant increase in runoff due to climate change and 2) people living in watersheds which cease to be water-stressed due to an increase in runoff. It is not appropriate to calculate the net effect of "increase in exposure" and "decrease in exposure", because the consequences of the two are not equivalent. A water-stressed watershed has an average annual runoff less than $1000m^3$/capita/year, a widely used indicator of water scarcity. This indicator may underestimate water stress in watersheds where per capita withdrawals are high, such as in watersheds with large withdrawals for irrigation.

Average annual runoff (30-year mean) is simulated at a spatial resolution of $0.5x0.5^o$ using a global hydrological model, MacPDM (Gosling and Arnell, 2011), and summed to the watershed scale. Climate change has a "significant" effect on average annual runoff when

the change from the baseline is greater than the estimated standard deviation of 30-year mean annual runoff: this varies between 5 and 10%, with higher values in drier areas.

The pattern of climate change from 21 GCMs was applied to MacPDM, under two emissions scenarios; 1) SRES A1B and 2) an aggressive mitigation scenario where emissions follow A1B up to 2016 but then decline at a rate of 5% per year thereafter to a low emissions floor (denoted A1B-2016-5-L). Both scenarios assume that population changes through the 21st century following the SRES A1 scenario as implemented in IMAGE 2.3 (van Vuuren et al., 2007). The application of 21 GCMs is an attempt to quantify the uncertainty due to climate modelling, although it is acknowledged that only one impacts model is applied (MacPDM). Simulations were performed for the years 2030, 2050, 2080 and 2100. Following Warren et al. (2010), changes in the population affected by increasing or decreasing water stress represent the additional percentage of population affected due to climate change, not the absolute change in the percentage of the affected population relative to present day.

Results

The results for the USA are presented in Figure 13. Simulations with all GCMs are consistent in showing a moderate increase in water stress under A1B emissions. The proportion of the population experiencing increased water stress peaks around the 2050 for the majority of models, under both emission scenarios. By 2100 the median population exposed to increased water stress due to climate change under the A1B emission scenario is around 7%. This is lower under the mitigation scenario; around 5%.

A number of the climate models also indicate that some of the population will experience decreased water stress, but this proportion is very small, under both emission scenarios throughout the century.

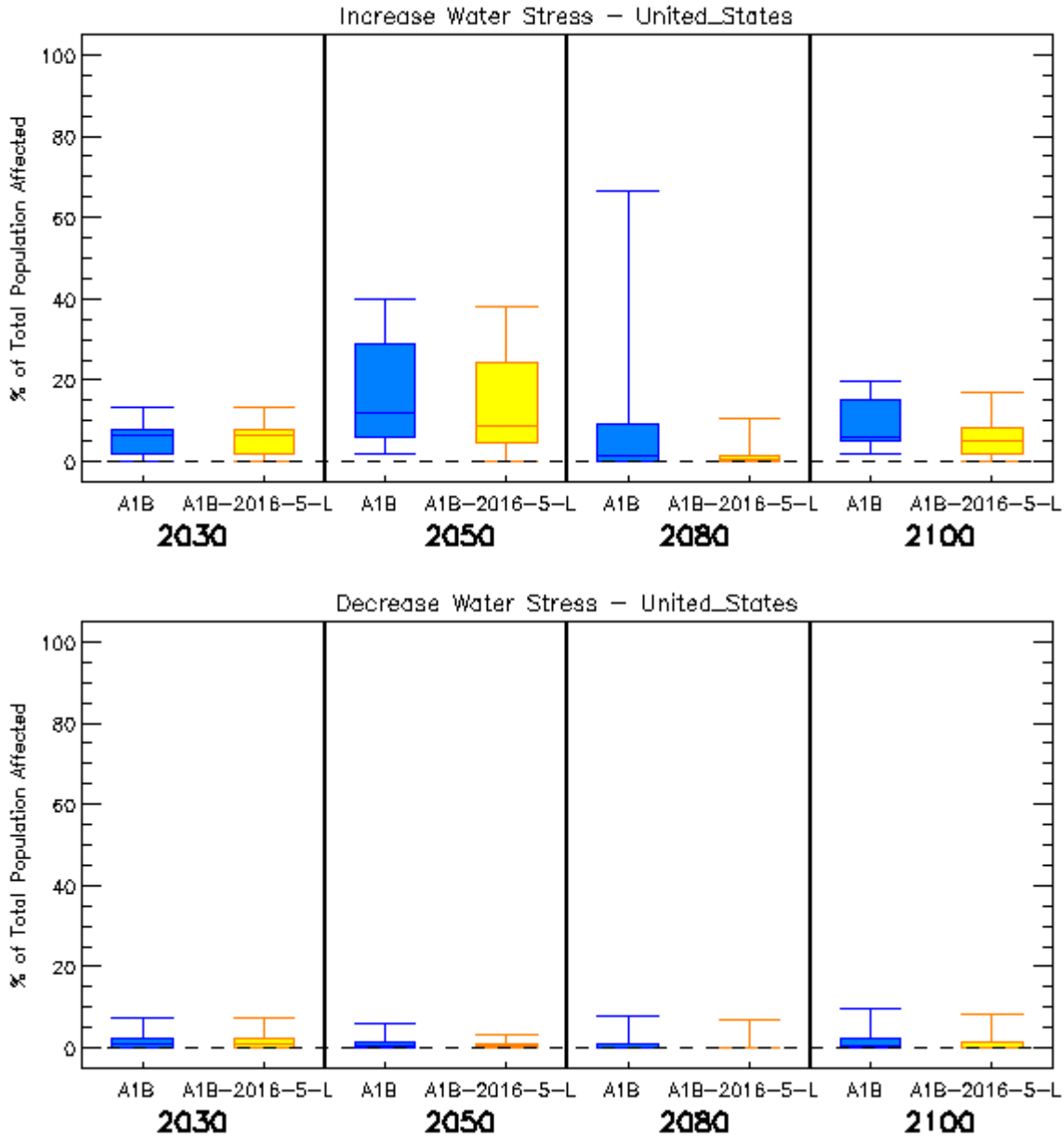

***Figure 13**. Box and whisker plots for the impact of climate change on increased water stress (top panel) and decreased water stress (bottom panel) in the USA, from 21 GCMs under two emissions scenarios (A1B and A1B-2016-5-L), for four time horizons. The plots show the 25th, 50th, and 75th percentiles (represented by the boxes), and the maximum and minimum values (shown by the extent of the whiskers).*

Pluvial flooding and rainfall

Headline

The IPCC AR4 noted that under climate change scenarios, the largest precipitation increases were projected to be in the northeast USA. Studies since then have also pointed to increasing mean and extreme precipitation in the northeast USA, which is suggested in observational analyses and projected in 21st century simulations. Mean precipitation is generally expected to decrease in the southwest USA with smaller changes to extreme precipitation events.

Supporting literature

Introduction

Pluvial flooding can be defined as flooding derived directly from heavy rainfall, which results in overland flow if it is either not able to soak into the ground or exceeds the capacity of artificial drainage systems. This is in contrast to fluvial flooding, which involves flow in rivers either exceeding the capacity of the river channel or breaking through the river banks, and so inundating the floodplain. Pluvial flooding can occur far from river channels, and is usually caused by high intensity, short-duration rainfall events, although it can be caused by lower intensity, longer-duration events, or sometimes by snowmelt. Changes in mean annual or seasonal rainfall are unlikely to be good indicators of change in pluvial flooding; changes in extreme rainfall are of much greater significance. However, even increases in daily rainfall extremes will not necessarily result in increases in pluvial flooding, as this is likely to be dependent on the sub-daily distribution of the rainfall as well as local factors such as soil type, antecedent soil moisture, land cover (especially urbanisation), capacity and maintenance of artificial drainage systems etc. It should be noted that both pluvial and fluvial flooding can potentially result from the same rainfall event.

Assessments that include a global or regional perspective

Climate change studies

The IPCC AR4 (2007a) stated that annual mean precipitation is very likely to increase over northeast USA, and likely to decrease in the southwest USA with climate change. More

recently, a global-scale assessment presented by Sillmann and Roeckner (2008) found increases in extreme precipitation indices in GCM projections for the 21st century over the eastern parts of the USA. Changes were more intense under the A1B emissions scenario compared with the B1 scenario. Similarly, Washington et al. (2009) investigated climate change projections from an aggressive mitigation scenario (CO_2 stabilisation in 2100 at around 450ppm) compared with a non-mitigation scenario (CO_2 concentrations around 740ppm in 2100) at the global-scale. The non-mitigation scenario showed a 5-15% increase in precipitation over the northeast USA and Canada. Precipitation decreased by around 30-50% in the south-western United States. Under the mitigation scenario, the projected values were about half of the non-mitigation scenario.

A comprehensive assessment of climate change for North America was undertaken by Karl et al. (2009). The summary, in terms of future precipitation projections, is that northern areas could become wetter, and southern areas, particularly in the west, could become drier (see Figure 14). Confidence is higher for winter and spring projections, than for summer and fall projections. In some northern areas, warmer temperatures could result in more precipitation falling as rain, as opposed to snow. The amount of rain falling in the heaviest downpours has increased by approximately 20% in the past century, and this trend could continue (Karl et al., 2009), with the largest increases in the wettest locations. Model projections indicate continued increases in the heaviest downpours during this century, but lighter precipitation is projected to decrease (see Figure 15). Heavy downpours that are now 1-in-20-year occurrences are projected to occur about every 4 to 15 years by the end of this century, depending on location, and the intensity of heavy downpours is also projected to increase. The 1-in-20-year heavy downpour is expected to be between 10-25% heavier by the end of the 21st century than it is now (Karl et al., 2009).

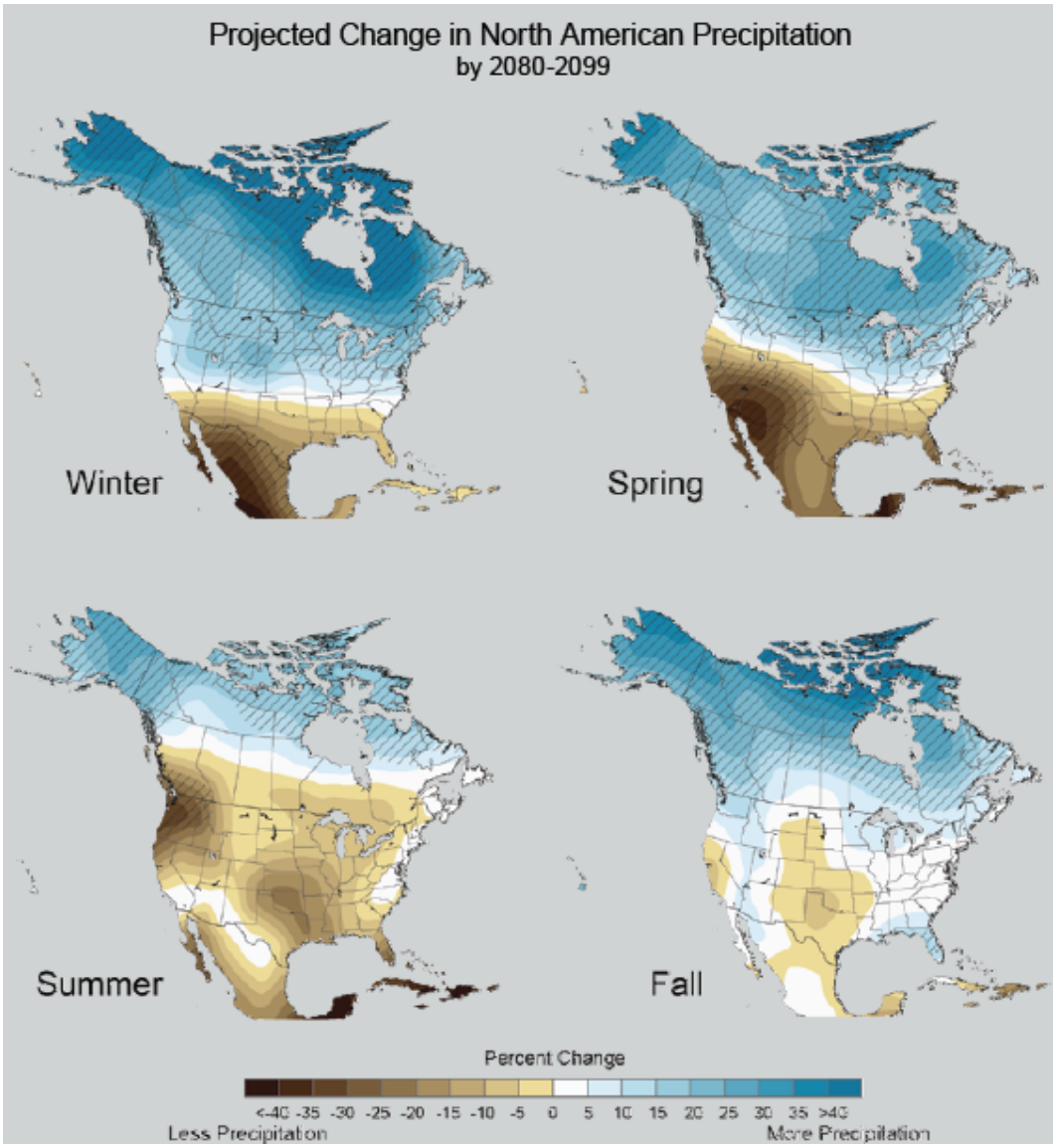

Figure 14. *Maps showing projected future changes in precipitation relative to the recent past as simulated by 15 climate models. The simulations are for the late 21st century under a high emissions scenario. High agreement across the 15 climate models in the sign of change is denoted by the hatched areas. The figure is from Karl et al. (2009).*

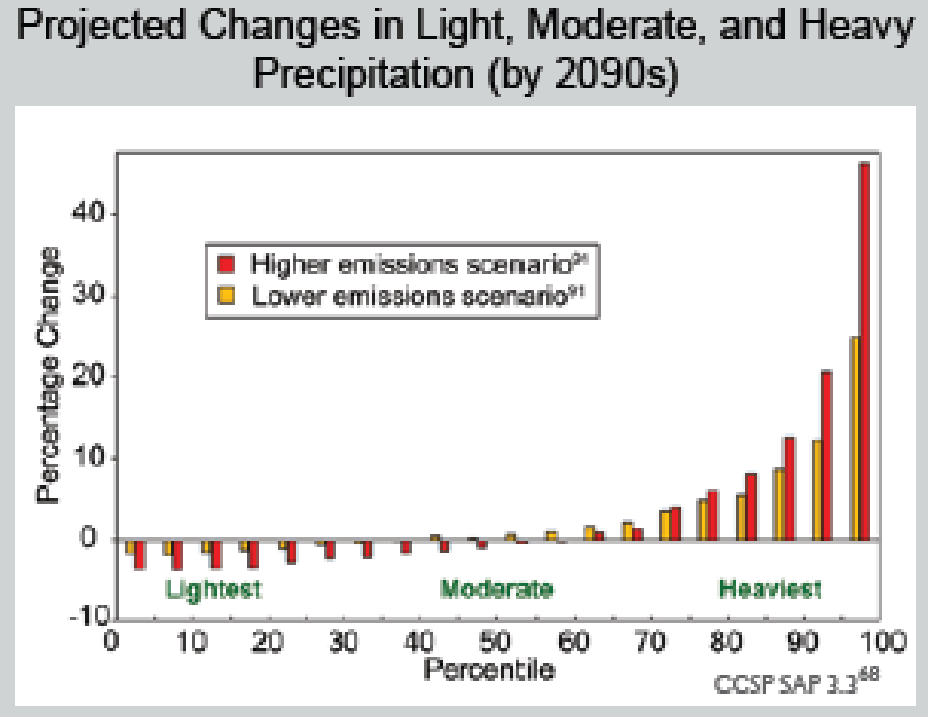

Figure 15. *Projected changes from the 1990s average to the 2090s average in the amount of precipitation falling in light, moderate and heavy events in North America, under a high and low emissions scenario. Projected changes are displayed in 5% increments from the lightest drizzles to the heaviest downpours. The figure is from Karl et al. (2009).*

National-scale or sub-national scale assessments

Recent past

Flooding often occurs when heavy precipitation persists for weeks to months in large river basins. Such extended periods of heavy precipitation have been increasing over the past century, most notably in the past two to three decades in the USA (Kunkel and et al., 2008).

Peterson et al. (2008) noted that observational studies over the North American region found an increase in average daily precipitation, increases in the number of days exceeding the 95th and 99th percentiles of daily precipitation, and also the maximum 1 and 5 day precipitation events. Similarly, a long-term study of observations (1870-2005) for the north-eastern USA (Brown et al., 2010) indicated few significant trends were present in the precipitation indices studied, but they did display a tendency towards wetter conditions.

Climate change studies

A study for the Pacific north-west region (Elsner et al., 2010) evaluated projected changes in snow water equivalent (SWE), soil moisture, runoff and stream-flow under the A1B and B1 emissions scenarios, for the 2020s, 2040s and 2080s. The analysis showed that April 1st SWE is projected to decrease by 38% (B1) to 46% (A1B) by the 2040s (compared to the

1917-2006 mean). Annual runoff across Washington State was projected to change little by the 2020s, then increase by around 2-3% by the 2040s, and around 4-6% by the 2080s driven mainly by projected increases in winter precipitation.

A study by Bell et al. (2004) for California, found that changes in precipitation exceeding the 95th percentile followed changes in mean precipitation, with decreases in heavy precipitation in most areas, under climate change. In a large river basin in the Pacific Northwest, increases in rainfall over snowfall, plus rain-on-snow events increased extreme runoff by 11%, which could contribute to more severe flooding. Likewise, applying a 25km resolution RCM, Diffenbaugh et al. (2005) found widespread increases in extreme precipitation events under an SRES A2 emissions scenario across the USA, which they determined to be significant. Over the North American region as a whole, observational studies have found an increase in average daily precipitation, increases in the number of days exceeding the 95th and 99th percentiles of daily precipitation, and also the maximum 1 and 5 day precipitation events.

An assessment by Moser et al. (2008) for California, considered a mitigation scenario in which global-mean warming was limited to 2°C, in addition to the standard SRES emissions scenarios. The mitigation scenario, referred to as the “policy scenario” assumed emission reductions in the industrialized nations of about 30% below 1990 levels by 2020, about 80% by 2050, and extremely low emissions by the end of this century. It also assumed eventual reductions from the developing world so that overall global emissions by 2050 are reduced by 50% with more drastic reductions after 2050. The study highlights an increased risk of winter flooding as a result of increased winter rainfall (i.e. higher temperature and decreased snowfall).

As an example of city level projections, a study for Chicago (Vavrus and Van Dorn, 2010) analysed statistically downscaled projections of climate model output, based upon SRES A1FI and B2 emissions scenarios. Extreme precipitation events were simulated to increase, especially in winter and spring.

Fluvial Flooding

Headline

Recent studies demonstrate large uncertainties in estimating fluvial flooding under climate change scenarios across the USA. At least one global modelling study has projected a strong increase in flood frequency in parts of Southern USA, the East Coast states and the Pacific Northwest, but a decrease in other parts of the country. Results from the AVOID programme, based on climate projections from 21 GCMs, show that for the USA as a whole the model projections are evenly balanced between increasing and decreasing flood risk in the early 21st century, but later in the century the models show a greater tendency towards increasing flood risk, especially in the A1B scenario. A thorough analysis of potential future changes in flooding frequency in rivers across the USA, based on the latest hydrological modelling techniques and climate change scenarios and accounting for the various sources of uncertainty, seems to be warranted.

Supporting literature

Introduction

This section summarises findings from a number of post IPCC AR4 assessments on river flooding in the United States to inform and contextualise the analysis performed by the AVOID programme for this project. The results from the AVOID work are discussed in the next section.

Fluvial flooding involves flow in rivers either exceeding the capacity of the river channel or breaking through the river banks, and so inundating the floodplain. A complex set of processes is involved in the translation of precipitation into runoff and subsequently river flow (routing of runoff along river channels). Some of the factors involved are; the partitioning of precipitation into rainfall and snowfall, soil type, antecedent soil moisture, infiltration, land cover, evaporation and plant transpiration, topography, groundwater storage. Determining whether a given river flow exceeds the channel capacity, and where any excess flow will go, is also not straightforward, and is complicated by the presence of artificial river embankments and other man-made structures for example. Hydrological models attempt to

simplify and conceptualise these factors and processes, to allow the simulation of runoff and/or river flow under different conditions. However, the results from global-scale hydrological modelling need to be interpreted with caution, especially for smaller regions, due to the necessarily coarse resolution of such modelling and the assumptions and simplifications this entails (e.g. a 0.5^{o} grid corresponds to landscape features spatially averaged to around 50-55km for mid- to low-latitudes). Such results provide a consistent, high-level picture, but will not show any finer resolution detail or variability. Smaller-scale or catchment-scale hydrological modelling can allow for more local factors affecting the hydrology, but will also involve further sources of uncertainty, such as in the downscaling of global climate model data to the necessary scale for the hydrological models. Furthermore, the application of different hydrological models and analysis techniques often makes it difficult to compare results for different catchments.

The average annual cost of floods in the USA has been estimated at about $2 billion, and in the last half of the 20th century an average of 110 people per year died in flood-related accidents (Ntelekos et al., 2010). With climate change, the largest increases in heavy precipitation events are projected in the Midwest and the Northeast of the USA (Karl et al., 2009). But even regions such as the Southwest that are projected to become drier on average may experience increased flood risk, due to an increased fraction of winter precipitation falling as rain instead of snow and more rain on snow events (Karl et al., 2009). Although these general trends are well understood, surprisingly few modelling studies have been undertaken to project changes in flood hazard in the large river basins of the USA, or at a national-scale.

Assessments that include a global or regional perspective

Climate change studies

A global modelling study presented by Hirabayashi et al. (2008), applied a single GCM under the A1B emissions scenario. The authors projected local increases in flood frequency in the next few decades (2001-2030) in the southern USA (Texas to Northern Florida). A decrease in flood hazard was projected for most of the western USA with the exception of the Pacific Northwest where a strong increase was found. In this region, the return period of what was a 100-year flood event in the 20th century was projected to decrease to less than 40 years. By the end of the century (2071-2100) this trend was reinforced. The return period of a 100-year flood was projected to decrease to 30 years or less in parts of southern USA (centred on Texas) and the East Coast states, suggesting that extreme discharge levels may become three times more likely. Strong decreases in return period were also found in the Pacific Northwest. In the Columbia River, the current 100-year flood level was projected to occur

once every three years with climate change, and the annual flood peak to occur two to three months earlier in the year. In much of the rest of the country, including the Western mountain and plateau region and the Great Plains, an increase in the return period of 100-year discharge levels was simulated, suggesting that such extreme floods could occur less frequently. In the Mississippi River the return period of a 100-year flood increased to about 150 years, and an even stronger decrease in flood hazard was projected for the Colorado River. A decrease in flooding frequency was also found in most of Alaska. In the Yukon River, the return period of a 100-year flood increased to more than 300 years, with little change in the timing of the peak flow. Whilst the simulations presented by Hirabayashi et al. (2008) provide useful details across the USA, it is important to note that the projections are based upon a single GCM and emissions scenario. To this end, the uncertainty in the projections is essentially large, because projections from other GCMs and scenarios are overlooked.

Similar patterns under climate change were also reported by Nohara et al. (2006). The authors applied 19 GCMs under the A1B emissions scenario for the end of the 21st century (2081-2100). However their results presented a wide spread in response among the different climate models in river basins such as the Mississippi and Yukon, suggesting large modelling uncertainty.

In view of these uncertainties, and the potential implications of an increase in flood risk, a thorough analysis of potential future changes in flooding frequency in rivers in the United States, based on the latest hydrological modelling techniques and climate change scenarios and accounting for the various sources of uncertainty, seems to be warranted.

National-scale or sub-national scale assessments

Recent past

20th century warming has already led to changes in flood risk in the western USA (Hamlet and Lettenmaier, 2007). In cold river basins where snow dominates the annual hydrological cycle, the warming has led to reductions in spring snowpack and hence reductions in snowmelt flood peaks. Warmer transient basins along the coast in Washington, Oregon, and California, in particular, tend to show increased flood risk (Hamlet and Lettenmaier, 2007).

Climate change studies

Ntelekos et al. (2010) estimated that annual flood costs in the US may increase sharply by the end of the 21st century ranging from about $7 to $19 billion current US dollars, depending on the economic growth rate and the emissions scenarios. Ntelekos et al. (2010) furthermore

estimated that the annual flood costs could be about $2.3 billion per year higher under a high emissions scenario (A2) compared with a low emissions scenario (B1). This result included projections of urban expansion and the study notes that infrastructure, including roads, bridges and embankments will continue to play a major role in determining the extent of floodplains.

Raff et al. (2009) present projections of flood frequency for four catchments across the western USA. Although they found different trends in annual maximum flood discharge in each of these basins, in all four of them the upper end of the distributions showed increases with time. Raff et al. (2009) argue that it is the most infrequent of floods that often define the flood hazard and risk at a location and all four of the basins were found to show an increase in annual maximum flood values for rare events.

AVOID programme results

To quantify the impact of climate change on fluvial flooding and the inherent uncertainties, the AVOID programme calculated an indicator of flood risk for all countries reviewed in this literature assessment based upon the patterns of climate change from 21 GCMs (Warren et al., 2010). This ensures a consistent methodological approach across all countries and takes consideration of climate modelling uncertainties.

Methodology

The effect of climate change on fluvial flooding is shown here using an indicator representing the percentage change in average annual flood risk within a country, calculated by assuming a standardised relationship between flood magnitude and loss. The indicator is based on the estimated present-day (1961-1990) and future flood frequency curve, derived from the time series of runoff simulated at a spatial resolution of 0.5°x0.5° using a global hydrological model, MacPDM (Gosling and Arnell, 2011). The flood frequency curve was combined with a generic flood magnitude–damage curve to estimate the average annual flood damage in each grid cell. This was then multiplied by grid cell population and summed across a region, producing in effect a population-weighted average annual damage. Flood damage is thus assumed to be proportional to population in each grid cell, not the value of exposed assets, and the proportion of people exposed to flood is assumed to be constant across each grid cell (Warren et al., 2010).

The national values are calculated across major floodplains, based on the UN PREVIEW Global Risk Data Platform (preview.grid.unep.ch). This database contains gridded estimates, at a spatial resolution of 30 arc-seconds (0.00833°x0.00833°), of the estimated frequency of flooding. From this database the proportion of each 0.5°x0.5° grid cell defined as floodplain was determined, along with the numbers of people living in each 0.5°x0.5° grid cell in flood-prone areas. The floodplain data set does not include "small" floodplains, so underestimates actual exposure to flooding. The pattern of climate change from 21 GCMs was applied to MacPDM, under two emissions scenarios; 1) SRES A1B and 2) an aggressive mitigation scenario where emissions follow A1B up to 2016 but then decline at a rate of 5% per year thereafter to a low emissions floor (denoted A1B-2016-5-L). Both scenarios assume that population changes through the 21st century following the SRES A1 scenario as implemented in IMAGE 2.3 (van Vuuren et al., 2007). The application of 21 GCMs is an attempt to quantify the uncertainty due to climate modelling, although it is acknowledged that only one impacts model is applied (MacPDM). Simulations were performed for the years 2030, 2050, 2080 and 2100. The result represents the change in flood risk due to climate change, not the change in flood risk relative to present day (Warren et al., 2010).

Results

The results for the USA as a whole are presented in Figure 16. By the 2030s, the models project a range of changes in mean fluvial flooding risk over the United States in both scenarios, with some models projecting decreases and others increases. The largest decrease projected for the 2030s is −40%, and the largest increase is +20%. The mean across all projections is for no significant change in the average annual flood risk.

By 2100 the model projections show a greater tendency towards an increase in flood risk, and the difference in projections from the different models becomes greater. Both these aspects of the results are more pronounced for the A1B scenario than the mitigation scenario. Under the mitigation scenario, more than a quarter of the models still project a lower flood risk (down to approximately −50%), but a majority project an increase. The mean of all projections is an increase of 10%, and the upper projection is approximately +50%. Under the A1B scenario, only a small number of models project a decreased flood risk (down to −60%). The largest projected increase is approximately +170%,while the mean of all projections is an increase in average annual flood risk of about +50%.

So for the USA as a whole, at first the models are evenly balanced between increasing and decreasing flood risk in both scenarios, but later in the century the models show a greater

tendency towards increasing flood risk in both scenarios, but especially A1B. The differences between the model projections are greater later in the century and particularly for A1B.

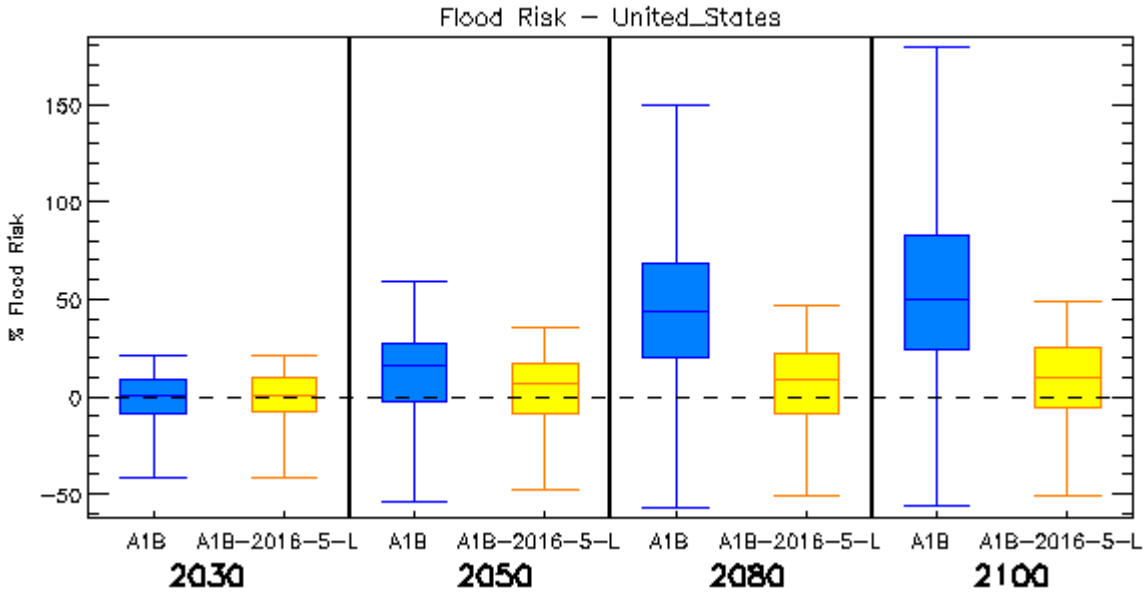

Figure 16. *Box and whisker plots for the percentage change in average annual flood risk within the USA, from 21 GCMs under two emissions scenarios (A1B and A1B-2016-5-L), for four time horizons. The plots show the 25th, 50th, and 75th percentiles (represented by the boxes), and the maximum and minimum values (shown by the extent of the whiskers).*

Tropical cyclones

Headline

Most studies reviewed here suggest that the frequency of tropical cyclones in the North Atlantic could decrease with climate change, which may result in fewer cyclones striking the eastern USA and the Gulf Coast. Complex sub-basin-scale changes in cyclone frequency, however, could lead to increasing cyclone counts in some coastal regions and decreases in others. The impact of climate change on cyclones near Hawaii is highly uncertain, due to the lack of model agreement on the sign of the change in cyclone frequency in the East Pacific. The majority of studies reviewed here show that tropical cyclone intensities and cyclone rainfall could increase in both the North Atlantic and the East Pacific, particularly for the most intense cyclones. These stronger storms could potentially cause an increase in cyclone damages in the USA due to climate change.

Supporting literature

Introduction

Tropical cyclones are different in nature from those that exist in mid-latitudes in the way that they form and develop. There remains an overall large uncertainty in the current understanding of how tropical cyclones might be affected by climate change because conclusions are based upon a limited number of studies. Moreover, the majority of tropical-cyclone projections are from either coarse-resolution global models or from statistical or dynamical downscaling techniques. The former are unable to represent the most-intense storms, whereas the very patterns used for the downscaling may change in itself under climate change. To this end, caution should be applied in interpreting model-based results, even where the models are in agreement.

Assessments that include a global or regional perspective

The USA is affected by tropical cyclones in the North Atlantic, including the Caribbean and the Gulf of Mexico, and the East Pacific. Cyclones in the latter basin affect the island of Hawaii. Since modelling studies separate their projections of tropical-cyclone activity with climate change by basin, the results here are organised similarly.

North Atlantic

Assessment of cyclone frequency

The majority of studies that focus on North Atlantic tropical cyclone activity with climate change, particularly those with high-resolution climate models, conclude that the frequency of tropical cyclones in the North Atlantic could decrease with global climate change. Knutson et al. (2008) applied an 18km RCM to downscale the ensemble-mean of 18 GCMs under the A1B emissions scenario. The RCM spontaneously generates tropical-cyclone-like disturbances, which either develop into cyclones or decay, depending on the background conditions provided by the 18 GCMs. The model realistically simulates observed tropical-cyclone frequencies, but its limited resolution prevents it from producing the most intense cyclones observed. When applied to the ensemble-mean climate from the 18 GCMs, the RCM simulated a 27% decrease in tropical cyclones in the North Atlantic, with an 18% decrease in the number of hurricanes and an 8% decrease in the frequency of major hurricanes (categories 3, 4 and 5), for the 2080-2099 time horizon. The authors concluded that increasing vertical wind shear and decreases in relative humidity were the key driving factors in reducing cyclone frequencies in a warmer climate. The decreases in frequency were stronger in the western Atlantic than in the east, which suggests that the number of landfalling storms in the USA could be reduced by more than the 27% decrease across the entire basin.

GCM simulations have also projected a decrease in cyclones in the North Atlantic basin. With the Italian coupled GCM SINTEX-G, at 120km resolution, Gualdi et al. (2008) found that cyclone frequency decreased by 14% in a $2xCO_2$ climate. Bengtsson et al. (2007) applied the ECHAM5 GCM at 60km and 40km resolutions respectively under the A1B emissions scenario. The model simulated 8% and 13% decreases in North Atlantic cyclones, respectively by the end of the 21st century. Experiments with the Hadley Centre atmospheric model (HadAM3) at 100km resolution demonstrated a 30% reduction in cyclone frequencies under the IPCC IS95a greenhouse-gas emissions scenario for the 2081-2100 time horizon (McDonald et al., 2005). Zhao et al. (2009) applied the 50km GFDL GCM with four simulated SST distributions from; 1) the CMIP3 multiple-GCM ensemble-mean, 2) the HadCM3 GCM, 3) the GFDL GCM, and 4) the ECHAM5 GCM. All SSTs distributions were for the A1B emissions scenario for the 2081-2100 time horizon. The authors found considerable variability among the models and between the individual models and the ensemble-mean in cyclone frequencies, emphasizing the uncertainty in basin-scale projections. Whilst the HadCM3 GCM simulated a 62% decrease in cyclone frequency, the GFDL and ECHAM5 GCMs showed nearly no change in cyclone frequency in the North

Atlantic. Chauvin et al. (2006) applied the ARPEGE RCM at 50km resolution with simulations from two GCMs for the 2090-2099 time horizon; the CNRM GCM under the SRES B2 emissions scenario and the HadCM3 GCM under the SRES A2 emission scenario. The simulation driven by the CNRM GCM simulated an 18% increase in North Atlantic tropical cyclones, while the HadCM3-driven simulation simulated a 25% decrease in cyclone counts

Murakami and Wang (2010) applied the 20km MRI atmosphere-only GCM, driven by the ensemble-mean warming trend in SSTs simulated by the CMIP3 multiple-GCM ensemble under the A1B emissions scenario and present-day inter-annual SST variability. A 25-year simulation of this high-resolution model demonstrated a considerable shift in tropical-cyclone genesis regions to the north and east compared to the present-day climate. This also caused a shift in cyclone tracks, such that the model simulated fewer storms in the western North Atlantic and more in the eastern half of the basin. The reduced genesis in the western North Atlantic was due to a drying of the mid-troposphere and remotely forced anomalous descent, rather than local changes in thermodynamic forcing. The anomalous descent in the west resulted from increased ascending motion in the eastern half of the basin, itself the result of large simulated SST increases there, which supported the increased genesis in the eastern North Atlantic. These results support the conclusion of Knutson et al. (2008), that the number of landfalling storms in the eastern USA could be reduced with climate change.

Garner et al. (2009) applied a 16km resolution RCM to downscale an ensemble of 18 GCMs under the A1B emissions scenario for the North Atlantic in August-October only. The ensemble-mean change in SST, wind, temperature and humidity from the 18 GCMs for the 2081-2100 time horizon was compared with reanalysis data for 1981-2000. The RCM simulated a 20-30% decrease in cyclone frequencies throughout the North Atlantic. The authors noted that the wind shear increased appreciably in the Caribbean, which could suggest a decrease in cyclones in the Gulf of Mexico that exceeded the basin average. Sugi et al. (2009) applied the JMA climate model at 60km and 20km resolutions respectively with SSTs from three individual GCMs as well as the CMIP3 multiple-GCM ensemble mean, for a total of eight simulations. All simulations were under the A1B emissions scenario at the end of the 21st century. The authors observed an even greater spread among the GCMs for the North Atlantic. From these eight simulations, two showed a decrease in North Atlantic cyclone counts, three simulated an increase in cyclone frequency, and the remaining three demonstrated no change from the present-day frequency. It is noted that the responses of tropical cyclones in other basins around the globe were more consistent between the experiments; the North Atlantic has the most uncertainty of all basins in this study.

Whilst some studies have found an increase in North Atlantic cyclone frequencies, the weight of evidence - particularly that from high-resolution simulations - points to an overall decrease in frequency.

Assessment of cyclone intensity

Whilst the overall *frequency* of cyclones may decrease, the *intensity* of North Atlantic cyclones could increase, particularly for the most-intense cyclones. North Atlantic cyclones have been growing stronger over the past 30 years, a trend that has been linked to warming ocean-surface temperatures (Elsner et al., 2008). It is unclear if this warming trend can be attributed to anthropogenic climate change, however, or if it is due to natural, multi-decadal variations in ocean temperatures (Gutowski et al., 2008).

Oouchi et al. (2006) applied the JMA atmosphere-only model at 20km resolution, using SSTs from the MRI GCM under the A1B emissions scenario. The authors concluded that the mean maximum wind speed of tropical cyclones increased by 11%, while the maximum wind speed of the most intense storm in the North Atlantic each year increased by an average of 20%, for the 2080-2099 time horizon. The 18km RCM applied by Knutson et al. (2008) simulated a 3% increase in mean cyclone intensity, but a doubling of the most intense storms in the model (those with wind speeds stronger than 45m s^{-1}) for the 2080-2099 time horizon under an A1B emission scenario. Using the GFDL hurricane model at 9km resolution, Bender et al. (2010) downscaled the CMIP3 multiple-GCM ensemble-mean (18 GCMs) and four individual GCMs, all using the A1B emissions scenario. The results are presented in Figure 17. The authors concluded that the frequency of category 4 and category 5 storms could double by 2100, supporting the results presented by Knutson et al. (2008). Knutson and Tuleya (2004) applied nine GCMs under a 1% per year CO_2 increase scenario. The authors found that North Atlantic cyclone wind speeds increased by 1-6% after an 80-year simulation. Vecchi and Soden (2007) conducted a similar study using the CMIP3 ensemble of GCMs and found no change in mean intensity.

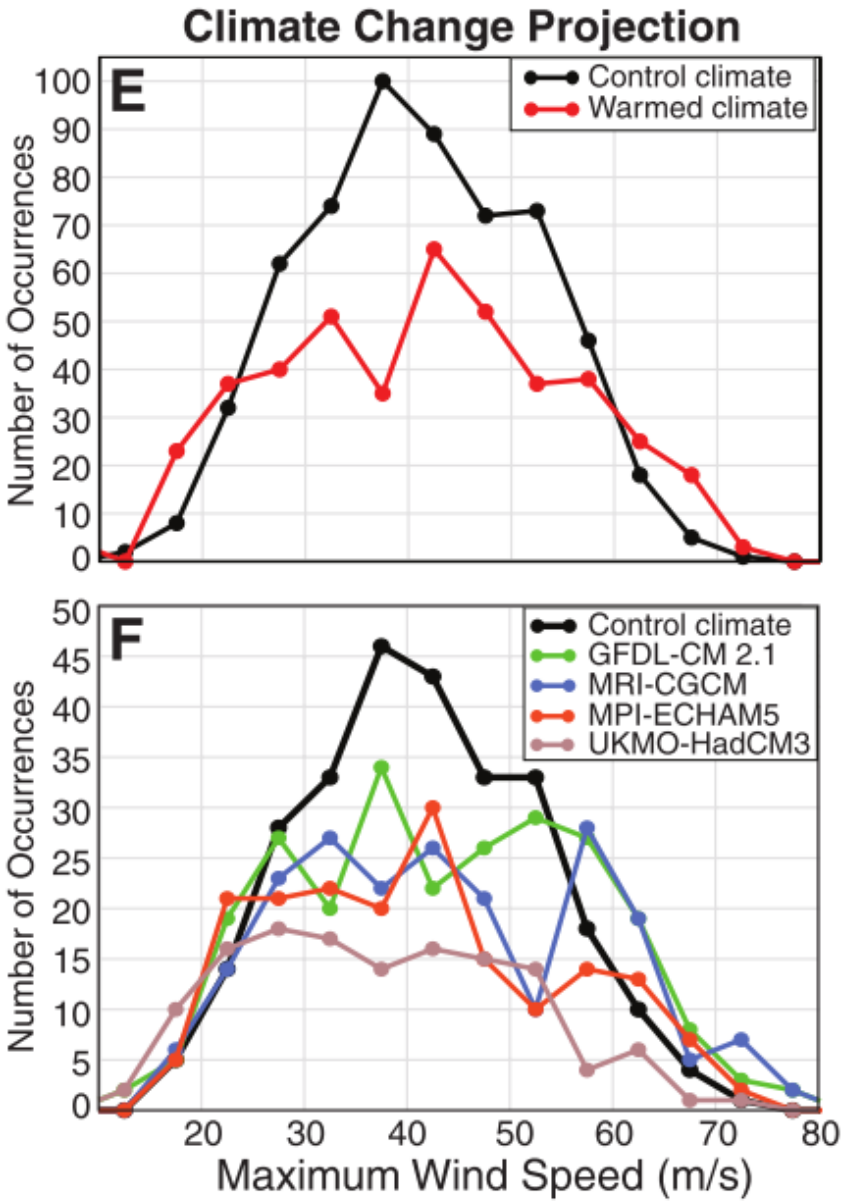

Figure 17. *The simulated maximum wind speeds of North Atlantic tropical cyclones from the GFDL operational hurricane model. The top panel displays simulations for the present-day climate (black line) and under climate change with the A1B emissions scenario (red line) using the ensemble-mean large-scale atmospheric conditions and SSTs from 18 GCMs. The bottom panel shows the same as the top panel, except here the climate change scenario is simulated by four separate GCMs. The figure is from Bender et al. (2010).*

Zhao and Held (2010) also observed increases in cyclone intensity, using the same 50km GFDL GCM and future GCM SST distributions applied by Zhao et al. (2009), i.e. 1) the ensemble mean from 18 GCMs, 2) the HadCM3 GCM, 3) the GFDL GCM, and 4) the ECHAM5 GCM; but with a statistical adjustment to the simulated tropical-cyclone intensities. The adjustment was calibrated by comparing modelled tropical cyclones using SSTs from 1981-2008 to observed cyclones, then applied to the modelled tropical-cyclones for 2081-

2100 under the A1B emissions scenario. Using this method, Zhao and Held (2010) were able to separate simulated intensity changes into a component that was associated with a change in the frequency of storms (i.e., the authors found a positive correlation between cyclone frequency and intensity) and a purely climate-change-driven component. Zhao and Held (2010) argued that the climate-change component should be independent of the spatial pattern of SST warming simulated by the individual CMIP3 GCMs, thus removing a considerable source of uncertainty. In this framework, climate change was responsible for a 5-10 ms^{-1} increase in the wind speed of strong North Atlantic storms, defined as those with wind speeds of 30-60 ms^{-1}, or approximately a 17% increase.

Assessment of precipitation change

In addition to wind-speed increases, the intensity of precipitation near the centre of tropical cyclones is expected to strengthen under climate change (Gutowski et al., 2008). Knutson et al. (2008) observed a 37% increase in precipitation within 50km of the storm centre for North Atlantic cyclones, a 23% increase within 100km and a 10% increase within 400km, for the 2080-2099 time horizon under A1B emissions. This result is supported by Knutson and Tuleya (2004); the authors applied the CMIP2 ensemble of GCMs and the 9km GFDL GCM, and observed a 22% increase in precipitation within 100km of the tropical cyclone centre, after 80-years of a 1% per year CO_2 increase scenario. Chauvin et al. (2006) also found a statistically significant, substantial increase in precipitation when downscaling the HadCM3 GCM under the A2 emissions scenario with the ARPEGE 50km climate model, for the 2090-2099 time horizon. These increases in precipitation agree with global studies that did not consider specific basins (Bengtsson et al., 2007, Gualdi et al., 2008, Hasegawa and Emori, 2005, Yoshimura et al., 2006).

East Pacific

Hawaii is only rarely affected by tropical cyclones. Many cyclones weaken before they reach the island and so cause only minor damage. The results for the East Pacific basin are reviewed here but they may be of little use for Hawaii due to the island's small size relative to the basin. No studies have considered Hawaii independently from the East Pacific basin. Such results would not be reliable, given the limited resolution of the models used to simulate the impact of climate change on tropical cyclones, as well as the lack of confidence in those models' abilities to simulate sub-basin-scale changes in cyclone activity. Note that where studies have previously been introduced for the North Atlantic basin, the details of their simulations will not be repeated here, for conciseness.

Assessment of cyclone frequency

Bengtsson et al. (2007) reported an increase in eastern Pacific tropical cyclones, with a 4% increase in the 60km resolution model and a 7% increase in the 40km resolution model. These increases were due to an overall eastward shift in Pacific cyclogenesis (cyclone formation), itself due to an decrease in vertical wind shear—which is conducive to cyclogenesis—in the East Pacific and an increase in shear and in atmospheric stability in the West Pacific. McDonald et al. (2005) also concluded that climate change could cause large increases in East Pacific cyclone frequencies. The 2081-2100 time horizon in their 100km HadAM3 simulation showed a 80% increase in the number of tropical cyclones in the East Pacific, which was statistically significant at the 5% level. Similarly, in three of the four experiments conducted by Zhao et al. (2009), the frequency of cyclones in the East Pacific basin increased, with the increases ranging from 15% to 61%. The fourth simulation, showed a decrease of 23%.

Decreases in West Pacific cyclone frequency were reported by Oouchi et al. (2006) using the 20km resolution JMA climate model, under A1B emissions for the 2080-2099 time horizon. Oouchi et al. (2006) found 34% fewer cyclones in the East Pacific under the climate-change scenario, which the authors concluded were due to increased atmospheric stability in a warmer world; the model simulated a 10% increase in the global dry static stability, defined as the difference in potential temperature between the 250hPa level of the atmosphere and the land surface. Further evidence for decreases in East Pacific cyclone frequency is presented by Sugi et al. (2009). The authors applied the JMA climate model at 60km and 20km resolutions respectively, with SSTs from three individual GCMs as well as the CMIP3 multiple-GCM ensemble mean, for a total of eight simulations. All simulations were under the A1B emissions scenario at the end of the 21st century. In all eight of their experiments, the frequency of East Pacific cyclones decreased. The magnitudes of the decreases were reasonably consistent, ranging from 25% to 50% across the eight experiments.

Further complicating projections of cyclone frequency, two studies have found approximately no change in cyclone frequency in the East Pacific relative to the present-day climate. Gualdi et al. (2008) found that East Pacific cyclones decreased by 3% in their 2x CO_2 experiment, which is well inside the range of natural variability. Also, Emanuel et al. (2008) applied a hybrid statistical-dynamical downscaling method to seven GCMs under the A1B emissions scenario for the 2180-2200 time horizon. The technique they applied “seeds” large numbers of tropical-cyclone vortices into each basin, then uses the models' large-scale climate fields (e.g., SSTs, wind shear, relative humidity) to determine whether the storms grow into

cyclones or simply decay. By comparing the A1B scenario simulations for 2180-2200 to downscaled reanalysis data for 1980-2000, the authors concluded that East Pacific cyclone numbers could decrease by 5%. Two of the seven GCMs simulated an increase in cyclone frequencies, however, while four simulated decreases and one showed nearly no change.

Assessment of cyclone intensity

Despite uncertainty in projections of cyclone *frequency*, it is possible that cyclone *intensities* in the East Pacific could increase, particularly for the most intense storms. For instance, Bengtsson et al. (2007) reported a 33% increase in the frequency of Northern Hemisphere storms with wind speeds exceeding 50 m s^{-1}, under the A1B emissions scenario by the end of the 21st century. The authors reported that "most of this increase" occurred in the East Pacific and the North Atlantic, but did not present quantitative results for each basin. Knutson and Tuleya (2004) applied nine GCMs under a 1% per year CO_2 increase scenario and found that the wind speeds of East Pacific cyclones increased by 5-16% at the time of CO_2 doubling. Similarly, Vecchi and Soden (2007) applied 18 GCMs under the A1B emissions scenario and found that the mean model projection was a 3.5% increase in East Pacific cyclone wind speeds by 2100. Oouchi et al. (2006) observed a relatively smaller intensification in their 20km JMA climate model experiment, with the mean wind speed of East Pacific cyclones increasing by 0.6%, for the 2080-2099 time horizon under an A1B emission scenario.

It is therefore possible that East Pacific cyclone *intensities* could increase with climate change, particularly for the most intense storms. This is in agreement with findings for global cyclones (Kitoh et al., 2009, McDonald et al., 2005, Oouchi et al., 2006).

Assessment of cyclone damages

Even when combined with a decrease in cyclone frequency, the projected strengthening of North Atlantic cyclones, particularly for the most intense cyclones, could increase cyclone damages in the USA. Mendelsohn et al. (2011) applied the cyclone "seeding" method described by Emanuel et al. (2008) to climate projections from four GCMs under the A1B emission scenario, then constructed a damage model to estimate the damages from each landfalling storm. With the Emanuel et al. (2008) method, cyclone-like disturbances are randomly generated in the large-scale environment simulated by a climate model under a climate change scenario. Similar to the method described by Knutson et al. (2008), the storms can then grow or decay, as determined by the climate model's atmospheric conditions and the underlying SST. All four of the GCMs considered by Mendelsohn et al. (2011) projected an increase in tropical-cyclone damages for the USA, but the amounts of

additional damage were highly variable. Against a baseline of $26.3 billion per year in damages, two of the models simulated approximately a 50% increase; the CNRM GCM ($14.5 billion increase) and the MIROC GCM ($13.1 billion increase). Damages doubled with the ECHAM5 GCM ($31.7 billion increase) and tripled with the GFDL GCM ($60.9 billion increase). Whilst it is possible that tropical-cyclone damages could increase in the USA as a result of climate change, it is not possible to quantify robustly, what the magnitude of these damages could be, largely to the large uncertainties in magnitudes of the decrease in cyclone frequency and increase in cyclone intensities.

National-scale or sub-national scale assessments

Literature searches yielded no post IPCC AR4 results for national-scale or sub-national scale studies for this impact sector.

Coastal regions

Headline

Studies published after the IPCC AR4 suggests that the USA is highly vulnerable to sea level rise (SLR). This supports conclusions from the IPCC AR4. More regional detail is now available, however. One study shows that by the 2070s, the number of people exposed to SLR with climate change could increase from 6.7 million in present to 12.9 million under A1B emissions; an aggressive mitigation scenario could reduce this by around 0.5 million.

Supporting literature

Assessments that include a global or regional perspective

The USA is highly vulnerable to SLR with climate change (Hanson et al., 2011, Hanson et al., 2010, Irish et al., 2010). The IPCC AR4 concluded that at the time, understanding was too limited to provide a best estimate or an upper bound for global SLR in the twenty-first century (IPCC, 2007b). However, a range of SLR, excluding accelerated ice loss effects was published, ranging from 0.19m to 0.59m by the 2090s (relative to 1980-2000), for a range of scenarios (SRES A1FI to B1). The IPCC AR4 also provided an illustrative estimate of an additional SLR term of up to 17cm from acceleration of ice sheet outlet glaciers and ice streams, but did not suggest this is the upper value that could occur. Although there are published projections of SLR in excess of IPCC AR4 values (Nicholls et al., 2011), many of these typically use semi-empirical methods that suffer from limited physical validity and further research is required to produce a more robust estimate. Linking sea level rise projections to temperature must also be done with caution because of the different response times of these two climate variables to a given radiative forcing change.

Nicholls and Lowe (2004) previously showed that mitigation alone would not avoid all of the impacts due to rising sea levels, adaptation would likely be needed too. Recent work by van Vuuren et al. (2011) estimated that, for a world where global mean near surface temperatures reach around 2°C by 2100, global mean SLR could be 0.49m above present levels by the end of the century. Their sea level rise estimate for a world with global mean temperatures reaching 4°C by 2100 was 0.71m, suggesting around 40% of the future

increase in sea level to the end of the 21st century could be avoided by mitigation. A qualitatively similar conclusion was reached in a study by Pardaens et al. (2011), which examined climate change projections from two GCMs. They found that around a third of global-mean SLR over the 21st century could potentially be avoided by a mitigation scenario under which global-mean surface air temperature is near-stabilised at around 2°C relative to pre-industrial times. Under their baseline business-as-usual scenario the projected increase in temperature over the 21st century is around 4°C, and the sea level rise range is 0.29-0.51m (by 2090-2099 relative to 1980-1999; 5% to 95% uncertainties arising from treatment of land-based ice melt and following the methodology used by the IPCC AR4). Under the mitigation scenario, global mean SLR in this study is projected to be 0.17-0.34m.

The IPCC 4th assessment (IPCCa) followed Nicholls and Lowe (2004) for estimates of the numbers of people affected by coastal flooding due to sea level rise. Nicholls and Lowe (2004) projected for the North America region that an additional 100 thousand people per year could be flooded due to sea level rise by the 2080s relative to the 1990s for the SRES A2 Scenario (note this region also includes other countries, such as Mexico and Canada). However, it is important to note that this calculation assumed that protection standards increased as GDP increased, although there is no additional adaptation for sea level rise. More recently, Nicholls et al. (2011) also examined the potential impacts of sea level rise in a scenario that gave around 4°C of warming by 2100. Readings from Figure 3 from Nicholls et al. (2011) for the North America Atlantic region suggest that less than an approximate 3 million additional people could be flooded for a 0.5 m SLR (assuming no additional protection), with less than an additional 3 million people flooded in the North America Pacific region. Nicholls et al. (2011) also looked at the consequence of a 2m SLR by 2100, however as we consider this rate of SLR to have a low probability we don't report these figures here.

Two recent global-scale assessments of the impact of SLR on the globe's coasts include national-scale impact estimates for the USA (Hanson et al., 2011, Hanson et al., 2010). Both studies suggest that the USA is highly vulnerable to SLR. Hanson et al. (2010) investigated population exposure to global SLR, natural and human subsidence/uplift, and more intense storms and higher storm surges, for 136 port cities across the globe. Future city populations were calculated using global population and economic projections, based on the SRES A1 scenario up to 2030. The study accounted for uncertainty on future urbanization rates, but estimates of population exposure were only presented for a rapid urbanisation scenario, which involved the direct extrapolation of population from 2030 to 2080. All scenarios assumed that new inhabitants of cities in the future will have the same relative exposure to flood risk as current inhabitants. The study is similar to a later study presented by Hanson et al. (2011) except here, different climate change scenarios were considered, and published estimates of exposure are available for more countries. Future water levels were generated from temperature and thermal expansion data related to greenhouse gas emissions with

SRES A1B (un-mitigated climate change) and under a mitigation scenario where emissions peak in 2016 and decrease subsequently at 5% per year to a low emissions floor (2016-5-L). Table 10 shows the aspects of SLR that were considered for various scenarios and Table 11 displays regional population exposure for each scenario in the 2030s, 2050s and 2070s. By comparing the projections in Table 11 with the estimates for exposure in the absence of climate change that are presented in Table 12, the vulnerability of the USA to SLR is clear. The USA is third only to China and India for the globe's most highly impacted countries to SLR. In present day there are around 6.7 million people in the USA exposed to SLR and in the absence of climate change in the 2070s this increases to around 10.7 million. With climate change in the 2070s, and under the FAC (Future City All Changes) scenario the exposed population is 12.9 million under un-mitigated A1B emissions, which implies the incremental impact of climate change is around 2.2 million people. Hanson et al. (2010) also demonstrated that aggressive mitigation scenario could avoid an exposure of around 0.5 million people in the USA, relative to un-mitigated climate change (see Table 12) in 2070.

Scenario		**Water levels**				
		Climate			**Subsidence**	
Code	**Description**	**More intense storms**	**Sea-level change**	**Higher storm surges**	**Natural**	**Anthropogenic**
FNC	Future city	**V**	x	x	X	x
FRSLC	Future City Sea-Level Change	**V**	**V**	x	**V**	x
FCC	Future City Climate Change	**V**	**V**	**V**	**V**	x
FAC	Future City All Changes	**V**	**V**	**V**	**V**	**V**

Table 10. *Summary of the aspects of SLR considered by Hanson et al. (2010). 'V' denotes that the aspect was considered in the scenario and 'x' that it was not.*

Rapid urbanisation projection																
2030						2050						2070				
Country	Ports	Water level projection				Country	Ports	Water level projection				Country	Ports	Water level projection			
		FAC	FCC	FRSLC	FNC			FAC	FCC	FRSLC	FNC			FAC	FCC	FRSLC	FNC
CHINA	15	17,100	15,500	15,400	14,600	**CHINA**	15	23,000	19,700	18,700	17,400	**CHINA**	15	27,700	22,600	20,800	18,600
INDIA	6	11,600	10,800	10,300	9,970	**INDIA**	6	16,400	14,600	13,600	12,500	**INDIA**	6	20,600	17,900	15,600	13,900
US	17	8,990	8,960	8,830	8,460	**US**	17	11,300	11,200	10,800	9,970	**US**	17	12,800	12,700	12,100	10,700
JAPAN	6	5,260	4,610	4,430	4,390	**JAPAN**	6	6,440	5,280	5,000	4,760	**JAPAN**	6	7,800	5,970	5,580	5,070
INDONESIA	4	1,420	1,200	1,200	1,170	**INDONESIA**	4	2,110	1,610	1,610	1,500	**INDONESIA**	4	2,680	1,830	1,830	1,530
BRAZIL	10	833	833	833	802	**BRAZIL**	10	929	929	929	879	**BRAZIL**	10	940	940	940	864
UK	2	497	497	478	459	**UK**	2	609	609	564	521	**UK**	2	716	716	640	569
CANADA	2	459	433	422	405	**CANADA**	2	549	512	486	457	**CANADA**	2	614	585	545	489
REP. OF KOREA	3	344	344	331	441	**REP. OF KOREA**	3	361	361	341	318	**REP. OF KOREA**	3	377	377	325	303
GERMANY	1	257	257	253	248	**GERMANY**	1	287	287	273	269	**GERMANY**	1	309	309	290	280
RUSSIA	1	177	177	177	177	**RUSSIA**	1	202	202	173	173	**RUSSIA**	1	226	226	197	169
AUSTRALIA	5	162	162	157	157	**AUSTRALIA**	5	197	197	191	181	**AUSTRALIA**	5	196	196	186	175
SOUTH AFRICA	2	30	30	30	29	**SAUDI ARABIA**	1	33	33	33	27	**SAUDI ARABIA**	1	38	38	38	29
SAUDI ARABIA	1	24	24	24	22	**SOUTH AFRICA**	2	28	28	28	27	**SOUTH AFRICA**	2	30	30	30	27
FRANCE	1	15	15	15	15	**FRANCE**	1	19	19	19	17	**FRANCE**	1	23	23	23	18
ITALY	1	2	2	2	2	**ITALY**	1	4	4	4	3	**ITALY**	1	6	6	6	4
MEXICO	0	0	0	0	0	**MEXICO**	0	0	0	0	0	**MEXICO**	0	0	0	0	0

Table 11. *National estimates of population exposure (1,000s) for each water level projection (ranked according to exposure with the FAC (Future City All Changes) scenario) under a rapid urbanisation projection for the 2030s, 2050s and 2070s. Estimates for present day exposure and in the absence of climate change (for 2070 only) for comparison are presented in Table 12. Data is from Hanson et al. (2010) and has been rounded down to three significant figures.*

Country	Ports	Population exposure				Exposure avoided
		Current	2070. Rapid urbanisation, FAC water level scenario			
			No climate change	A1B un-mitigated	Mitigated (2016-5-L)	
CHINA	15	8,740	18,600	27,700	26,500	1,140
UNITED STATES	17	6,680	10,700	12,800	12,300	505
RUSSIA	1	189	169	226	197	28
JAPAN	6	3,680	5,070	7,800	7,290	515
SOUTH AFRICA	2	24	27	30	29	0
INDIA	6	5,540	13,900	20,600	18,900	1,670
BRAZIL	10	555	864	940	926	14
MEXICO	0	0	0	0	0	0
CANADA	2	308	489	614	599	15
AUSTRALIA	5	99	175	196	190	6
INDONESIA	4	602	1,530	2,680	2,520	156
REP. OF KOREA	3	294	303	377	343	34
UK	2	414	569	716	665	51
FRANCE	1	13	18	23	20	2
ITALY	1	2	4	6	6	0
GERMANY	1	261	280	309	295	15
SAUDI ARABIA	1	15	29	38	35	3

Table 12. *Exposed population (1,000s) in present (current), and in the 2070s in the absence of climate change (no climate change), with unmitigated climate change (A1B un-mitigated), and mitigated climate change (mitigated 2016-5-L), under the rapid urbanisation and FAC (Future City All Changes) water level scenarios. The final column shows the potential avoided exposure, as a result of mitigation. Data is from Hanson et al. (2010) and has been rounded down to three significant figures.*

Hanson et al. (2011) also present estimates of the exposure of the world's large port cities (population exceeding one million inhabitants in 2005) to coastal flooding due to SLR and storm surge, now and in the 2070s. Population exposure was calculated as a function of elevation against water levels related to the 1 in 100 year storm surge. The analysis assumed a homogenous SLR of 0.5m by 2070. For tropical storms a 10% increase in extreme water levels was assumed, with no expansion in affected area; while for extratropical storms, a 10% increase in extreme water levels was assumed. A uniform 0.5 m decline in land levels was assumed from 2005 to the 2070s in those cities which are historically susceptible (usually port cities located in deltas). This approach provided a variable change in extreme water level from around 0.5m in cities only affected by global SLR, to as much as 1.5m for cities affected by global SLR, increased storminess and human-induced subsidence. Population projections were based upon the UN medium variant, where global population stabilises at around 9 billion by 2050. Figure 18 shows that the USA was the 5th highest country simulated to show an increased exposure from SLR relative to present in the 2070s. Generally, exposure change in developing country cities is more strongly driven by socioeconomic changes, while developed country cities see a more significant effect from climate change.

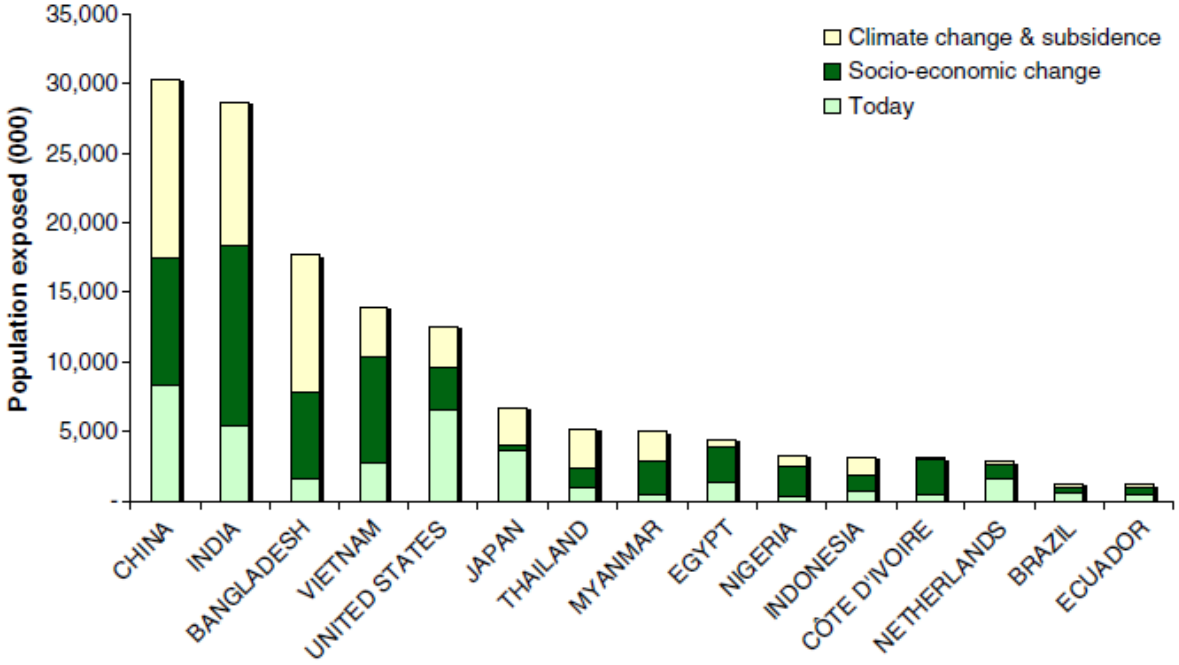

Figure 18. *The top 15 countries in the 2070s for exposure to SLR, based upon a global analysis of 136 port cities (Hanson et al., 2011). The proportions associated with current exposure, climate change and subsidence, and socio-economic changes are displayed.*

To further quantify the impact of SLR and some of the inherent uncertainties, the DIVA model was used to calculate the number of people flooded per year for global mean sea level increases (Brown et al., 2011). The DIVA model (DINAS-COAST, 2006) is an integrated model of coastal systems that combines scenarios of water level changes with socio-economic information, such as increases in population. The study uses two climate scenarios; 1) the SRES A1B scenario and 2) a mitigation scenario, RCP2.6. In both cases an SRES A1B population scenario was used. The results are shown in Table 13.

	A1B		**RCP**	
	Low	**High**	**Low**	**High**
Additional people flooded (1000s)	58.01	775.83	44.89	258.75
Loss of wetlands area (% of country's total wetland)	33.95%	50.46%	33.52%	44.15%

Table 13. *Number of additional people flooded (1000s), and percentage of total wetlands lost by the 2080s under the high and low SRES A1B and mitigation (RCP 2.6) scenarios (Brown et al., 2011).*

National-scale or sub-national scale assessments

Several national-scale assessments of the impact of SLR on coastal USA support the suggestion from global-scale studies (Hanson et al., 2011, Hanson et al., 2010) that the USA is highly vulnerable to climate change (Irish et al., 2010, Kirshen et al., 2008, Lam et al., 2009, Titus et al., 1991, Wu et al., 2009). Lam et al. (2009) estimated the vulnerability of the USA to SLR by calculating the amount of people who lived within a certain distance of the US coastline and below a certain elevation from present sea level. Lam et al. (2009) showed that 19 million people live within 1km of the US coastline and that 11.6 million people live below 3m elevation, and 22 million live below 6m elevation. 6.3 million people were found to live 1km from the coast and with less than 3m elevation. Titus et al. (1991) estimated that the loss of land within 1m of the high water mark across the USA was of the order of 35,700 km^2, based on a sample of 46 coastal sites selected at regular intervals along the coast.

More recently, Kirshen et al. (2008) investigated how magnitudes of the 100-year flood elevation might be effected by climate change, along the northeastern USA, which is highly vulnerable to present and future coastal flooding (Wu et al., 2009). Changes were estimated for SRES B1 and A1FI scenarios and for high and low climate sensitivities. Under the A1FI emissions scenario, by 2050, the elevation of the 2005 100-year event may be equalled or exceeded at least every 30 years at all the locations Kirshen et al. (2008) considered (Table

14). In more exposed US cities such as Boston, Massachusetts and Atlantic City, New Jersey, this could occur at the considerably higher frequency of every 8 years or less. Under the B1 emissions scenario, by 2050, the elevation of the 2005 100-year event may be equalled or exceeded at least every 70 years at all sites. In Boston and Atlantic City, this could occur every 30 years or less. The potential impacts of such changes in SLR for this region of USA were explored by Wu et al. (2009). The study investigated the impact of SLR estimated from five GCMs driven by two emissions scenarios (A2 and B2), for the Mid and Upper-Atlantic region of the USA. Sub-regional estimates of the area subject to inundation are displayed in Table 14. An assessment of the impact of SLR on the city of Corpus Christi, along the Gulf of Mexico coastline, found that hurricane flooding is projected to rise between 20% and 70% by the 2030s, resulting in an increase in property damages and impacted population (Irish et al., 2010). Under an A1B emissions scenario, Irish et al. (2010) estimated that the amount of land inundated in the region could double by the 2080s.

Location and scenario	100-year storm surge elevation (m)			Recurrence interval of 2005 100- year Anomaly (years)	
	2005	2050	2100	2050	2100
Boston- B1 lo	3.0	3.2	3.5	3	2
Boston—A1FI hi	3.0	3.4	4.2	2	2
Woods Hole—B1 lo	3.0	3.1	3.3	50	35
Woods Hole—A1FI hi	3.0	3.3	4.0	25	2
New London—B1 lo	2.2	2.3	2.4	70	50
New London—A1FI hi	2.2	2.3	3.1	30	3
New York City—B1 lo	2.8	2.9	3.0	50	30
New York City—A1FI hi	2.8	3.1	3.7	30	3
Atlantic City—B1 lo	2.4	2.8	3.4	6	2
Atlantic City—A1FI hi	2.4	3.1	4.1	2	2

Table 14. *Estimated storm surge elevations for 2005, 2050 and 2100 for each site considered by Kirshen et al. (2008). Estimates were made for two emissions scenarios (A1FI and B1) and high (hi) and low (lo) climate sensitivities. Data is from Kirshen et al. (2008).*

State	Minimum	B2 mean	A2 mean	Maximum
Massachusetts	140	150	155	168
Rhode Island	32	34	35	38
Connecticut	76	80	81	85
New York	247	266	275	292
New Jersey	337	404	424	468
Delaware	210	224	230	243
Maryland	764	841	893	1,051
Virginia	506	572	675	768
Total	**2,312**	**2,571**	**2,767**	**3,112**

Table 15. *The area (km^2) subject to inundation at mean sea level under different SLR scenarios. The minimum and maximum values across five GCMs and two emissions scenarios are presented, as well as the mean across the five GCMs for each scenario. Data is from Wu et al. (2009).*

Mousavi et al. (2011) assessed the impact of climate change on SLR for Corpus Christi, Texas. They found that hurricane flood elevation (meteorologically generated storm surge plus sea level rise) could, on average, rise by 0.3m by the 2030s and by 0.8m by the 2080s. For catastrophic-type hurricane surge events, flood elevations were projected to rise by as much as 0.5m and 1.8m by the 2030s and 2080s, respectively.

References

AINSWORTH, E. A. & MCGRATH, J. M. 2010. Direct Effects of Rising Atmospheric Carbon Dioxide and Ozone on Crop Yields. *In:* LOBELL, D. & BURKE, M. (eds.) *Climate Change and Food Security.* Springer Netherlands.

ALLISON, E. H., PERRY, A. L., BADJECK, M.-C., NEIL ADGER, W., BROWN, K., CONWAY, D., HALLS, A. S., PILLING, G. M., REYNOLDS, J. D., ANDREW, N. L. & DULVY, N. K. 2009. Vulnerability of national economies to the impacts of climate change on fisheries. *Fish and Fisheries,* 10**,** 173-196.

ARNELL, N., OSBORNE, T., HOOKER, J., DAWSON, T., PERRYMAN, A. & WHEELER, T. 2010a. Simulation of AVOIDed impacts on crop productivity and food security. *Work stream 2, Report 17 of the AVOID programme (AV/WS2/D1/R17).*

ARNELL, N., WHEELER, T., OSBORNE, T., ROSE, G., GOSLING, S., DAWSON, T., PENN, A. & PERRYMAN, A. 2010b. The implications of climate policy for avoided impacts on water and food security. *Work stream 2, Report 6 of the AVOID programme (AV/WS2/D1/R06).* London: Department for Energy and Climate Change (DECC).

ARNELL, N. W. 2004. Climate change and global water resources: SRES emissions and socio-economic scenarios. *Global Environmental Change,* 14**,** 31-52.

AVNERY, S., MAUZERALL, D. L., LIU, J. F. & HOROWITZ, L. W. 2011. Global crop yield reductions due to surface ozone exposure: 2. Year 2030 potential crop production losses and economic damage under two scenarios of O_3 pollution. *Atmospheric Environment,* 45**,** 2297-2309.

BELL, J. L., SLOAN, L. C. & SNYDER, M. A. 2004. Regional changes in extreme climatic events: A future climate scenario. *Journal of Climate,* 17**,** 81-87.

BENDER, M. A., KNUTSON, T. R., TULEYA, R. E., SIRUTIS, J. J., VECCHI, G. A., GARNER, S. T. & HELD, I. M. 2010. Modeled impact of anthropogenic warming on the frequency of intense Atlantic hurricanes. *Science,* 327**,** 454-8.

BENGTSSON, L., HODGES, K. I., ESCH, M., KEENLYSIDE, N., KORNBLUEH, L., LUO, J.-J. & YAMAGATA, T. 2007. How may tropical cyclones change in a warmer climate? *Tellus A,* 59**,** 539-561.

BETTS, R. A., BOUCHER, O., COLLINS, M., COX, P. M., FALLOON, P. D., GEDNEY, N., HEMMING, D. L., HUNTINGFORD, C., JONES, C. D., SEXTON, D. M. H. & WEBB, M. J. 2007. Projected increase in continental runoff due to plant responses to increasing carbon dioxide. *Nature,* 448**,** 1037-1041.

BROWN, P. J., BRADLEY, R. S. & KEIMIG, F. T. 2010. Changes in Extreme Climate Indices for the Northeastern United States, 1870–2005. *Journal of Climate,* 23**,** 6555-6572.

BROWN, S., NICHOLLS, R., LOWE, J.A. and PARDAENS, A. (2011), Sea level rise impacts in 24 countries. Faculty of Engineering and the Environment and Tyndall Centre for Climate Change Research, University of Southampton.

CHAKRABORTY, S. & NEWTON, A. C. 2011. Climate change, plant diseases and food security: an overview. *Plant Pathology,* 60**,** 2-14.

CHANGNON, S. A. 2008. Assessment of flood losses in the United States. *Journal of Contemporary Water Research and Education,* 138**,** 38-44.

CHAUVIN, F., ROYER, J.-F. & DÉQUÉ, M. 2006. Response of hurricane-type vortices to global warming as simulated by ARPEGE-Climat at high resolution. *Climate Dynamics,* 27**,** 377-399.

CHEUNG, W. W. L., LAM, V. W. Y., SARMIENTO, J. L., KEARNEY, K., WATSON, R. E. G., ZELLER, D. & PAULY, D. 2010. Large-scale redistribution of maximum fisheries catch potential in the global ocean under climate change. *Global Change Biology,* 16**,** 24-35.

CIFUENTES, L., BORJA-ABURTO, V. H., GOUVEIA, N., THURSTON, G. & DAVIS, D. L. 2001. Assessing the health benefits of urban air pollution reductions associated with climate change mitigation (2000-2020): Santiago, Sao Paulo, Mexico City, and New York City. *Environmental health perspectives,* 109**,** 419-425.

DIFFENBAUGH, N. S., PAL, J. S., TRAPP, R. J. & GIORGI, F. 2005. Fine-scale processes regulate the response of extreme events to global climate change. *Proceedings of the National Academy of Sciences of the United States of America,* 102**,** 15774-15778.

DINAS-COAST Consortium. 2006 DIVA 1.5.5. Potsdam, Germany: Potsdam Institute for Climate Impact Research (on CD-ROM).

DOLL, P. 2009. Vulnerability to the impact of climate change on renewable groundwater resources: a global-scale assessment. *Environmental Research Letters,* 4.

DOLL, P. & SIEBERT, S. 2002. Global modeling of irrigation water requirements. *Water Resources Research*. Vol: 38 Issue: 4. Doi: 10.1029/2001WR000355.

EBI, K.L., BALBUS, J., KINNEY, P.L., LIPP, E., MILLS, D., O'NEILL, M.S., & WILSON, M., 2008: Effects of global change on human health.In: *Analyses of the Effects of Global Change on Human Healthand Welfare and Human Systems* [Gamble, J.L. (ed.), K.L. Ebi, F.G.Sussman, and T.J. Wilbanks (authors)]. Synthesis and AssessmentProduct 4.6. U.S. Environmental Protection Agency, Washington, DC, pp. 39-87.

ELSNER, J. B., KOSSIN, J. P. & JAGGER, T. H. 2008. The increasing intensity of the strongest tropical cyclones. *Nature,* 455**,** 92-5.

ELSNER, M. M., CUO, L., VOISIN, N., DEEMS, J. S., HAMLET, A. F., VANO, J. A., MICKELSON, K. E. B., LEE, S. Y. & LETTENMAIER, D. P. 2010. Implications of 21st century climate change for the hydrology of Washington State. *Climatic Change,* 102**,** 225-260.

EMANUEL, K., SUNDARARAJAN, R. & WILLIAMS, J. 2008. Hurricanes and Global Warming: Results from Downscaling IPCC AR4 Simulations. *Bulletin of the American Meteorological Society,* 89**,** 347-367.

FALKENMARK, M., ROCKSTRÖM, J. & KARLBERG, L. 2009. Present and future water requirements for feeding humanity. *Food Security,* 1**,** 59-69.

FAO. 2008. *Food and Agricultural commodities production* [Online]. Available: http://faostat.fao.org/site/339/default.aspx [Accessed 1 June 2011].

FISCHER, G. 2009. World Food and Agriculture to 2030/50: How do climate change and bioenergy alter the long-term outlook for food, agriculture and resource availability? *Expert Meeting on How to Feed the World in 2050.* Food and Agriculture Organization of the United Nations, Economic and Social Development Department.

FUNG, F., LOPEZ, A. & NEW, M. 2011. Water availability in +2°C and +4°C worlds. *Philosophical Transactions of the Royal Society A: Mathematical, Physical and Engineering Sciences,* 369**,** 99-116.

GARNER, S. T., HELD, I. M., KNUTSON, T. & SIRUTIS, J. 2009. The Roles of Wind Shear and Thermal Stratification in Past and Projected Changes of Atlantic Tropical Cyclone Activity. *Journal of Climate,* 22**,** 4723-4734.

GERTEN D., SCHAPHOFF S., HABERLANDT U., LUCHT W., SITCH S. 2004 . Terrestrial vegetation and water balance: hydrological evaluation of a dynamic global vegetation model *International Journal Water Resource Development* 286:249–270.

GORNALL, J., BETTS, R., BURKE, E., CLARK, R., CAMP, J., WILLETT, K., WILTSHIRE, A. 2010. Implications of climate change for agricultural productivity in the early twenty-first century. *Phil. Trans. R. Soc. B*, DOI: 10.1098/rstb.2010.0158.

GOSLING, S., TAYLOR, R., ARNELL, N. & TODD, M. 2011. A comparative analysis of projected impacts of climate change on river runoff from global and catchment-scale hydrological models. *Hydrology and Earth System Sciences,* 15**,** 279–294.

GOSLING, S. N. & ARNELL, N. W. 2011. Simulating current global river runoff with a global hydrological model: model revisions, validation, and sensitivity analysis. *Hydrological Processes,* 25**,** 1129-1145.

GOSLING, S. N., BRETHERTON, D., HAINES, K. & ARNELL, N. W. 2010. Global hydrology modelling and uncertainty: running multiple ensembles with a campus grid. *Philosophical Transactions of the Royal Society A: Mathematical, Physical and Engineering Sciences,* 368**,** 4005-4021.

GROISMAN, P. Y. & KNIGHT, R. W. 2008. Prolonged dry episodes over the conterminous united states: New tendencies emerging during the last 40 years. *Journal of Climate,* 21**,** 1850-1862.

GUALDI, S., SCOCCIMARRO, E. & NAVARRA, A. 2008. Changes in Tropical Cyclone Activity due to Global Warming: Results from a High-Resolution Coupled General Circulation Model. *Journal of Climate,* 21**,** 5204-5228.

GUTOWSKI, W. J., HEGERL, G. C., HOLLAND, G. J., KNUTSON, T. R., MEARNS, L. O., STOUFFER, R. J., WEBSTER, P. J., WEHNER, M. F., ZWIERS, F. W., BROOKS, H. E., EMANUEL, K. A., KOMAR, P. D., KOSSIN, J. P., KUNKEL, K. E., MCDONALD, R., MEEHL, G. A. & TRAPP, R. J. 2008. Causes of Observed Changes in Extremes and Projections of Future Changes. Regions of Focus: North America, Hawaii, Caribbean, and U.S. Pacific Islands. *In:* KARL, T. R., MEEHL, G. A., MILLER, C. D., HASSOL, S. J., WAPLE, A. M. & MURRAY, W. L. (eds.) *Weather and Climate Extremes in a Changing Climate. Regions of Focus: North America, Hawaii, Caribbean, and U.S. Pacific Islands.* Washington, D.C.: Department of Commerce, National Oceanic and Atmospheric Administration's National Climate Data Center.

HAMLET, A. F. & LETTENMAIER, D. P. 2007. Effects of 20th century warming and climate variability on flood risk in the western U.S. *Water Resources Research,* 43**,** W06427, doi:10.1029/2006WR005099.

HANSON, S., NICHOLLS, R., RANGER, N., HALLEGATTE, S., CORFEE-MORLOT, J., HERWEIJER, C. & CHATEAU, J. 2011. A global ranking of port cities with high exposure to climate extremes. *Climatic Change,* 104**,** 89-111.

HANSON, S., NICHOLLS, R., S, H. & CORFEE-MORLOT, J. 2010. The effects of climate mitigation on the exposure of worlds large port cities to extreme coastal water levels. London, UK.

HARDING, R., BEST, M., BLYTH, E., HAGEMANN, D., KABAT, P., TALLAKSEN, L.M., WARNAARS, T., WIBERG, D., WEEDON, G.P., van LANEN, H., LUDWIG, F., HADDELAND, I. 2011. Preface to the “Water and Global Change (WATCH)” special collection: Current knowledge of the terrestrial global water cycle. *Journal of Hydrometeorology*, DOI: 10.1175/JHM-D-11-024.1

HASEGAWA, A. & EMORI, S. 2005. Tropical Cyclones and Associated Precipitation over the Western North Pacific : T106 Atmospheric GCM Simulation for Present-day and Doubled CO_2 Climates. *Simulation,* 1**,** 148-151.

HATFIELD, J., K. BOOTE, P. FAY, L. HAHN, C. IZAURRALDE, B.A. KIMBALL,T. MADER, J. MORGAN, D. ORT, W. POLLEY, A. THOMSON, and D. WOLFE,2008: Agriculture. In: *The Effects of Climate Change on Agriculture,Land Resources, Water Resources, and Biodiversity in the United States* [Backlund, P., A. Janetos, D. Schimel, J. Hatfield,K. Boote, P. Fay, L. Hahn, C. Izaurralde, B.A. Kimball, T. Mader,J. Morgan, D. Ort, W. Polley, A. Thomson, D. Wolfe, M.G. Ryan,S.R. Archer, R. Birdsey, C. Dahm, L. Heath, J. Hicke, D. Hollinger,T. Huxman, G. Okin, R. Oren, J. Randerson, W. Schlesinger, D.Lettenmaier, D. Major, L. Poff, S. Running, L. Hansen, D. Inouye,B.P. Kelly, L. Meyerson, B. Peterson, and R. Shaw (eds.)]. Synthesis and Assessment Product 4.3. U.S. Department of Agriculture, Washington, DC, pp. 21-74.

HAYHOE, K., CAYAN, D., FIELD, C. B., FRUMHOFF, P. C., MAURER, E. P., MILLER, N. L., MOSER, S. C., SCHNEIDER, S. H., CAHILL, K. N., CLELAND, E. E., DALE, L., DRAPEK, R., HANEMANN, R. M., KALKSTEIN, L. S., LENIHAN, J., LUNCH, C. K., NEILSON, R. P., SHERIDAN, S. C. & VERVILLE, J. H. 2004. Emissions pathways, climate change, and

impacts on California. *Proceedings of the National Academy of Sciences of the United States of America,* 101**,** 12422-12427.

HAYHOE, K., WAKE, C. P., HUNTINGTON, T. G., LUO, L. F., SCHWARTZ, M. D., SHEFFIELD, J., WOOD, E., ANDERSON, B., BRADBURY, J., DEGAETANO, A., TROY, T. J. & WOLFE, D. 2007. Past and future changes in climate and hydrological indicators in the US Northeast. *Climate Dynamics,* 28**,** 381-407.

HIRABAYASHI, Y., KANAE, S., EMORI, S., OKI, T. & KIMOTO, M. 2008. Global projections of changing risks of floods and droughts in a changing climate. *Hydrological Sciences Journal-Journal Des Sciences Hydrologiques,* 53**,** 754-772.

HOFF, H., FALKENMARK, M., GERTEN, D., GORDON, L., KARLBERG, L. & ROCKSTROM, J. 2010. Greening the global water system. *Journal of Hydrology,* 384**,** 177-186.

IFPRI. 2010. *International Food Policy Research Institute (IFPRI) Food Security CASE maps. Generated by IFPRI in collaboration with StatPlanet.* [Online]. Available: www.ifpri.org/climatechange/casemaps.html [Accessed 21 June 2010].

IGLESIAS, A., GARROTE, L., QUIROGA, S. & MONEO, M. 2009. Impacts of climate change in agriculture in Europe. PESETA-Agriculture study. *JRC Scientific and Technical Reports.*

IGLESIAS, A. & ROSENZWEIG, C. 2009. Effects of Climate Change on Global Food Production under Special Report on Emissions Scenarios (SRES) Emissions and Socioeconomic Scenarios: Data from a Crop Modeling Study. . Palisades, NY: Socioeconomic Data and Applications Center (SEDAC), Columbia University.

IPCC 2007a. Climate Change 2007: The Physical Science Basis. Contribution of Working Group I to the Fourth Assessment Report of the Intergovernmental Panel on Climate Change *In:* SOLOMON, S., QIN, D., MANNING, M., CHEN, Z., MARQUIS, M., AVERYT, K. B., TIGNOR, M. & MILLER, H. L. (eds.). Cambridge, United Kingdom and New York, NY, USA.

IPCC 2007b. Climate Change 2007: Impacts, Adaptation and Vulnerability. Contribution of Working Group II to the Fourth Assessment Report of the Intergovernmental Panel on Climate Change. *In:* PARRY, M. L., CANZIANI, O. F., PALUTIKOF, J. P., VAN DER LINDEN, P. J. & HANSON, C. E. (eds.). Cambridge, UK.

IRISH, J. L., FREY, A. E., ROSATI, J. D., OLIVERA, F., DUNKIN, L. M., KAIHATU, J. M., FERREIRA, C. M. & EDGE, B. L. 2010. Potential implications of global warming and barrier island degradation on future hurricane inundation, property damages, and population impacted. *Ocean & Coastal Management,* 53**,** 645-657.

JACOB, K., GORNITZ, V. & ROSENZWEIG, C. 2007. Vulnerability of the New York City Metropolitan Area to Coastal Hazards, Including Sea-Level Rise: Inferences for Urban Coastal Risk Management and Adaptation Policies. *Managing coastal vulnerability***,** 141.

KARL, T. R., MELILLO, J. M. & PETERSON, T. C. (eds.) 2009. *Global Climate Change Impacts in the United States.,* New York: Cambridge University Press.

KIRSHEN, P., WATSON, C., DOUGLAS, E., GONTZ, A., LEE, J. & TIAN, Y. 2008. Coastal flooding in the Northeastern United States due to climate change. *Mitigation and Adaptation Strategies for Global Change,* 13**,** 437-451.

KITOH, A., OSE, T., KURIHARA, K., KUSUNOKI, S., SUGI, M. & GROUP, K. T.-M. 2009. Projection of changes in future weather extremes using super-high-resolution global and regional atmospheric models in the KAKUSHIN Program : Results of preliminary experiments Abstract :. *Group,* 53**,** 49-53.

KNUTSON, T. R., SIRUTIS, J. J., GARNER, S. T., VECCHI, G. A. & HELD, I. M. 2008. Simulated reduction in Atlantic hurricane frequency under twenty-first-century warming conditions. *Nature Geosci,* 1**,** 359-364.

KNUTSON, T. R. & TULEYA, R. E. 2004. Impact of CO_2-Induced Warming on Simulated Hurricane Intensity and Precipitation : Sensitivity to the Choice of Climate Model and Convective Parameterization. *Journal of Climate***,** 3477-3495.

KUNKEL, K. E. & ET AL. 2008. Observed changes in weather and climate extremes. In: Weather and Climate Extremes in a Changing Climate: Regions of Focus: North America, Hawaii, Caribbean, and U.S. Pacific Islands *Synthesis and Assessment Product 3.3. U.S. Climate Change Science Program.* Washington DC.

LAM, N. S. N., ARENAS, H., LI, Z. & LIU, K. B. 2009. An Estimate of Population Impacted by Climate Change Along the U. S. Coast. *Journal of Coastal Research***,** 1522-1526.

LATIF, M. & KEENLYSIDE, N. S. 2009. El Niño/Southern Oscillation response to global warming. *Proceedings of the National Academy of Sciences of the United States of America,* 106**,** 20578-20583.

LOBELL, D. B., SCHLENKER, W. & COSTA-ROBERTS, J. 2011. Climate Trends and Global Crop Production Since 1980. *Science*, 333(6042), 616-620.

LUCK, J., SPACKMAN, M., FREEMAN, A., TRE¸BICKI, P., GRIFFITHS, W., FINLAY, K. & CHAKRABORTY, S. 2011. Climate change and diseases of food crops. *Plant Pathology,* 60**,** 113-121.

MANSUR, E. T., MENDELSOHN, R. & MORRISON, W. 2005. A discrete-continuous choice model of climate change impacts on energy. *SSRN Yale SOM Working Paper No. ES-43 (abstract number 738544)***,** 45.

MCCARTHY, K., PETERSON, D. J., SASTRY, N. & POLLARD, M. 2006. The repopulation of New Orleans after Hurricane Katrina. Technical Report. Santa Monica, RAND Gulf States Policy Institute. Available online: http://www.rand.org.

MCDONALD, R. E., BLEAKEN, D. G., CRESSWELL, D. R., POPE, V. D. & SENIOR, C. A. 2005. Tropical storms: representation and diagnosis in climate models and the impacts of climate change. *Climate Dynamics,* 25**,** 19-36.

MENDELSOHN, R. 2001. *Global Warming and the American Economy: A Regional Assessment of Climate Change,* Cheltenham, UK, Edward Elgar Publishing.

MENDELSOHN, R., EMANUEL, K. & CHONABAYASHI, S. 2011. The Impact of Climate Change on Global Tropical Cyclone Damages.

MOSER, S. C. & ET AL. 2008. The Future is Now. An Update on Climate Change Science, Impacts and Response Options for California. PIER Energy-Related Environmental Research, CEC-500-2008-071, Sacramento, CA.

MOUSAVI, M. E., IRISH, J. L., FREY, A. E., OLIVERA, F. & EDGE, B. L. 2011. Global warming and hurricanes: the potential impact of hurricane intensification and sea level rise on coastal flooding. *Climatic Change,* 104**,** 575-597.

MUNICH REINSURANCE COMPANY 2009. World map of natural hazards, http://www.esri.com/mapmuseum/mapbook_gallery/volume25/pdf/mapbook25_20.pdf accessed 13th Sept 2011.

MURAKAMI, H. & WANG, B. 2010. Future Change of North Atlantic Tropical Cyclone Tracks: Projection by a 20-km-Mesh Global Atmospheric Model. *Journal of Climate,* 23**,** 2699-2721.

NATIONAL RESEARCH COUNCIL, 2010. Adapting to the Impacts of Climate Change. National Academies Press, Washington DC, ISBN 978-0-309-14591-6, 292pp.

NELSON, G. C., ROSEGRANT, M. W., PALAZZO, A., GRAY, I., INGERSOLL, C., ROBERTSON, R., TOKGOZ, S., ZHU, T., SULSER, T. & RINGLER, C. 2010. Food Security, Farming and Climate Change to 2050. *Research Monograph, International Food Policy Research Institute.* Washington, DC.

NICHOLLS, R. J. and LOWE, J. A. (2004). "Benefits of mitigation of climate change for coastal areas." *Global Environmental Change* **14**(3): 229-244.

NICHOLLS, R. J., MARINOVA, N., LOWE, J. A., BROWN, S., VELLINGA, P., DE GUSMÃO, G., HINKEL, J. and TOL, R. S. J. (2011). "Sea-level rise and its possible impacts given a 'beyond 4◦C world' in the twenty-first century." *Philosophical Transactions of the Royal Society A* 369: 1-21.

NING, L., TAYLOR, T., WEI, J., CHUNLIAN, J., CORREIA, J., LEUNG, L. R. & PAK CHUNG, W. 2010. Climate Change Impacts on Residential and Commercial Loads in the Western U.S. Grid. *Power Systems, IEEE Transactions on,* 25**,** 480-488.

NOHARA, D., KITOH, A., HOSAKA, M. & OKI, T. 2006. Impact of climate change on river discharge projected by multimodel ensemble. *Journal of Hydrometeorology,* 7**,** 1076-1089.

NTELEKOS, A. A., OPPENHEIMER, M., SMITH, J. A. & MILLER, A. J. 2010. Urbanization, climate change and flood policy in the United States. *Climatic Change,* 103**,** 597-616.

OOUCHI, K., YOSHIMURA, J., YOSHIMURA, H., MIZUTA, R., KUSUNOKI, S. & NODA, A. 2006. Tropical Cyclone Climatology in a Global-Warming Climate as Simulated in a 20 km-Mesh Global Atmospheric Model: Frequency and Wind Intensity Analyses. *Journal of the Meteorological Society of Japan,* 84**,** 259-276.

PARDAENS, A. K., LOWE, J., S, B., NICHOLLS, R. & DE GUSMÃO, D. 2011. Sea-level rise and impacts projections under a future scenario with large greenhouse gas emission reductions. *Geophysical Research Letters,* 38**,** L12604.

PARRY, M. L., ROSENZWEIG, C., IGLESIAS, A., LIVERMORE, M. & FISCHER, G. 2004. Effects of climate change on global food production under SRES emissions and socio-economic scenarios. *Global Environmental Change-Human and Policy Dimensions,* 14**,** 53-67.

PETERSON, T. C., ZHANG, X. B., BRUNET-INDIA, M. & VAZQUEZ-AGUIRRE, J. L. 2008. Changes in North American extremes derived from daily weather data. *Journal of Geophysical Research-Atmospheres,* 113.

RAFF, D. A., PRUITT, T. & BREKKE, L. D. 2009. A framework for assessing flood frequency based on climate projection information. *Hydrology and Earth System Sciences,* 13**,** 2119-2136.

RAHMSTORF, S. 2010. A new view on sea level rise. *Nature Reports Climate Change,* 4**,** 44-45.

RAMANKUTTY, N., EVAN, A. T., MONFREDA, C. & FOLEY, J. A. 2008. Farming the planet: 1. Geographic distribution of global agricultural lands in the year 2000. *Global Biogeochemical Cycles,* 22**,** GB1003.

RAMANKUTTY, N., FOLEY, J. A., NORMAN, J. & MCSWEENEY, K. 2002. The global distribution of cultivable lands: current patterns and sensitivity to possible climate change. *Global Ecology and Biogeography,* 11**,** 377-392.

REICHLER, T. & KIM, J. 2008. How well do coupled models simulate today's climate? *Bulletin of the American Meteorological Society,* 89**,** 303.

ROCKSTROM, J., FALKENMARK, M., KARLBERG, L., HOFF, H., ROST, S. & GERTEN, D. 2009. Future water availability for global food production: The potential of green water for increasing resilience to global change. *Water Resources Research,* 45.

SILLMANN, J. & ROECKNER, E. 2008. Indices for extreme events in projections of anthropogenic climate change. *Climatic Change,* 86**,** 83-104.

SMAKHTIN, V., REVENGA, C. & DOLL, P. 2004. A pilot global assessment of environmental water requirements and scarcity. *Water International,* 29**,** 307-317.

STRZEPEK, K., YOHE, G., NEUMANN, J. & BOEHLERT, B. 2010. Characterizing changes in drought risk for the United States from climate change. *Environmental Research Letters,* 5.

SUGI, M., MURAKAMI, H. & YOSHIMURA, J. 2009. A reduction in global tropical cyclone frequency due to global warming. *SOLA,* 5**,** 164-167.

TATSUMI, K., YAMASHIKI, Y., VALMIR DA SILVA, R., TAKARA, K., MATSUOKA, Y., TAKAHASHI, K., MARUYAMA, K. & KAWAHARA, N. 2011. Estimation of potential changes in cereals production under climate change scenarios. *Hydrological Processes,*Special Issue: Japan Society of Hydrology and water resources, 25 (17), 2715-2725.

TITUS, J. G., PARK, R. A., LEATHERMAN, S. P., WEGGEL, J. R., GREENE, M. S., MAUSEL, P. W., BROWN, S., GAUNT, C., TREHAN, M. & YOHE, G. 1991. Greenhouse effect and sea level rise: the cost of holding back the sea. *Coastal Management,* 19**,** 171-204.

VAN LIESHOUT, M., KOVATS, R., LIVERMORE, M. & MARTENS, P. 2004. Climate change and malaria: analysis of the SRES climate and socio-economic scenarios. *Global Environmental Change,* 14**,** 87-99.

VAN VUUREN, D., DEN ELZEN, M., LUCAS, P., EICKHOUT, B., STRENGERS, B., VAN RUIJVEN, B., WONINK, S. & VAN HOUDT, R. 2007. Stabilizing greenhouse gas concentrations at low levels: an assessment of reduction strategies and costs. *Climatic Change,* 81**,** 119-159.

VAN VUUREN, D. P., ISAAC, M., KUNDZEWICZ, Z. W., ARNELL, N., BARKER, T., CRIQUI, P., BERKHOUT, F., HILDERINK, H., HINKEL, J., HOF, A., KITOUS, A., KRAM, T., MECHLER, R. & SCRIECIU, S. 2011. The use of scenarios as the basis for combined assessment of climate change mitigation and adaptation. *Global Environmental Change,* 21**,** 575-591.

VAVRUS, S. & VAN DORN, J. 2010. Projected future temperature and precipitation extremes in Chicago. *Journal of Great Lakes Research,* 36**,** 22-32.

VECCHI, G. A. & SODEN, B. J. 2007. Effect of remote sea surface temperature change on tropical cyclone potential intensity. *Nature,* 450**,** 1066-70.

VÖRÖSMARTY, C. J., MCINTYRE, P. B., GESSNER, M. O., DUDGEON, D., PRUSEVICH, A., GREEN, P., GLIDDEN, S., BUNN, S. E., SULLIVAN, C. A., LIERMANN, C. R. & DAVIES, P. M. 2010. Global threats to human water security and river biodiversity. *Nature,* 467**,** 555-561.

WARREN, R., ARNELL, N., BERRY, P., BROWN, S., DICKS, L., GOSLING, S., HANKIN, R., HOPE, C., LOWE, J., MATSUMOTO, K., MASUI, T., NICHOLLS, R., O'HANLEY, J., OSBORN, T., SCRIECRU, S. (2010) The Economics and Climate Change Impacts of Various Greenhouse Gas Emissions Pathways: A comparison between baseline and policy emissions scenarios, AVOID Report, AV/WS1/D3/R01. http://www.metoffice.gov.uk/avoid/files/resources-researchers/AVOID_ WS1_D3_01_20100122.pdf.

WASHINGTON, W. M., KNUTTI, R., MEEHL, G. A., TENG, H. Y., TEBALDI, C., LAWRENCE, D., BUJA, L. & STRAND, W. G. 2009. How much climate change can be avoided by mitigation? *Geophysical Research Letters,* 36. L08703, doi:10.1029/2008GL037074.

WEHNER, M., EASTERLING, D. R., LAWRIMORE, J. H., HEIM, R. R., VOSE, R. S. & SANTER, B. D. 2011. Projections of Future Drought in the Continental United States and Mexico. *Journal of Hydrometeorology*.

WILBANKS, T. J., ROMERO LANKAO, P., BAO, M., BERKHOUT, F., CAIRNCROSS, S., CERON, J.-P., KAPSHE, M., MUIR-WOOD, R. & ZAPATA-MARTI, R. 2007. Industry, settlement and society. *In:* PARRY, M. L., CANZIANI, O. F., PALUTIKOF, J. P., VAN DER LINDEN, P. J. & HANSON, C. E. (eds.) *Climate Change 2007: Impacts, Adaptation and Vulnerability. Contribution of Working Group II to the Fourth Assessment Report of the Intergovernmental Panel on Climate Change.* Cambridge, UK: Cambridge University Press.

WOOD, E.F., ROUNDY, J.K., TROY, T.J., van BEEK, L.P.H., BIERKENS, M.F.P., BLYTH, E., de ROO, A., DOLL, P., EK, M., FAMIGLIETTI, J., GOCHIS, D., van de GIESEN, N., HOUSER, P., JAFFE, P.R., KOLLET, S., LEHNER, B., LETTENMAIER, D.P., PETERS-LIDARD, C., SIVAPALAN, M., SHEFFIELD, J., WADE, A. & WHITEHEAD, P. 2011. Hyperresolution global land surface modelling: Meeting a grand challenge for monitoring Earth's terrestrial water. *Water Resources Research,* 47, W05301.

WORTH, T. 2010. Climate Change and Crop Insurance in the United States. *OECD-INEA-FAO Workshop on agriculture and adaptation to climate change.*

WOS. 2011. *Web of Science* [Online]. Available: http://thomsonreuters.com/products_services/science/science_products/a-z/web_of_science [Accessed August 2011].

WRIGHT, K. & HOGAN, C. 2008. The Potential Impacts of Global Sea Level Rise on Transportation Infrastructure, Phase 1-Final Report. District of Columbia, Maryland, North Carolina and Virginia: Center for Climate Change and Environmental Forecasting.

WU, S.-Y., NAJJAR, R. & SIEWERT, J. 2009. Potential impacts of sea-level rise on the Mid- and Upper-Atlantic Region of the United States. *Climatic Change,* 95**,** 121-138.

WU, W., TANG, H., YANG, P., YOU, L., ZHOU, Q., CHEN, Z. & SHIBASAKI, R. 2011. Scenario-based assessment of future food security. *Journal of Geographical Sciences,* 21**,** 3-17.

YOSHIMURA, J., SUGI, M. & NODA, A. 2006. Influence of Greenhouse Warming on Tropical Cyclone Frequency. *Journal of the Meteorological Society of Japan,* 84**,** 405-428.

ZHAO, M. & HELD, I. M. 2010. An Analysis of the Effect of Global Warming on the Intensity of Atlantic Hurricanes Using a GCM with Statistical Refinement. *Journal of Climate,* 23**,** 6382-6393.

ZHAO, M., HELD, I. M., LIN, S.-J. & VECCHI, G. A. 2009. Simulations of Global Hurricane Climatology, Interannual Variability, and Response to Global Warming Using a 50-km Resolution GCM. *Journal of Climate,* 22**,** 6653.

Acknowledgements

Funding for this work was provided by the UK Government Department of Energy and Climate Change, along with information on the policy relevance of the results.

The research was led by the UK Met Office in collaboration with experts from the University of Nottingham, Walker Institute at the University of Reading, Centre for Ecology and Hydrology, University of Leeds, Tyndall Centre — University of East Anglia, and Tyndall Centre — University of Southampton.

Some of the results described in this report are from work done in the AVOID programme by the UK Met Office, Walker Institute at the University of Reading, Tyndall Centre — University of East Anglia, and Tyndall Centre — University of Southampton.

The AVOID results are built on a wider body of research conducted by experts in climate and impact models at these institutions, and in supporting techniques such as statistical downscaling and pattern scaling.

The help provided by experts in each country is gratefully acknowledged — for the climate information they suggested and the reviews they provided, which enhanced the content and scientific integrity of the reports.

The work of the independent expert reviewers at the Centre for Ecology and Hydrology, University of Oxford, and Fiona's Red Kite Climate Consultancy is gratefully acknowledged.

Finally, thanks go to the designers, copy editors and project managers who worked on the reports.

Met Office
FitzRoy Road, Exeter
Devon, EX1 3PB
United Kingdom

Tel: 0870 900 0100
Fax: 0870 900 5050
enquiries@metoffice.gov.uk
www.metoffice.gov.uk

Produced by the Met Office.